5-2018

The Regulation of DNA Methylation in Mammalian Development and Cancer

Nicolas Veland

Follow this and additional works at: https://digitalcommons.library.tmc.edu/utgsbs_dissertations

Part of the Amino Acids, Peptides, and Proteins Commons, Biological Factors Commons, Cancer Biology Commons, Cells Commons, Molecular Biology Commons, Molecular Genetics Commons, and the Nucleic Acids, Nucleotides, and Nucleosides Commons

TMC LIBRARY
Health Sciences Resource Center

THE REGULATION OF DNA METHYLATION IN MAMMALIAN

DEVELOPMENT AND CANCER

by

Jaime Nicolas Veland, B.S.

APPROVED:

_____
Taiping Chen, Ph.D.
Advisory Professor

_____
Mark T. Bedford, Ph.D.

_____
Sharon Y. R. Dent, Ph.D.

_____
Kevin M. McBride, Ph.D.

_____
Gregory K. Wilkerson, D.V.M., Ph.D., D.A.C.V.P.

APPROVED:

_____
Dean, The University of Texas
MD Anderson Cancer Center UTHealth Graduate School of Biomedical Sciences

THE REGULATION OF DNA METHYLATION IN MAMMALIAN

DEVELOPMENT AND CANCER

A

DISSERTATION

Presented to the Faculty of

The University of Texas

MD Anderson Cancer Center UTHealth

Graduate School of Biomedical Sciences

in Partial Fulfillment

of the Requirements

for the Degree of

DOCTOR OF PHILOSOPHY

by

Jaime Nicolas Veland, B.S.

Houston, Texas

May, 2018

EPIGRAPH

"Go confidently in the direction of your dreams! Live the life you have imagined."

-- Henry David Thoreau (1817 – 1862)

DEDICATION

This dissertation is dedicated to my mother, who deeply inspired me to become a scientist at a very early age, and whose hard work and sacrifice has allowed me to pursue my dream and taught me to always give the best of myself in everything I do.

This research work is also greatly dedicated to my wife Marta, who has tremendously supported me since the first step of this long journey, and who truly encouraged me to follow my dream to become a scientist, despite the difficulties that arise in the way. Her care and affection were essential for me in order to reach the finish line.

Finally, this research work is also dedicated to my daughter Gabriela, whose laughs and joys fueled me up in the last hard stretch of this journey, and motivated me not only to be a good scientist, but also to be a great person.

ACKNOWLEDGMENTS

I would like to thank all the people that contribute to make this research work possible:

In the first place, to Dr. Taiping Chen, my mentor, for his extraordinary guidance, remarkable mentoring, unconditional support, significant motivation, outstanding scientific discussions, and fundamental advices in both scientific and personal matters. In particular, for all the time and efforts dedicated to all the different aspects of my scientific education, including, but not limited to, achieving good experimental and technical skills, maximizing my experimental productivity, developing critical and independent scientific thinking, acquiring good communication skills, both oral and written, and contributing to my development as a good laboratory member and scientist.

To Dr. Mark T. Bedford, for all his amazing advices, essential support, scientific discussions and critical suggestions, which play key roles in my formation as a scientist and the development of this research work.

To Dr. Sharon Y.R. Dent, for her important advices, outstanding support, critical suggestions and integral example of scientific leadership, which inspire me and are fundamental for my scientific training and education.

To the rest of my advisory committee members, Dr. Kevin M. McBride and Dr. Gregory K. Wilkerson, for their incredible support, important suggestions, time and efforts for participating in all the committee meetings, which tremendously contribute to my scientific training.

ABSTRACT

THE REGULATION OF DNA METHYLATION IN MAMMALIAN

DEVELOPMENT AND CANCER

Jaime Nicolas Veland, B.S.

Advisory Professor: Taiping Chen, Ph.D.

DNA methylation is an essential epigenetic modification in mammals, as it plays important regulatory roles in multiple biological processes, such as gene transcription, maintenance of chromosomal structure and genomic stability, genomic imprinting, retrotransposon silencing, and X-chromosome inactivation. Dysregulation of DNA methylation is associated with various human diseases. For example, cancer cells usually show global hypomethylation and regional hypermenthylation, which have been implicated in genomic instability and tumor suppressor silencing, respectively. Although great progress has been made in elucidating the biological functions of DNA methylation over the last several decades, how DNA methylation patterns and levels are regulated and dysregulated is not well understood. This dissertation focuses on the molecular mechanisms involved in the regulation of DNA methylation during mammalian development and in cancer. Using mouse embryonic stem cells (mESCs), an ideal model system for studying DNA methylation, I have discovered novel regulatory mechanisms that play important roles in *de novo* and maintenance DNA methylation. In one project, I show that Dnmt3L, a key regulator of *de novo* methylation, facilitates Dnmt3a-mediated methylation by stabilizing Dnmt3a2, the major Dnmt3a isoform in mESCs, thus uncovering a new role for Dnmt3L and providing a plausible explanation for the functional specificity of Dnmt3L. In a separate project, I

demonstrate that PRMT6, an arginine methyltransferase responsible for asymmetric dimethylation of histone H3 arginine 2 (H3R2me2a), negatively regulates maintenance DNA methylation by impairing the recruitment of the Dnmt1-Uhrf1 complex to chromatin, thereby identifying a novel crosstalk between histone arginine methylation and DNA methylation. Moreover, I show that PRMT6 upregulation contributes to global DNA hypomethylation in cancer. Lastly, my work results in the identification of an intestine-specific Dnmt1 protein product that originates from a proteolytic cleavage event, which could shed light on the regulation of DNA methylation in intestinal stem cells (ISCs). In summary, the research work in this dissertation advances our understanding of the regulatory network that controls DNA methylation changes in normal developmental processes and pathological conditions.

TABLE OF CONTENTS

LIST OF FIGURES

LIST OF TABLES

CHAPTER 1 : INTRODUCTION

Part of this chapter is based upon: Veland N & Chen T. (2017) Mechanisms of DNA Methylation and Demethylation during Mammalian Development. In Handbook of Epigenetics, 2nd Edition. (ed. Tollefsbol T.), Elsevier Inc. Academic Press, pp11-24.

Table 1 was adapted from the original version used in: Nicholson TB, Veland N, Chen T. (2015) Writers, Readers, and Erasers of Epigenetic Marks. In Epigenetic Cancer Therapy. (ed. Gray S.G.), Elsevier Inc. Academic Press, pp. 31-66.

Used with permission of Elsevier.

1.1 OVERVIEW OF DNA METHYLATION

DNA methylation, the covalent addition of a methyl group to the fifth position of cytosine (i.e. 5-methylcytosine, 5mC), was initially discovered as epi-cytosine by Rollin D. Hotchkiss more than 60 years ago (1). Subsequent studies revealed that DNA methylation is the most common form of DNA modification, which plays important roles in the regulation of chromatin structure and gene expression. DNA methylation is present in various organisms including many animals, plants and fungi. In mammals, DNA methylation mostly occurs in the context of CpG dinucleotides, with 60-80% of all CpGs in the genome being methylated, although non-CpG (i.e. CpA, CpT or CpC) methylation is abundant in specific tissues and cell types, including embryonic stem cells (ESCs), oocytes, and brain tissue (2). DNA methylation is essential for mammalian development and plays key roles in multiple biological processes such as genomic imprinting, X-chromosome inactivation, and transposon silencing (3). Consistent with its pleiotropic roles, DNA methylation patterns are altered in pathological conditions. For example, cancer cells usually exhibit global hypomethylation and local hypermethylation, which contribute to genomic instability and tumor suppressor silencing, respectively (4).

5mC is not randomly distributed in the genome. In general, repetitive DNA sequences, including transposable elements and centromeric and pericentric satellite DNA, are heavily methylated. In contrast, CpG islands (CGIs, 1-2 kilobases of GC-rich regions) present in gene promoters are usually depleted of DNA methylation, with some exceptions. For example, CpGs on the inactive X chromosome in female cells are hypermethylated, and CpGs in imprinting control regions (ICRs) exhibit allele-specific methylation. On the other hand, gene bodies, especially exons, are often highly methylated. Unlike promoter methylation, which correlates with gene silencing, gene body methylation is often associated with transcriptional activity (5).

In 1975, Holliday and Pugh and Riggs proposed that DNA methylation could be important for cellular memory by serving as a heritable epigenetic mark through cell division. Based on the complementarity of CpG/CpG dyads, they reasoned that methylated CpG sites could be replicated semi-

conservatively during DNA replication (6, 7). The theory would predict the existence of two DNA methyltransferase activities: *de novo* methyltransferase(s) methylate unmodified DNA to establish DNA methylation patterns, and maintenance methyltransferase(s) methylate newly formed hemi-methylated CpG sites during DNA replication to maintain the patterns (Figure 1). The hypothesis was subsequently validated, to a large extent, by the identification of DNA methyltransferases with distinct expression patterns, biochemical properties, and biological functions (8).

DNA methylation patterns and levels are determined by the opposing actions of the methylation and demethylation machineries. The methylation machinery includes DNA methyltransferases (DNMTs), which catalyze the transfer of a methyl group from the methyl donor *S*-adenosyl-L-methionine (AdoMet or SAM) to the C-5 position of cytosines. There are four active DNMTs in mammals: DNMT1 is mainly responsible for maintaining DNA methylation patterns during DNA replication, whereas DNMT3A and DNMT3B function primarily as *de novo* methyltransferases that establish DNA methylation patterns (8). Recently, a new family member named DNMT3C is been found exclusively in rodents, where it plays a specific role in *de novo* methylation at retrotransposons during spermatogenesis (9). DNMT2, a protein with conserved DNMT catalytic motifs, turned out to be an aspartic acid tRNA methyltransferase and has been renamed tRNA aspartic acid (D) methyltransferase 1 (TRDM1) (10). From a chemical perspective, DNA methylation is considered a relatively stable modification. However, global demethylation occurs in pre-implantation embryos and primordial germ cells (PGCs), and locus-specific demethylation takes place during cellular differentiation. DNA demethylation can be achieved by replication-dependent "passive" dilution of 5mC and replication-independent "active" processes (11, 12). Great progress has been made in understanding the mechanisms of demethylation over the last several years, thanks to the discovery that the ten-eleven translocation (TET) family of proteins - TET1, TET2, and TET3 - function as 5mC dioxygenases that convert 5mC to 5-hydroxymethylcytosine (5hmC), 5-formylcytosine (5fC), and 5-carboxylcytosine (5caC) (13-16). There is compelling evidence that 5hmC, 5fC, and 5caC serve as intermediates for DNA demethylation (11, 12).
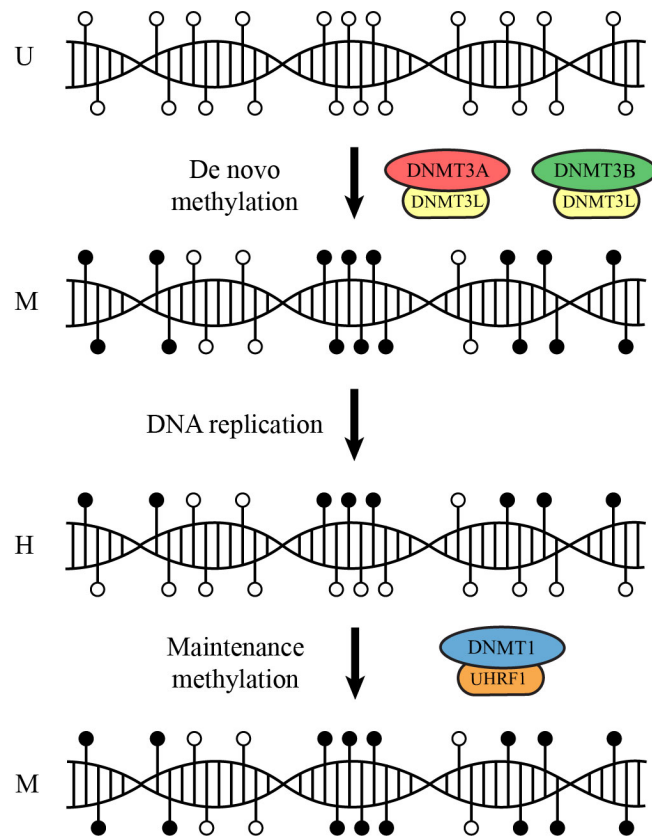
Figure 1: Overview of mechanisms of DNA methylation.

During early development, *de novo* methylation adds methyl groups to specific CpG sites on both DNA strands (resulting in symmetric CpG methylation) and establishes DNA methylation patterns. After each round of DNA replication, the methylated CpG sites become hemi-methylated, as the newly replicated daughter DNA strand is unmethylated. Maintenance methylation recognizes hemi-methylated CpG sites and "copies" the DNA methylation pattern of the parental strand onto the daughter strand. Open and black filled circles indicate unmethylated and methylated CpG dinucleotides, respectively. U, unmethylated DNA; M, methylated DNA; H, hemi-methyalted DNA. The enzymes and their major accessary factors involved at different steps of DNA methylation are indicated.

1.2 DE NOVO DNA METHYLATION DURING MAMMALIAN DEVELOPMENT

After fertilization, both the maternal and paternal genomes undergo global DNA demethylation during preimplantation development. As a result, DNA methylation marks inherited from gametes are largely erased by the blastocyst stage, with the exception of those in ICRs and some retrotransposons. After implantation, a wave of *de novo* methylation occurs in the epiblast to establish the initial pattern of DNA methylation (Figure 1) (17). DNA methylation shows further changes during cellular differentiation, and the patterns are then stably maintained in a lineage-specific manner after successive cell divisions. Similar epigenetic reprogramming events also take place during gametogenesis, including global demethylation in PGCs. Subsequently, a new round of *de novo* DNA methylation takes place in germ cells, which have already passed sex-determination, resulting in different methylation patterns in male and female gametes (sperm and egg) (3, 17). *De novo* methylation is mediated by DNMT3A and DNMT3B. A third member of the DNMT3 family, DNMT3-like (DNMT3L), has no catalytic activity, but is an important regulator of *de novo* methylation (Figure 2) (8).
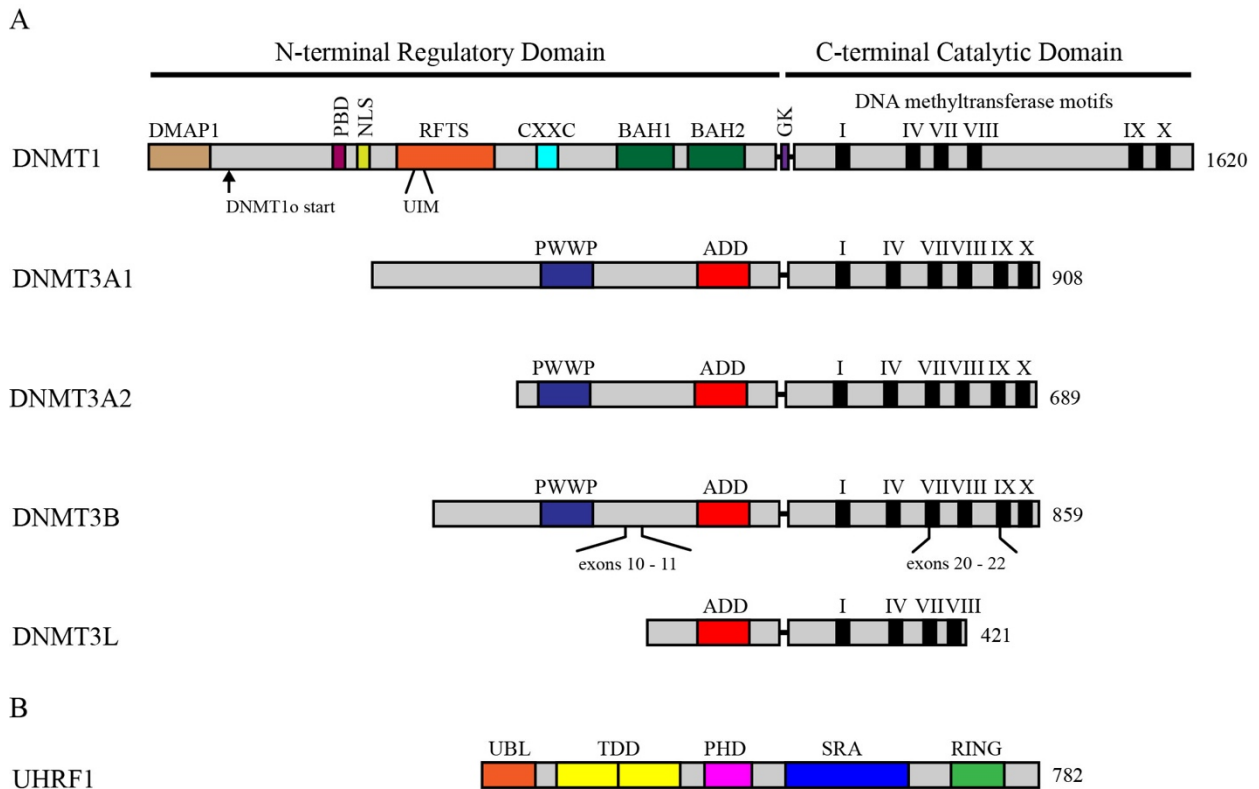
Figure 2: Schematic diagram of major proteins involved in DNA methylation.

A. Protein domain architecture of mouse DNA methyltransferases (DNMTs). The DNMT1 and DNMT3 families of proteins share conserved catalytic motifs (I-X) in their C-terminal catalytic domains. DNMT3L lacks catalytic activity because some essential motifs are missing or mutated. The N-terminal regions of DNMT1 and DNMT3 proteins have little sequence similarity, with distinct domains that contribute to their functional specificities. DMAP1: DNA methyltransferase associated protein 1; PBD: PCNA-binding domain; NLS: nuclear localization sequence; RFTS: replication foci targeting sequence; UIM: ubiquitin interacting motif; CXXC: cysteine-rich motif; BAH: bromo-adjacent homology; GK: glycine/lysine-rich linker; I-X: DNA methyltransferase conserved catalytic motifs; PWWP: proline-tryptophan-tryptophan-proline; ADD: ATRX-DNMT3-DNMT3L. The start site of the DNMT1o isoform is indicated. Locations of the most common alternatively spliced exons (exons 10, 11, 20, 21, 22) in DNMT3B are also indicated. B. Protein domain architecture of mouse UHRF1. UBL: ubiquitin-like domain; TTD: tandem tudor domain; PHD: plant homeodomain; SRA: SET and RING associated; RING: Really Interesting New Gene.

DNMT3A and DNMT3B

The *DNMT3A* and *DNMT3B* genes were initially identified by searching an expressed sequence tag (EST) database using bacterial type II cytosine-5 methyltransferase sequences as queries. Their protein products have a similar structural organization, including a C-terminal catalytic domain that contains sequence motifs characteristic of all DNA methyltransferases (prokaryotic and eukaryotic) and an N-terminal regulatory domain that is distinct from that of DNMT1 (Figure 2) (18). The N-terminal regions of DNMT3A/3B contain a variable region (not conserved between DNMT3A and DNMT3B), followed by two conserved domains implicated in chromatin binding. The PWWP domain, an ~150-residue domain with a conserved proline-tryptophan-tryptophan-proline (PWWP) motif, is necessary for heterochromatin targeting and mediates binding to trimethylated lysine 36 of histone H3 (H3K36me3) marks (19-21). The ADD (ATRX-DNMT3-DNMT3L) domain, composed of two C_4-type zinc fingers (GATA binding protein 1 (GATA1) and plant homeodomain (PHD)-type), interacts with the N-terminal tail of histone H3 with unmodified lysine 4 (H3K4) (22, 23). Recent structural studies revealed that the ADD domain of DNMT3A interacts with its catalytic domain and blocks its DNA-binding affinity, resulting in autoinhibition. Unmodified histone H3 tail (but not H3 tail with H3K4me3) can disrupt the interaction between the ADD and the catalytic domains, leading to DNMT3A activation (24). These findings indicate that DNMT3A and DNMT3B act as both "writers" and "readers" of epigenetic marks and that their activities and specificities are regulated by specific histone modifications.

The conclusion that DNMT3A and DNMT3B function primarily as *de novo* methyltransferases is based on several lines of evidence. First, DNMT3A and DNMT3B expression correlates with *de novo* methylation during development. Specifically, DNMT3A and DNMT3B are highly expressed in early embryos (as well as ESCs) and developing germ cells, and their expression is significantly downregulated in somatic cells and when ESCs are differentiated (18). In ESCs, DNMT3A transcription is mostly driven by an internal promoter, resulting in a shorter isoform known as DNMT3A2, which lacks the N-terminal 219 (mouse) or 223 (human) amino acids of full-length DNMT3A1 (Figure 2). DNMT3A2 expression decreases with ESC differentiation and is replaced by the DNMT3A1 isoform, which is ubiquitously expressed at low levels in most somatic tissues (25). DNMT3B produces multiple

alternatively spliced isoforms (~30 reported to date), many of which lack catalytic activity but may play regulatory roles in DNA methylation (26). In ESCs, the full-length isoform DNMT3B1, a catalytically active form, is the predominant product, and other isoforms, including the inactive DNMT3B6, are also expressed. In most somatic cells, DNMT3B expression is low, usually with both active (e.g. DNMT3B2) and inactive (e.g. DNMT3B3) isoforms (18, 25).

Second, biochemical studies indicate that DNMT3A and DNMT3B behave as *de novo* methyltransferases do. In particular, recombinant DNMT3A and DNMT3B proteins show no preference for hemi-methylated DNA over unmethylated DNA *in vitro*, unlike DNMT1, which preferentially methylates hemi-methylated DNA (18, 27). Furthermore, *in vitro* and *in vivo* target analyses indicate that DNMT3A and DNMT3B could methylate cytosines at non-CpG sites such as CpA and CpT, albeit with lower efficiency compared to CpG methylation (28). Non-CpG methylation, which cannot be maintained during DNA replication, is mediated by *de novo* methyltransferases.

Third, genetic studies provide definitive evidence for the involvement of DNMT3A and DNMT3B in *de novo* DNA methylation. Targeted disruption of both DNMT3A and DNMT3B blocks *de novo* methylation in mouse ESCs (mESCs) and early embryos, but has no effect on the maintenance of methylation at imprinted loci (29). Moreover, DNMT3A and DNMT3B cause *de novo* methylation when overexpressed in mammalian cells or ectopically expressed in transgenic flies or budding yeast (30-33). While DNMT3A and DNMT3B methylate many genomic loci redundantly, they also have preferred and distinct targets. For example, DNMT3A is more efficient than DNMT3B in methylating major satellite repeats at pericentric heterochromatin, whereas DNMT3B preferentially methylates minor satellite repeats in centromeric regions (32). Characterization of *DNMT3A* and *DNMT3B* knockout (KO) mice suggest that these enzymes play distinct roles in developmental processes. *DNMT3A* KO mice develop to term and show no overt defects at birth, but die at ~4 weeks of age. In contrast, disruption of *DNMT3B* leads to embryonic lethality at ~E12.5, with multiple developmental defects. *DNMT3A/3B* double KO (DKO) embryos exhibit more severe defects and die earlier (before E11.5) than *DNMT3B* KO embryos (29). DNA methylation analysis of E9.5 embryos indicate that DNMT3B is largely responsible for methylation of germline-specific genes, pluripotency genes, and many developmental genes and

DNMT3A and DNMT3B redundantly methylate some specific genes such as Brdt, Dpep3, Cytip, and Crygd (34). Conditional gene KO studies indicate that DNMT3A, but not DNMT3B, is essential for *de novo* methylation during gametogenesis, including the establishment of DNA methylation imprints (35). Indeed, immunofluorescence experiments show abundant expression of DNMT3A, but not DNMT3B, in fully grown oocytes (36).

Consistent with their important roles in developmental processes in mice, *DNMT3A* and *DNMT3B* mutations are associated with human diseases (37). Somatic *DNMT3A* mutations occur frequently in acute myeloid leukemia (AML) and other hematologic malignancies (37). Many *DNMT3A* mutations have been identified, with the majority (>50%) of cases affecting Arg882 (R882) in the catalytic domain. Although almost all reported *DNMT3A* mutations in leukemia occur in only one allele, there is evidence that DNMT3A R882 mutant proteins have dominant-negative effects by interacting with wild-type DNMT3A to form functionally deficient complexes (38). *DNMT3A* mutations are also associated with Tatton Brown Rahman syndrome, an overgrowth disorder (37). Hypomorphic *DNMT3B* mutations account for ~50% of cases with ICF (Immunodeficiency, Centromeric instability, and Facial anomalies) syndrome, a rare recessive autosomal disorder characterized by hypomethylation of special genomic regions (most notably classical satellites 2 and 3 repeats) and chromosomal defects in lymphocytes and antibody deficiency, as well as facial dysmorphism, failure to thrive, and mental retardation (37). Several other ICF genes – *ZBTB24* (zinc-finger- and BTB domain-containing 24), *CDCA7* (cell division cycle associated 7), and *HELLS* (helicase, lymphoid-specific) – have also been identified (39, 40). HELLS (also known as LSH), a DNA helicase involved in chromatin remodeling, has been shown to regulate DNA methylation by affecting DNMT3B targeting to chromatin (41). However, little is known about the biological functions of ZBTB24 and CDCA7 and, in particular, their links to DNA methylation.

DNMT3L

DNMT3L was originally identified by sequence database analysis. The protein product contains an ADD domain, but not a PWWP domain, in the N-terminal region. Its C-terminal region shares

sequence homology with the catalytic domains of DNMT3A and DNMT3B, but lacks some sequence motifs essential for catalytic activity, including those required for AdoMet (methyl donor) binding (Figure 2) (8).

Although DNMT3L has no methyltransferase activity, biochemical and genetic evidence suggests that it is an important regulator of *de novo* methylation. DNMT3L interacts with DNMT3A and DNMT3B and significantly enhances their catalytic activity (42). Crystallographic studies reveal that the C-terminal region of DNMT3L directly interacts with the catalytic domain of DNMT3A, and the DNMT3A/3L dimer further dimerizes through DNMT3A-DNMT3A interaction, forming a tetramer with two active sites (43). Biochemical and structural data also indicate that the ADD domain of DNMT3L binds to the N-terminal tail of histone H3, specifically recognizing unmodified lysine 4 (H3K4), suggesting that DNMT3L plays a role in determining the specificity of *de novo* methylation (22). The expression pattern of DNMT3L during development is similar to that of DNMT3A and DNMT3B, with high expression in developing germ cells, early embryos and ESCs and low expression in most somatic tissues (42). *DNMT3L* KO mice are viable and grossly normal, suggesting that zygotic DNMT3L is not essential for development. However, both male and female KO mice fail to reproduce (42, 44). *DNMT3L* KO males have reduced testis size and are sterile, as they are unable to produce mature sperm (azoospermia). The spermatogenesis defect is due to loss of DNA methylation in germ cells, which results in reactivation of retrotransposons, inducing genomic instability, meiotic catastrophe, and ultimately apoptosis (45). On the other hand, *DNMT3L* KO females produce oocytes and are able to conceive, but their embryos die by mid-gestation due to failure to establish DNA methylation imprints in oocytes (42, 44). These studies suggest that DNMT3L is a critical accessory factor for DNMT3A for *de novo* methylation during gametogenesis. Indeed, the phenotype of *DNMT3L* KO mice is almost identical to that of mice with conditional *DNMT3A* deletion in germ cells (35).

The genetic studies described above suggest that DNMT3L is functionally more important for DNMT3A than for DNMT3B *in vivo*, contrary to biochemical evidence that DNMT3L is equally efficient in stimulating the catalytic activities of both DNMT3A and DNMT3B *in vitro*. Little is known about what determines the functional specificity of DNMT3L. In contrast to the strong evidence that

supports the essential role for DNMT3L in *de novo* methylation during gametogenesis, its role in mESCs is poorly understood and controversial. It has been shown that Dnmt3L is required to silence ectopic integrated retroviral DNA in mESCs, and that Dnmt3L deficiency decreases their DNA methylation over time in culture (46, 47). Moreover, Dnmt3L heterochromatin foci localization depends on the presence of Dnmt3a2, but not on Dnmt3a or Dnmt3b, probably due to the specific interaction between Dnmt3L and Dnmt3a2 in mESCs (48). Together, these studies suggest that Dnmt3L is a positive regulator of *de novo* DNA methylation in mESCs. However, a recent report by Neri and colleagues suggests dual roles for Dnmt3L, both as a negative and positive regulator of DNA methylation, depending on genomic regions, in mESCs (49). In **Chapter 3** of this dissertation, I aim to clarify the role of Dnmt3L and elucidate the molecular mechanism involved in *de novo* DNA methylation using Dnmt3L-deficienct mESCs.

1.3 MAINTENANCE DNA METHYLATION DURING MAMMALIAN DEVELOPMENT

Once DNA methylation patterns are established during early embryogenesis, they are maintained in somatic cells in a cell type-specific manner. During each round of DNA replication, DNA becomes hemi-methylated, as only CpGs on the parental strand remain methylated while CpGs on the newly replicated daughter strand are unmethylated. To re-establish the symmetry of CpG methylation and keep the specificity, the maintenance DNA methyltransferase activity recognizes hemi-methylated CpGs and methylates the corresponding CpGs on the daughter strand. Biochemical, cellular, and genetic evidence suggests that DNMT1 is the major maintenance methyltransferase (8). In addition, a multi-domain protein, UHRF1 (ubiquitin-like with PHD and RING finger domains 1), is essential for directing DNMT1 to DNA replication sites (50, 51).

DNMT1

Mouse *DNMT1*, the first mammalian DNA methyltransferase gene identified (52), has several transcription start sites and produces two major protein products. Transcripts initiated within a somatic

cell-specific exon encode the full-length DNMT1 protein that is expressed in somatic cell types, whereas transcripts initiated within an oocyte-specific exon utilize a downstream AUG as the translation initiation codon, resulting in the DNMT1o isoform that lacks the N-terminal 118 amino acids of full-length DNMT1 (Figure 2) (8). Both isoforms are equally functional in maintaining DNA methylation, although DNMT1o is more stable than DNMT1 (53).

DNMT1 has an N-terminal regulatory domain and a C-terminal catalytic domain (Figure 2). While all DNMTs contain highly conserved DNA methyltransferase motifs in their catalytic domains, the DNMT1 and DNMT3 families show little sequence similarity in their regulatory domains. There are several unique domains in the N-terminal region of DNMT1 that confer its functional difference from DNMT3 enzymes. A region at the very N terminus mediates the interaction between DNMT1 and DNA methyltransferase associated protein 1 (DMAP1), a protein implicated in histone acetylation and ATM signaling. The DMAP1-interaction domain is absent in the more stable DNMT1o isoform (53), suggesting that this domain or the interaction between DNMT1 and DMAP1 may be involved in regulating DNMT1 stability. The DMAP1-interaction domain is followed by a proliferating cell nuclear antigen (PCNA) binding domain (PBD), which is required for the interaction with the DNA replication machinery, and a nuclear localization signal (NLS) (8). DNMT1 also contains a motif originally named as the replication foci-targeting sequence (RFTS). Recent evidence indicates that RFTS contains a ubiquitin-interacting motif (UIM) that recognizes ubiquitinated histone H3 at lysine 18 (H3K18ub), a histone modification that serves as a docking site for DNMT1 targeting to replication foci (54). Structural data obtained recently suggests that the RFTS domain also plays an autoinhibitory role in the regulation of DNMT1 activity by binding to the catalytic domain and blocks the catalytic center (55). Additionally, DNMT1 contains a CXXC domain, a cysteine-rich motif that binds unmethylated CpGs, and a pair of bromo-adjacent homology (BAH) domains, BAH1 and BAH2, with their role remaining unknown (8).

Biochemical assays reveal that DNMT1 preferentially methylates hemi-methylated CpG dinucleotides, although it is capable of methylating unmethylated substrates as well (27). *DNMT1* is constitutively expressed in proliferating cells. During S phase, DNMT1 is upregulated and associates

with the replication foci, suggesting that DNMT1-mediated methylation is coupled to DNA replication (56). Genetic inactivation of *DNMT1* in mESCs results in global loss of DNA methylation, but does not affect *de novo* methylation of integrated provirus DNA (57, 58). Taken together, these results suggest that DNMT1 functions primarily as a maintenance methyltransferase.

DNA methylation is dispensable in undifferentiated mESCs, as *DNMT1* KO, *DNMT3A/3B* DKO, and *DNMT1/3A/3B* triple KO (TKO) mESCs show no defects in viability and proliferation, but these cells die when induced to differentiate (29, 32, 58-60). A recent study shows that human ESCs (hESCs) require *DNMT1*, but not *DNMT3A* and *DNMT3B*, for survival (61). mESCs and hESCs represent different pluripotent states, with hESCs resembling the more mature epiblast state, which may explain the sensitivity of hESCs to hypomethylation. DNMT1 is also required for the survival of mouse embryonic fibroblasts (MEFs) and the human colorectal cancer cell HCT116 (62, 63). These findings suggest crucial roles for DNMT1 in cellular differentiation and in the viability of differentiated cells. Consistent with this notion, complete inactivation of *DNMT1* results in the arrest of mouse embryonic development around E9.5, when the embryo is in the process of differentiating into the three germ layers (58). In human, missense *DNMT1* mutations in the RFTS of the N-terminal regulatory domain, which likely result in hypomorphic alleles, have been identified in two related neurodegenerative disorders, hereditary sensory and autonomic neuropathy with dementia and hearing loss type IE (HSAN IE) and autosomal dominant cerebellar ataxia, deafness and narcolepsy (ADCA-DN) (37). While the mechanisms by which these mutations lead to the disease phenotypes are unknown, changes in DNA methylation and gene expression likely play an important role.

UHRF1

UHRF1, also known as nuclear protein of ~95-kDa (NP95 in mouse) and inverted CCAAT box-binding protein (ICBP90 in human), is a multi-domain protein. Genetic studies demonstrate that UHRF1 is essential for maintaining DNA methylation. Similar to the phenotype of DNMT1 deficiency, disruption of *UHRF1* leads to embryonic lethality and global DNA hypomethylation (50, 51, 64). Cellular studies also suggest functional interactions between DNMT1 and UHRF1. Both proteins are

enriched at DNA replication foci during the S phase in normal cells, but DNMT1 fails to localize to these foci in *UHRF1* KO cells (50, 51). These findings indicate that UHRF1 is a critical regulator of maintenance methylation by directing DNMT1 to hemi-methylated CpG sites.

UHRF1 has five conserved domains: a ubiquitin-like domain (UBL), a tandem tudor domain (TTD), a plant homeodomain (PHD), a SET and RING associated (SRA) domain, and a Really Interesting New Gene (RING) domain (Figure 2). The mechanisms by which UHRF1 controls DNMT1 localization and DNA methylation are complex, and all the conserved domains, with the exception of UBL, have been implicated. UHRF1 interacts with DNMT1 and likely mediates its recruitment to chromatin, as the TTD and PHD of UHRF1 act in combination to recognize the trimethylated lysine 9 of histone H3 (H3K9me3) mark, and additionally, the PHD finger binds to unmodified arginine 2 of histone H3 (H3R2) (65, 66). The SRA domain preferentially binds hemi-methylated DNA and likely plays an important role in loading DNMT1 onto newly synthesized DNA substrates (50, 51). The RING finger domain has E3 ubiquitin ligase activity. UHRF1 has been shown to ubiquitinate histone H3 at lysine 18 (H3K18ub) in mammalian cells (54) and at lysine 23 (H3K23ub) using the cell-free system of *Xenopus* egg extracts (67). Both studies show that UHRF1-dependent histone H3 ubiquitination is required for maintenance DNA methylation, suggesting that the H3 ubiquitination mark(s) provides a binding site(s) for DNMT1 (54, 67). Together, these studies indicate that a complex crosstalk between different histone modifications takes place in the regulation of maintenance DNA methylation.

The UHRF1 PHD finger specifically recognizes and binds unmodified, but not H3R2-methylated, N-terminal tail of H3, which suggests that H3R2 methylation might play a role in the regulation of maintenance DNA methylation. The role of arginine methylation in the regulation of DNA methylation is largely unknown. This site is the major substrate of PRMT6, an arginine methyltransferase responsible for asymmetric dimethylation of H3R2 (H3R2me2a) (68-70). In **Chapter 4** of this dissertation, I investigated whether H3R2me2a plays a role in the regulation of maintenance of DNA methylation by impairing the recruitment of UHRF1 to chromatin.

1.4 DNA METHYLATION IN CANCER

Cancer is a disease of genetic, as well as epigenetic, abnormalities. The latter is supported by a great outburst of knowledge in chromatin regulation and its importance to aberrant gene expression in cancer. This led to the concept of "the cancer epigenome", which encompasses countless alterations that are not caused by changes in the DNA sequence (i.e. mutations), and rather consist of covalent modifications to DNA, RNA and chromatin proteins, including histones and non-histone substrates. The epigenetics field is rapidly evolving, in part due to technological advances such as next-generation sequencing techniques, which have been widely applied to identifying the structure and organization of chromatin, including DNA methylation, and with this has transform our understanding of normal development and cancer (71).

In normal somatic cells, CGIs associated with gene promoters are usually devoid of DNA methylation, except in special genomic regions, such as genes located in the inactive X chromosome, inactive imprinted genes and germ-cell specific genes (5, 72). In contrast, alterations of DNA methylation patterns are frequently detected in cancer, as tumor cells present loci-specific CpG hypermethylation or global DNA hypomethylation (4) (Figure 3).
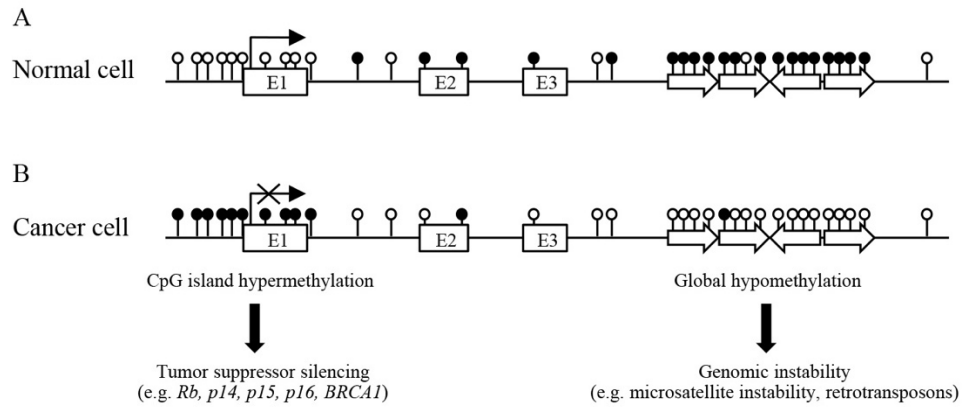
Figure 3: Alterations of DNA methylation patterns in cancer cells.

A. Typical DNA methylation patterns in normal cells, including high levels of methylation in repetitive sequences and gene bodies and lack of methylation in CGIs associated with promoter regions. B. Alterations in DNA methylation patterns frequently observed in cancer cells, including global hypomethylation and abnormal promoter hypermethylation, which contributes to genomic instability and tumor suppressor silencing, respectively. Open and black filled circles indicate unmethylated and methylated CpG dinucleotides, respectively. White boxes labeled with E indicate exons. Black horizontal thin arrow in Exon 1 indicates transcription, which is blocked in B as indicated by the cross. White horizontal thick arrow indicates repetitive sequences.

CpG island DNA hypermethylation

Specific gain of DNA methylation (i.e. DNA hypermethylation) in the CGIs of promoters, which is associated with transcriptional silencing, is among the most investigated epigenetic alteration in cancer, as multiple studies showed that most cancer types have high numbers of genes with hypermethylation, although the numbers vary in a patient-specific manner (4, 71-74). In certain cases, the affected CGIs control the expression of tumor suppressor genes, and therefore, DNA hypermethylation acts as an alternative mechanism for gene inactivation leading to tumor suppressor silencing and loss of function, favoring malignant transformation (4, 72). For example, promoters of tumor suppressor genes involved in pathways that control cell cycle progression, like *Rb, CDKN2A* and *p73*, or that regulate DNA repair, such as *MLH1, BRCA1, MGMT* and *WRN* are found hypermethylated in different tumor types. Additionally, key genes in cancer biology that are silenced by CGI promoter hypermethylation include *VHL, ER, RARβ2, APC, DKK1, GATA4, GATA5, ID4, DAPK*, and *HOXA9* (71, 72). Moreover, DNA hypermethylation has also been implicated in loss of monoallelic expression of imprinted genes (i.e. loss of imprinting) at the *H19* locus, leading to the activation of the insulin-like growth factor 2 (*IGF2*) and initiation of tumor development and progression of colon cancer (75-77).

Genomic studies in tumors revealed that cancer-specific mutations are frequently detected in genes that regulate DNA methylation, which may lead to DNA hypermethylation. For instance, mutations in *TET2*, *IDH1* (isocitrate dehydrogenase 1) and *IDH2* are found in different types of leukemias and brain cancer, including gliomas and other types of brain tumors, although they are mutually exclusive (4, 78, 79). TETs are enzymes that catalyze the oxidation of 5mC into 5hmC in a reaction dependent on the cofactor α-ketoglutarate (80). Patients with mutations in TET2 are commonly heterozygous and result in loss of function (79). Similarly, mutations of IDH1 and IDH2 impair their normal enzymatic functions and result in the abnormal conversion of α-ketoglutarate into 2-hydroxyglutarate, a metabolite that inhibits the catalytic activity of TET2 (78). As a consequence, inhibition of the TET pathway by different mechanisms results in DNA hypermethylation due to the accumulation of 5mC at specific regions. Interestingly, recent studies indicate that under normal

conditions, TET proteins reside at the CGIs of active promoters and enhancers and contribute to the maintenance of their hypomethylated state (81-84), suggesting that upon TET inhibition, these locations might become rapidly hypermethylated. Consistent with this hypothesis, *IDH1* mutations in gliomas correlate with CpG island DNA hypermethylation phenotype (CIMP), a concept used to classify different types of cancer (71).

Alternative mechanisms have also been proposed to explain DNA hypermethylation in cancer. One of them is strictly linked to bivalent promoters, which are those promoters that simultaneously contain the H3K4me3 active and H3K27me3 repressive marks and are associated with poised transcriptional state of genes required for ESC differentiation (85). Based on correlations observed in studies in colon cancer, it has been proposed that an epigenetic switch occurs at these promoters during tumorigenesis, where expanded population of stem cells undergo replacement of temporal H3K27me3 repression by a more stable silencing mediated by H3K9me3 and DNA methylation (71). However, these mechanisms require further characterization and validation.

Global DNA hypomethylation

Global loss of DNA methylation (i.e. DNA hypomethylation) was initially observed in human tumors compared to healthy tissue over 30 years ago (86), with *H-ras* and *K-ras* as the first examples of hypomethylated oncogenes in human cancer samples (87). Early studies comparing primary tumors, normal tissues and metastatic samples isolated from the same patients showed that DNA hypomethylation was progressive and correlates with metastatic capacity (86, 88). Subsequent studies revealed that global DNA hypomethylation is a common feature of cancer cells, where it has been associated to activation of oncogenes, derepression of retrotransposons and genomic instability (72). Several lines of evidence suggest the involvement of DNA hypomethylation as an early oncogenic event that leads to transformation and tumorigenesis. Firstly, treatment with DNA methylation inhibitors has been shown to convert low-metastatic cancer cell lines to high-metastatic versions, and animals fed with methyl-deficient diet result in global DNA hypomethylation and formation of liver tumors (89). Secondly, mice carrying a hypomorphic *Dnmt1* allele show genome-wide hypomethylation and develop

T cell lymphomas with a high frequency of chromosome 15 trisomy (90). Induction of DNA hypomethylation in $Nf1^{+/-} p53^{+/-}$ mice also promotes tumor development by increasing the rate of loss of heterozygosity, as a result of chromosomal instability due to hypomethylated centromeric and pericentric regions (91). Finally, DNA hypomethylation results in loss of imprinting, which may also contribute to tumorigenesis (92).

Recent correlation analysis between genomic and gene expression profiling in tumors samples has shed some light into the molecular aspects of this dysregulation, and a few mechanisms have been proposed to explain how DNA hypomethylation occurs in cancer cells. For instance, loss-of-function mutations in *DNMT3A* are commonly found in hematological malignancies in adults and are implicated in the development of leukemias (93). Experiments using mouse hematopoietic stem cells (HSCs) revealed that *Dnmt3a* deletion results in increased self-renewal capacity instead of differentiation, leading to the expansion of this population, suggesting a potential early mechanism for malignant transformation. Moreover, *Dnmt3a* deficient HSCs show substantial global DNA hypomethylation (94). Mice recipients of *Dnmt3a*-null HSCs develop multiple myeloid and lymphoid leukemias, recapitulating human malignancies containing *DNMT3A* mutations (95-97). In contrast, *Dnmt3a* heterozygous HSCs are prone to develop only myeloid leukemias (97), suggesting that *DNMT3A* behave as a haploinsufficient tumor suppressor gene in myeloid leukemias (93). In clear agreement with this hypothesis, 65% of the *DNMT3A* mutations found in acute myeloid leukemia (AML) are heterozygous missense mutations altering the residue R882 at the C-terminal catalytic domain of the protein (93). It has also been shown that the R882H mutation (R878H in mouse) has a dominant-negative effect on the wild-type DNMT3A protein, as the mutant DNMT3A can dimerize with wild-type protein (38), but the R882H mutation disrupts the formation of tetramers, which have significantly higher activity. Therefore, in the absence of functional tetramers, mutant DNMT3A dimers with impaired catalytic activity lead to global DNA hypomethylation observed in AML patients with R882 mutation (93, 97-99).

Furthermore, alterations of the maintenance methylation machinery have also been proposed to drive the loss of DNA methylation in cancer. In fact, upregulation of UHRF1 expression has been detected in different types of cancer and correlates with global DNA hypomethylation and tumorigenesis

19

(100-105). As mentioned previously, UHRF1 has E3 ubiquitin ligase activity through its RING domain and it has been shown to ubiquitinate DNMT1, DNMT3A and UHRF1 itself, leading to their degradation and consequently DNA hypomethylation in cancer cells (104, 106-108). Moreover, genetic experiments using zebrafish as a model demonstrate that overexpression of human UHRF1 in hepatocytes leads to mislocalization of DNMT1 in the nucleus and to the reduction of its protein levels due to proteosomal degradation, which results in global DNA hypomethylation and hepatocellular carcinoma (109). Importantly, DNA hypomethylation by UHRF1 overexpression causes p53-dependent senescence, and tumorigenesis only occurs after senescence is bypassed (109). In addition to the described mechanisms, many molecular defects that lead to DNA hypomethylation likely alter the function of the DNMT1-UHRF1 complex. For example, DNMT1 phosphorylation by AKT and/or PKC has been shown to abrogate the formation of the DNMT1-UHRF1 complex in cancer cells (110). Importantly, global DNA hypomethylation through disruption of the DNMT1-UHRF1 complex has also been reported to cause transformation in non-tumorigenic cells and development of tumors in mice (110, 111).

Despite the progress, the mechanisms underlying DNA hypomethylation in cancer are largely unclear. In **Chapter 4**, I identified a novel epigenetic mechanism that negatively regulates DNA methylation by inhibiting the recruitment of the DNMT1-UHRF1 complex to chromatin, which is dysregulated in cancer leading to global DNA hypomethylation.

1.5 CROSSTALK BETWEEN DNA METHYLATION AND ARGININE METHYLATION

The current knowledge about the activity and function of DNA methylation indicates that DNMTs do not have an evident specificity for target DNA sequences rather than CpG dinucleotides, which implies that the chromatin structure drives their correct targeting within the genome. Multiple lines of evidence support the interaction between DNA methylation and different epigenetic mechanisms. Indeed, the regulation of DNA methylation by histone modifications, particularly histone lysine methylation, is well documented. For example, H3K9me3 generally correlates with DNA

methylation, whereas H3K4me3 inhibits DNA methylation. However, much less is known about the crosstalk between DNA methylation and arginine methylation.

Arginine methylation

Modification of proteins by methylation of arginine residues is an important post-translational modification (PTM) that is involved in several biological process, including transcription regulation, DNA damage response, mRNA splicing and translation and modulation of different signaling pathways (112, 113). Recent proteomic studies indicate that arginine methylation is as common as other more studied PTMs, such as phosphorylation and ubiquitination, as it regulates the function of multiple cytoplasmic and nuclear targets, including histone and non-histone substrates (114). The major role for arginine methylation is the regulation of the binding by interacting proteins as, in contrast to other PTMs, methylation does not change the charge of arginine residues and instead creates a docking site for "readers", such as tudor domain-containing proteins (115). Consistent with its importance in multiple biological processes, dysregulation of arginine methylation is associated with multiple human diseases, including cancer (112, 113).

Arginine methylation is carried out by the protein arginine methyltransferase (PRMT) family, which consists of nine members that fall into three categories. Type I (PRMT1, PRMT2, PRMT3, PRMT4, PRMT6, and PRMT8) and type II (PRMT5 and PRMT9) enzymes catalyze the formation of ω-N^G-monomethylarginine (MMA) as an intermediate before generating ω-N^G,N^G-asymmetric dimethylarginine (aDMA) and ω-N^G,N'^G-symmetric dimethylarginine (sDMA), respectively, whereas the sole type III enzyme PRMT7 catalyzes only the formation of MMA (112, 116). Overexpression and mutation of PRMTs are frequently observed in cancer (Table 1).

Table 1: The human protein arginine methyltransferase family in cancer.

Enzyme	Other name	Modification	Cancer implication	References
PRMT1		ADMA	up to 5.5% overexpression (uterine, bladder, pancreas, breast, lung); up to 2.8% mutated (cervical, uterine, melanoma); other alterations (MLL)	(113, 117-121)
PRMT2		ADMA	up to 3.5% overexpression (ovarian, bladder, AML, sarcoma, breast); up to 2.8% mutated (colon, uterine, lung); up to 1.4% deletion (stomach, colon)	(113, 117, 118)
PRMT3		ADMA	up to 3.8% mutated (uterine, lung, stomach, colon, melanoma); up to 2% overexpression (bladder, stomach, sarcoma); regulated by DAL-1/4 tumor suppresor gene	(113, 117, 118, 122)
PRMT4	CARM1	ADMA	up to 11.3% overexpression (uterin, ovarian, ACyC, ACC, sarcoma, glioma, colon, breast, prostate, lung, liver); up to 2% mutated (uterine, bladder, lung, head and neck, melanoma)	(113, 117, 118, 120, 123-125)
PRMT5		SDMA	up to 4% mutated (uterine, head and neck, bladder, colon, melanoma, leukemia, lymphoma); up to 3% overexpression (ovarian, lung, sarcoma, glioma, breast, liver, glioblastoma)	(113, 117, 118, 126-128)
PRMT6		ADMA	up to 3.6% overexpression (prostate, melanoma, sarcoma, bladder, lung); up to 1.6% mutated (lung, uterine, liver)	(113, 117, 118, 121, 129)
PRMT7		MMA	up to 6.6% deletion (prostate, ovarian, breast, AML); up to 4% mutated (bladder, lung, uterine, stomach, melanoma, colon)	(113, 117, 118, 130)
PRMT8		ADMA	up to 11% overexpression (ovarian, uterine, bladder, glioma, sarcoma, head and neck, breast, glioblastoma); up to 7% mutated (lung, melanoma, colon)	(117, 118)
PRMT9		SDMA	up to 3.8% mutated (uterine, stomach, colon, bladder, lung, esophageal, liver, glioblastoma); up to 3.6% overexpression (uterine, prostate, ovarian, sarcoma, breast, lung)	(117, 118)

MMA, monomethylarginine; ADMA, asymmetric dimethylarginine; SDMA, symmetric dimethylarginine; AML, acute myeloid leukemia; ACyC, Adenoid Cystic Carcinoma; ACC, Adrenocortical Carcinoma. Adapted from the original version (131).

Regulation of DNA methylation by histone arginine methylation

A few studies explored the crosstalk between histone arginine methylation and DNA methylation. Zhao and colleagues reported that the protein arginine methyltransferase 5 (PRMT5) mediates histone H4R3 symmetric dimethylation (H4R3me2s), which serves as a binding site for DNMT3A through its ADD domain (132). However, this mechanism remains to be confirmed, as other studies reported evidence that does not support it (23, 133). Using biochemical approaches, Otani and colleagues were unable to reproduce the binding between the ADD domain of DNMT3A and H4R3me2s peptide (23). Likewise, another study using ChIP-seq analysis reported that, despite the fact that H4R3me2s was found in CpG-rich promoters, downregulation of this modification with PRMT5 knockdown did not alter DNA methylation (133). Therefore, the role of PRMT5 in *de novo* DNA methylation is still controversial.

A recent study identified the protein methyltransferase-like 23 (Mettl23) as a new arginine methyltransferase that catalyzes asymmetric dimethylation of histone H3 at arginine 17 (H3R17me2a) in maternal histone H3.3, and that this modification is required for the incorporation of H3.3 in the *de novo* assembly of paternal nucleosomes in zygotes (134). Notably, this study further showed that H3R17me2a and Mettl23 are required for the recruitment of TET3 to the male pronucleus, which results in the active demethylation of the paternal genome to facilitate efficient reprograming (134).

Together, these studies suggest possible roles for histone arginine methylation in the regulation of DNA methylation in mammals. Nevertheless, the functional and mechanistic links between arginine methylation and DNA methylation remain largely unknown.

PRMT6 and its role in cancer

PRMT6 is the primary enzyme responsible for catalyzing methylation of histone H3 at arginine 2 (H3R2) to generate the aDMA form (H3R2me2a), which is an epigenetic modification associated with transcriptional repression (68-70, 135). In fact, multiple studies have shown that PRMT6-dependent H3R2me2a is mutually exclusive with H3K4me3, and that it inhibits the recruitment of the MLL complex to the N-terminal tail of histone H3 (68-70, 135). Therefore, under normal conditions, PRMT6

acts a transcriptional repressor by inhibiting H3K4me3 and the recruitment of coactivator complexes to gene promoters.

Importantly, PRMT6 is frequently overexpressed in cancer cells and has been implicated in different tumorigenic functions involving the methylation of histones and non-histones targets (113). Among these, it has been shown that PRMT6 functions both as a transcription co-activator of oncogenic pathways and as a repressor of tumor suppressor genes (113, 136). Studies using cancer cell lines have reported that PRMT6 binds to the hormone receptors ER, AR, GR, and PR-B and facilitates their transcriptional functions (137, 138). It also binds to PELP1, a proto-oncogene in breast cancer that function as an ER co-activator (139). On the other hand, PRMT6 serve as a transcriptional repressor of cyclin-dependent kinase (CDK) inhibitors p21 and p16 in osteosarcoma and breast cancer cells, thus acting as an oncogene that promotes cell proliferation and prevents senescence (140-142). Moreover, p21 and p16 are also methylation substrates of PRMT6, which results in inhibition of their cell cycle regulatory functions (143, 144). PRMT6 also represses transcription of the tumor suppressor gene *Trp53*, and PRMT6 overexpression results in lower levels of p53 (145). In addition to regulating transcription, PRMT6 oncogenic functions also involve the regulation of alternative splicing (136, 138, 139).

The evidence described above indicates that PRMT6 has important roles in cancer development and progression. However, it is not clear whether PRMT6 activity is involved in the early steps of malignant transformation, or it is required for tumor progression. Moreover, the significance of the transcriptional functions of PRMT6 in tumorigenesis remains to be determined. In **Chapter 4** of this dissertation, I discovered a new role for PRMT6 as a negative regulator of maintenance DNA methylation and showed that upregulation of PRMT6 contributes to global loss of DNA methylation in cancer cells.

Part of this chapter is based upon: Veland, N., Hardikar, S., Zhong, Y., Gayatri, S., Dan, J., Strahl, B.D., Rothbart, S.B., Bedford, M.T. and Chen, T. (2017) The Arginine Methyltransferase PRMT6 Regulates DNA Methylation and Contributes to Global DNA Hypomethylation in Cancer. Cell Rep, 21, 3390-3397.

Used with permission of Elsevier.

Mice: The *Dnmt3L* null allele, generated by Hata et al. (42), was maintained on the 129 background. Zygotic *Dnmt3L* knock-out (*Dnmt3L* zKO) and *Dnmt3L* wild-type zygotes and blastocysts were obtained from inter-crosses between heterozygous (*Dnmt3L$^{+/-}$*) mice, whereas maternal *Dnmt3L* KO (*Dnmt3L* mKO) and double maternal and zygotic knock-out (*Dnmt3L* mzKO) zygotes and blastocysts were obtained from crosses between homozygous (*Dnmt3L$^{-/-}$*) females and *Dnmt3L$^{+/-}$* males.

Dnmt1$^{2lox/+}$ knock-in chimera mice were backcrossed into C57BL/6J strain background. Then, this mice were crossed with Zp3-Cre transgenic mice to activate the *3XFlag-Dnmt1* knock-in allele, and their female progeny was crossed with wild-type C57BL/6J mice to generate *Dnmt1$^{Flag/+}$* mice. Heterozygous intercrossed provide homozygous (*Dnmt1$^{Flag/Flag}$*) knock-in mice.

All procedures were performed according with the National Institutes of Health Guide for the Care and Use of Laboratory animals, with Institutional Care and Use Committee-approved protocols at The University of Texas MD Anderson Cancer Center (MDACC).

Isolation of zygotes and derivation of mouse embryonic stem cells from blastocysts: For isolation of zygotes and blastocysts, *Dnmt3L* heterozygous or homozygous null mice were superovulated and mated with wild-type males. Zygotes were collected from the oviducts at E0.5 and released into a hyaluronidase/M2 medium (Millipore) for dissociation. Derivation of mouse embryonic stem cells (mESCs) was performed essentially as previously described (146). Briefly, mice were euthanized at E3.5 and blastocysts were flushed out of the uterus using M2 medium (Sigma). Then, blastocysts were placed on a feeder cell layer of irradiated mouse embryonic fibroblasts in Serum-free ES medium with 2i, which consist of a 1:1 mixture of Dulbecco modified Eagle medium-F12/N-2 (DMEM-F12 supplemented with N-2, Invitrogen) and Neurobasal/B27 (Neurobasal supplemented with B27, Invitrogen) with 0.5% (vol/vol) penicillin- streptomycin (Invitrogen), 1 mM GlutaMAX (Invitrogen), 0.5 mM sodium pyruvate (Invitrogen), 0.1 mM non-essential amino acids (Invitrogen), 0.1 mM 2-mercaptoethanol (Sigma), 10^3 IU of LIF (Millipore), 1 μM PD0325901 and 3 μM CHIR99021 (S1036 and S2924, respectively, Selleckchem). After blastocyst hatching, the inner cell mass clumps were picked under the microscope and plated into 96-well plate with feeder cells. The newly established mESCs lines were expanded,

adapted to DMEM FBS mESC medium [DMEM supplemented with 15% fetal bovine serum (Invitrogen), 0.5% (vol/vol) penicillin- streptomycin (Invitrogen), 0.1 mM non-essential amino acids (Invitrogen), 0.1 mM 2-mercaptoethanol (Sigma), 10^3 IU of LIF (Millipore)] and then either frozen or used for further analysis. The cells were then normally grown on gelatin-coated petri dishes without feeder cells.

Cell culture and manipulations: For the generation of stable mESCs clones expressing Myc-Dnmt3L, Myc-Dnmt3L F297D, Myc-Dnmt3a1, Myc-Dnmt3a2, Myc-PRMT6 or Myc-PRMT6 E155Q, cells transfected with the corresponding plasmids were seeded at low density on dishes coated with feeder cells, selected with 6 μg/mL of Blasticidin S HCl (Gibco) for 7-10 days, and colonies were picked. Transfection was performed using Lipofectamine 2000 (Invitrogen). Experiments where cells were treated with cycloheximide (C4859, Sigma) were carried out at 100 μg/mL. MG-132 (M7449, Sigma) was used at 10 μM, while Bafilomycin A1 (B1793, Sigma) at 125nM. For all treatments, DMSO was used as control. Human cancer cell lines were cultured according to instructions of American Type Culture Collection. For PRMT6 knockdown, MCF7 cells transfected with shRNA plasmids were selected and maintained in medium containing 1 μg/ml of puromycin (Gibco). To inhibit PRMT6 activity, cells were treated with 10 μM of MS023 (147)

Antibodies: For Western blots: anti-Myc (Sigma M4439; 1:5,000), anti-Flag (Sigma F3165; 1:5,000), anti-DNMT1 (Cell Signaling 5032; 1:1,000), anti-DNMT1 N-terminal (Novus Biologicals 100-264; 1:1,000), anti-Dnmt3a (Abcam 13888; 1:2,000), anti-Dnmt3b (Abcam 13604; 1:2,000), anti-Dnmt3L (Cell Signaling 12309; 1:1,1000), anti-p53 (Cell Signaling 2524; 1:1,1000), anti-LC3B (Cell Signaling 2775; 1:1,1000), anti-UHRF1 (Cell Signaling 12387; 1:1,000), anti-PRMT6 (Bethyl A300-929A; 1:2,000), anti-PCNA (Cell Signaling 2586; 1:8,000), anti-Usp7 (Cell Signaling 4833; 1:1,000), anti-HP1α (Thermo Fisher PA5-17441; 1:2,000), anti-α-tubulin (Cell Signaling 2144; 1:2,000), anti-β-actin (Sigma A5441; 1:5,000), anti-H3R2me2a (Millipore 05-808; 1:2,000), anti-H3K4me3 (Active

27

Motif 39159; 1:2,000), anti-H3K9me3 (Millipore 07-442; 1:2,000), anti-H3 (Cell Signaling 9715; 1:8,000), anti-Oct4 (Abcam 19857; 1: 1,000), anti-Sox2 (Abcam 97959; 1: 1,000), anti-Nanog (Abcam 80892; 1: 1,000), and anti-pan asymmetric dimethyl arginine (Rme2a) (Cell Signaling 13522; 1:2,000). For immunofluorescence (IF): anti-Oct4 (Abcam 19857; 1:300), anti-Sox2 (Abcam 97959; 1:300), and anti-Nanog (Abcam 80892; 1:300). For chromatin immunoprecipitation (ChIP): anti-UHRF1 (Diagenode C15410258), anti-H3R2me2a (Abcam 175007), and anti-H3 (Abcam 1791). For DNA methylation: anti-5mC (Millipore MABE146; 1:1,000 for dot blot, 1:2,000 for IF, 2 μg for MeDIP), anti-5hmC (Active Motif 39769; dilution for 1:1,000 for IF).

Plasmid constructs: The vectors containing Myc-tagged *Dnmt3L*, *Dnmt3a1* and *Dnmt3a2* were generated by PCR amplification of the corresponding mouse cDNA from mESCs, using the primers indicated in Table 2. Amplified PCR products were cloned into the *pCAG-IRESblast* vector (32). The *pCAG-Myc-PRMT6-IRESblast* vector was generated by sub-cloning Myc-tagged human *PRMT6* cDNA into the *pCAG-IRESblast* vector. The *Dnmt3L F297D* and *PRMT6 E155Q* point mutations were introduced by PCR-based mutagenesis (see Table 2 for primer sequences). The *pGIPZ (tGFP-IRES-Puro)* control and *PRMT6* shRNA plasmids were obtained from GE Healthcare Dharmacon. Untagged *Dnmt1* with alternative translation start site were cloned into the of *pCAG-HA-IRESblast* (148), using *Spe*I and *Not*I to remove the HA tag.

Southern blot analysis: DNA methylation levels at major satellite repeats, minor satellite repeats and intracisternal A-particle (IAP) retrotransposons were analyzed by Southern blot after digestion of 2 μg of genomic DNA with the methylation-sensitive restriction enzymes *Mae*II (Roche) or *Hpa*II (New England Biolabs) as previously reported (32). Briefly, digested DNA was separated by agarose gel electrophoresis and then transferred onto nylon membranes. For hybridization, the membranes were incubated with biotin-labeled probes (500 ng for major and minor satellites and 2.5 μg for IAP)

overnight at 42°C. Signal detection was performed using North2South Chemiluminescent Hybridization and Detection Kit (Thermo Scientific). See Table 2 probes sequences.

Bisulfite sequencing: For bisulfite sequencing, genomic DNA was treated for bisulfite conversion using the EZ DNA Methylation kit (Zymo) and then used as template to amplify the 45S *rDNA* promoter with Taq DNA polymerase (Qiagen) using primers described in the Table 2. PCR conditions consisted of 40 cycles of denaturation at 94°C for 30 sec, annealing for 30 sec at 60°C and extension at 72°C for 30 sec. Following a final extension at 72°C for 5 min, PCR products were gel purified and directly ligated into pMiniT 2.0 using the NEB PCR cloning kit (New England Biolabs) according to the manufacturer's protocol. Qiagen Miniprep DNA was sequenced and results were analyzed with QUMA web-based quantification tool for methylation analysis (http://quma.cdb.riken.jp) (149). Percentages of methylated CpG sites were calculated from individual clones.

RNA isolation and RT-qPCR: Total RNA was from ESCs using the Tryzol (Invitrogen) according to the manufacturer's instruction, followed by reverse transcription (RT) using ProtoScript First Strand cDNA Synthesis kit (New England Biolabs) to generate cDNA. Relative quantification of mRNA levels was carried out by RT-qPCR using iTaq Universal SYBR Green Supermix (Bio-Rad) in the ABI 7900 Real-Time PCR system (Applied Biosystems) using primers provided in Table 2.

Chromatin immunoprecipitation (ChIP): ChIP experiments were performed according to the Abcam X-ChIP protocol with modifications. Briefly, a total of 1 x 10^7 of mESC or MCF7 cells were cross-linked with 1% formaldehyde for 10 min at room temperature. Fixation reaction was quenched with 125 mM glycine for 5 min. Cells were washed twice with 1X PBS, lysed in SDS buffer [50 mM Tris-HCl (pH 8.1), 10 mM EDTA, 1% SDS and 1X protease inhibitor cocktail (Thermo Scientific)] and sonicated for 50 cycles (30 sec ON, 30 sec OFF) using Bioruptor Plus (Diagenode) to obtain chromatin fragments of 300-500 bp. Sonicated chromatin was centrifuged at 14.5 K rpms for 10 min at 4°C, and the supernatant was 5-fold diluted with dilution buffer [16.7 mM Tris-HCl (pH 8.1), 167 mM NaCl, 1.2

mM EDTA, 1% Triton X-100, 0.1% SDS and 1X protease inhibitor cocktail (Thermo Scientific)]. Each sample was pre-cleared with 30 μl of Dynabeads M-280 sheep anti-rabbit IgG (Thermo Scientific) for 2 hours at 4°C, followed by incubation with specific antibodies overnight at 4°C. Samples were incubated with Dynabeads M-280 sheep anti-rabbit IgG for 1 hour at 4°C, followed by high stringency washes. Beads were eluted twice at room temperature in elution buffer (100 mM NaHCO$_3$, 1% SDS), and reverse cross-linking was performed overnight at 65°C with 200 mM NaCl. Samples were then incubated with RNase A at 37°C for 30 min followed by incubation with proteinase K at 55°C for 2 hours, and DNA was purified using the QIAquick PCR Purification kit (Qiagen). Enrichment at selected loci was detected by qPCR (see Table 2 for primer sequences) using iTaq Universal SYBR Green Supermix (Bio-Rad). Ct values were normalized against 1% input.

Methylated-DNA immunoprecipitation (MeDIP): MeDIP was performed as described previously (150). RNA-free genomic DNA was sonicated for 12 cycles (30 sec ON, 30 sec OFF) using Bioruptor Plus (Diagenode) to obtain DNA fragments of 300-1000 bp. After sonication, a portion of DNA was separated as input control. Each DNA sample was incubated with 2 μg of anti-5mC mouse antibody (Millipore) in MeDIP buffer [10 mM Na-Phosphate (pH 7.0), 140 mM NaCl, and 0.05% Triton X-100] for 3 hours at 4°C. Then, the samples were incubated with 30 μl of Dynabeads M-280 sheep anti-mouse IgG (Thermo Scientific) for 1 hour at 4°C, followed by three washes with MeDIP buffer. Beads were incubated with proteinase K overnight at 55°C in constant agitation, and DNA from MeDIP and input were purified using the QIAquick PCR Purification kit (Qiagen). Methylated DNA enrichment at selected loci was detected by qPCR (see Table 2 for primer sequences) using iTaq Universal SYBR Green Supermix (Bio-Rad). MeDIP Ct values were normalized against 1% input.

Table 2: Primers and Oligonucleotides used in this dissertation.

Assay	Target	Sequence (5' to 3')	Reference
Cloning	mDnmt3L (F)	AGGGAATTCCCGGGAGACACCTTCTTC	This study
Cloning	mDnmt3L (R)	TCAGAATTCTAAAGAGGAAGTGAGTTTTG	This study
Cloning	mDnmt3L F297D (F)*	CTGGTACATGgaCCAGTTCCACCGGATCCT	This study
Cloning	mDnmt3L F297D (R)*	GTGGAACTGGtcCATGTACCAGCCGGGACA	This study
Cloning	mDnmt3a1 (F)	CCTGAATTCGCCCTCCAGCGGCCCCGG	This study
Cloning	mDnmt3a2 (F)	TGCGAATTCGAATGCTGTGGAAGAGAAC	This study
Cloning	mDnmt3a (R)	CACGAATTCAGTTTGCCCCCATGTCCCT	This study
Cloning	mDnmt1 Δ1-607 (F)	CAAACTAGTCCACCATGGGTGCTACCAAGGAGAAG	This study
Cloning	mDnmt1 Δ1-650 (F)	ACAACTAGTCCACCATGAAGCGCCGCCGCTGTG	This study
Cloning	mDnmt1 Δ1-675 (F)	AGGACTAGTCCACCATGGTGAAGTTTGGTGGCAC	This study
Cloning	mDnmt1 Δ1-714 (F)	ATGACTAGTCCACCATGCCATCACCCAAAAAGCTG	This study
Cloning	mDnmt1 (R)	CATGCGGCCGCTAGTCCTTGGTAGCAGCCTCCTC	This study
Cloning	hPRMT6 (F)	GTAGAATTCGTCGCAGCCCAAGAAAAG	This study
Cloning	hPRMT6 E155Q (R)^	CCCATCCACTgGCTCACGATGGCATCCAC	This study
Cloning	hPRMT6 E155Q (F)^	CATCGTGAGCcAGTGGATGGGCTACGGAC	This study
Cloning	hPRMT6 (R)	GCTGAATTCAGTCCTCCATGGCAAAGTC	This study
Southern Blot	Major satellite repeat probe	TTAGAAATGTCCACTGTAGGACGTGGAATATGGCAAG	This study
Southern Blot	Minor satellite repeat probe	ACTGAAAAACACATTCGTTGGAAACGGGATTTGTAGAACAGTGTATATCAATGAGTTACAATGAG	This study
Southern Blot	IAP probe	GATGTAAGAATAAAGCTTTGCCGCAGAAGATTCTGGTCTG	This study
RT-qPCR	mDnmt3a (F)	GTTCTACCGCCTCCTGCATGATGC	This study
RT-qPCR	mDnmt3a (R)	GCCCTGTGTGCAGCAGACACTTC	This study
RT-qPCR	mDnmt3a1 (F)	GAGGCCTGGCCGGAAGCGCAAGCAC	This study
RT-qPCR	mDnmt3a1 (R)	GTCTCAGTTCCCTCTCCTTCAGCTG	This study
RT-qPCR	mDnmt3a2 (F)	GAGGGGCTGCACCTGGCCTTATG	This study
RT-qPCR	mDnmt3a2 (R)	AGCATCCCCTCCTACTGGCTCAG	This study
RT-qPCR	mDnmt3b (F)	GGAGGCCCATTAGAGTCCTGTCTC	This study
RT-qPCR	mDnmt3b (R)	CACCAATCACCAAGTCGAACGGGC	This study
RT-qPCR	mGAPDH (F)	AAGAGAGGCCCTATCCCAACTC	This study
RT-qPCR	mGAPDH (R)	TTGTGGGTGCAGCGAACTTTATTG	This study
RT-qPCR	mDnmt1 exon 4 (F)	TGGGCGGCCGCCATGGCAGACTCAAATAGATC	This study
RT-qPCR	mDnmt1 exon 6 (R)	GACGGATCCTAGTTCCCCTCTTCCGACTCTTC	This study
RT-qPCR	mDnmt1 exon 5 (F)	GAGAACCACCAGGCAGAC	This study
RT-qPCR	mDnmt1 exon 8 (R)	GTTCACATGGCTCTTCCGGACCCAG	This study
RT-qPCR	mDnmt1 exon 25 (F)	CTGTTCCTGGTGGGCGAGTGC	This study
RT-qPCR	mDnmt1 exon 26 (R)	GTAAGTCTTGCCATCCTCAG	This study
RT-qPCR	mDnmt1 exon 33 (F)	CATGGTGCTGAAGCTCACACTGCG	This study
RT-qPCR	mDnmt1 exon 34 (R)	CAGCCAAGATGATGGCCCTCCTTC	This study

ChIP-PCR	IAP (F)	CAAATAATCTGCGCATATGCCGA	(151)
ChIP-PCR	IAP (R)	GACCAGAATCTTCTGCGGCAA	(151)
ChIP-PCR	MSR (F)	TGATATACACTGTTCTACAAATCCCGTTTC	(152)
ChIP-PCR	MSR (R)	ATCAATGAGTTACAATGAGAAACATGGAAA	(152)
Bisulfite sequencing	Human *45S rDNA* promoter (F)	GTGTGTTTTGGGGTTGATTAGAG	This study
Bisulfite sequencing	Human *45S rDNA* promoter (R)	TCCGAAAACCCAACCTCTCCAAC	This study
ChIP-PCR & MeDIP-PCR	Human *HOXA2* promoter (F)	CGGTCCCCATACGGCTGTA	(69)
ChIP-PCR & MeDIP-PCR	Human *HOXA2* promoter (R)	CAGGCTGGGAATGGTCTGCT	(69)
ChIP-PCR & MeDIP-PCR	Human *CDKN1A* promoter (F)	TGCGTTCACAGGTGTTTCTG	(142)
ChIP-PCR & MeDIP-PCR	Human *CDKN1A* promoter (R)	CACATCCCGACTCTCGTCAC	(142)
ChIP-PCR & MeDIP-PCR	Human *GREB1C* promoter (F)	TTGTTGTAGCTCTGGGAGCA	(139)
ChIP-PCR & MeDIP-PCR	Human *GREB1C* promoter (R)	CAACCAGCCAAGAGGCTAAG	(139)

F, forward; R, reverse. Continuous underlined sequences indicate *Eco*RI site, spaced underlined sequences indicate *Spe*I site and double underlined sequence indicate *Not*I site used for cloning. *Primers used together with mDnmt3L (F) and mDnmt3L (R) to generate mDnmt3L F297D mutation (altered nucleotide in lower case). ^Primers used together with hPRMT6 (F) and hPRMT6 (R) to generate hPRMT6 E155Q mutation (altered nucleotide in lower case).

Immunofluorescence (IF) analysis: Zygotes were fixed in 3.7% paraformaldehyde in PBS for 30 min at room temperature and permeabilized for 15 min in 0.1% Triton X-100 in PBS at room temperature. For 5mC and 5hmC staining, conditions were essentially as previously described (153). Images were taken with Olympus IX51 inverted fluorescence microscope at 60X magnification. For mESCs IF, cells were cultured on gelatin-coated glass coverslips, fixed with 3.7% paraformaldehyde and then permeabilized with 0.1% Triton X-100. After blocking with 1% bovine serum albumin and 10% donkey serum (Sigma), cells were incubated with primary antibodies at 4 °C overnight. Finally, cells were labeled with Alexa Fluor conjugated secondary antibodies and nuclear stained with DAPI. For 5mC IF, the cells were incubated with 2N HCl at room temperature for 40 min and then neutralized with 0.1 M sodium borate (pH 9.0) for 15 min before the blocking step. Images were taken with Olympus IX51 inverted fluorescence microscope at 40X magnification.

Isolation of small intestinal crypts: The duodenum section of small intestine from 6-8 weeks old mice was removed and flushed with 1X PBS. Intestinal crypts were isolated essentially as previously described (154). Briefly, intestine pieces were incubated in constant agitation at 4°C with cold crypt chelating buffer (2 mM EDTA in 1X DPBS) and then epithelium was disassociated from basement membrane by gently agitation in cold dissociation buffer (54.9 mM D-sorbitol, 43.4 mM sucrose in 1X DPBS). Cell suspension was then filtered with 70 μm cell strainer to remove villi. Crypts were purified by centrifugation 150 g for 10 min in dissociation buffer and purity was verified under microscope. Sufficient amount of intestinal crypts was obtained from one mouse preparation to be divided in three separate tubes to extract protein, DNA and RNA.

Immunohistochemistry on tissue sections: Duodenum was initially processed as describe above for crypt isolation. Duodenum pieces were formalin fixed and embedded in paraffin and longitudinal 4 μm sections were prepared. After dewaxing and re-hydration, antigen retrieval was achieved in citrate buffer pH 6.0 at 96°C for 20 min. Immunohistochemistry was performed using standard procedures.

Western blot and immunoprecipitation: For regular analysis of whole cell extracts by western blots, mESCs were lysed in cold RIPA buffer [50 mM Tris-HCl (pH 8.8), 150 mM NaCl, 1% Triton X-100, 0.5% Sodium Deoxycholate, 0.1% SDS, 1 mM EDTA, 3 mM $MgCl_2$, and 1X protease inhibitor cocktail (Thermo Scientific 1861279)]. Immunoprecipitation was performed in lysis buffer [20mM Tris-HCl (pH 7.9), 150 mM NaCl, 0.1% NP-40, 1 mM EDTA, 3 mM $MgCl_2$, 10% Glycerol, 1X protease inhibitor cocktail (Thermo Scientific 1861279)] using Protein A/G UltraLink Resin beads (Thermo Fisher 53133). Western blots were performed according to standard procedures. Quantification of westerns blots by densitometry was carried out using NIH Image J software (155).

Mass spectrometry proteomic analysis: After Flag immunoprecipitation using M2 beads (Sigma), protein samples were eluted from beads using 3X Flag peptide (Sigma) under constant agitation for 1 hour at 4°C, and sample volume was concentrated by centrifugation using columns. Then, samples were separated by PAGE, gels were Coomasie stained and protein bands were excised from the gel. After in-gel trypsin digestion, samples were run on the Dionex LC and Orbitrap Fusion for LC-MS/MS with a 30 minute run time. Peptide mapping analysis was performed using Scaffold version 4.8 (Proteome Software).

Dot blot analyses: RNA-free genomic DNA was denatured in 0.4 N NaOH, 10 mM EDTA at 95°C for 10 min before spotting various amounts (0.25-1 μg) on nylon membranes using a Bio-Dot apparatus (Bio-Rad). The membranes were then incubated with anti-5mC antibody (1:1,000) overnight at 4°C. Enhanced chemiluminescence signal detection was carried out in the ImageQuant LAS 4000 imaging system (GE Healthcare Life Sciences) with a CCD camera using chemiluminescence filter and automatic exposure settings. To verify equal loading of different DNA samples, membranes were stained with SYTOX Green nuclei acid stain (Invitrogen S7020; 1:10,000) for 10 minutes at room temperature. Fluorescent green signal was detected using the Cy2 filter and automatic exposure settings. Dot blot quantification was carried out by densitometry using the NIH Image J software (155).

Reduced Representation Bisulfite Sequencing (RRBS) and Bioinformatics Analyses:
Experiment: RRBS libraries were made from 1 μg of genomic DNA, according to published protocols (156, 157). In brief, the genomic DNA was digested with *Msp*I, end-repaired and A-tailed, and Illumina-compatible cytosine-methylated adaptors (Bio Scientific) were ligated to the enzyme-digested DNA. Size-selected fragments representing sequences from 40 to 170 bp were bisulfite-converted using the EZ DNA Methylation-Gold Kit (Zymo Research) and library preparation was done by PCR amplification. The libraries were sequenced using 36 bases single-read protocol on Illumina HiSeq 2000 instrument. Three biological replicates were prepared for each condition (one Dnmt3L KO sample was discarded in the later analysis due to the quality problem). 12-35 million reads were generated per sample. **Mapping:** The adapters were removed from the 3' ends of the reads by Trim Galore! version 0.4.1 (https://www.bioinformatics. babraham.ac.uk/projects/trim_galore/) and cutadapt version 1.9.1 (158). Then, the reads were mapped to mouse genome mm10 by the bisulfite converted read mapper Bismark version 0.16.1 (159) and Bowtie version 1.1.2 (160). 95-96% reads were mapped to the mouse genome, with 65-68% uniquely mapped. 8-23 million uniquely mapped reads were used in the final analysis.

Methylation Calling: The methylation percentages for the CpG sites were calculated by the bismark_methylation_extractor script from Bismark and an in-house Perl script. **Differential Methylation:** the differential methylation between conditions was statistically assessed by R/Bioconductor package methylKit version 0.9.5 (161) at site resolution and 500 bp tile resolution. Only the CpG sites with read coverage ≥ 20 or the tiles that have at least three CpG sites with coverage ≥ 10 in all the samples were qualified for the test. The CpG sites or 500 bp tiles with qvalue ≤ 0.01 and methylation difference $\geq 25\%$ were called as differentially methylated. **Gene Annotation:** each site or tile was assigned to a location relative to the nearby genes: upstream (-5k to -1k from TSS), promoter (-1k to +0.5k from TSS), exon, intron, TES (-0.5k to +1k from TES), downstream (+1k to +5k from TES) and intergenic. In the case a site/tile could be assigned to multiple locations relative to different genes, one location was chosen following this order: promoter > upstream > TES > downstream > exon > intron > intergenic. The genes are the RefSeq genes (162) downloaded from UCSC genome browser (http://genome.ucsc.edu/) on July 17, 2015.

MeDIP-seq: The raw reads and the peaks called for shGFP and shDnmt3L were obtained from Neri et al. (49), data accessible at NCBI Gene Expression Omnibus (GEO) database, accession GSE44642. The reads were mapped to mouse genome mm9 by Bowtie version 1.1.2 (160), with at most 1 mismatch allowed, and only the reads that were mapped to unique position were retained. To avoid PCR bias, for multiple reads that were mapped to the same genomic position, only one copy was retained for further analysis. The overlapping or book-ended peaks of shGFP and shDnmt3L were merged, and the number of reads in each of the merged peaks was counted for shGFP and shDnmt3L separately. The differential methylation between shGFP and shDnmt3L was statistically assessed by binomial test on each merged peak, with the hypothesized probability of success determined by the total number of reads mapped to the two samples or the number of reads mapped to all the merged peaks in the two samples. The pvalues were corrected to false discovery rate (FDR) by Benjamini & Hochberg (BH) method. The peaks with FDR≤ 0.05 and fold change ≥ 2 were called as differentially methylated between shGFP and shDnmt3L.

Histone acid extraction: Cells were lysed in cold mild lysis buffer containing 10 mM Tris-HCl (pH 7.5), 150 mM NaCl, 5 mM EDTA, 1% Triton X-100, 1X protease inhibitor cocktail (Thermo Scientific 1861279), and 1X phosphatase inhibitor cocktail (Thermo Scientific 78427). Lysates were then sonicated in Bioruptor Plus (Diagenode) for 10 cycles (5 sec ON, 30 sec OFF), centrifuged at 14,500 rpm in 4°C for 15 minutes, and final pellets were washed once in mild lysis buffer. To extract histones, pellets were resuspended in 0.8 N HCl, sonicated for 20 cycles (15 sec ON, 30 sec OFF) and incubated at 4°C for 1 hour in constant agitation. Soluble histones were clarified by centrifugation at 13,000 rpm in 4°C for 10 min and neutralized with 2 M Tris-HCl (pH 8.0).

Nuclear fractionation: Nuclear fractionation in mESCs was carried out as described previously (163) with the following modification: buffer B was replaced by buffer N [15 mM Tris-HCl (pH 7.5), 200 mM NaCl, 60 mM KCl, 5 mM $MgCl_2$, 1 mM $CaCl_2$, 0.3% NP-40, and 1X protease inhibitor cocktail (Thermo Scientific)]. For experiments in MCF7, NaCl in buffer N was adjusted to 100 mM.

Quantification of nuclear fractionation data: Areas from Western blots were measured by densitometry using the NIH Image J software (155). UHRF1 areas were normalized against PCNA or HP1α areas for soluble or chromatin fractions, respectively. UHRF1 percentages of soluble and chromatin fractions from three independent nuclear fractionation experiments were plotted using GraphPad Prism 6.

In vitro arginine methylation assay: *In vitro* arginine methylation reactions were performed in 30 μl of 1X PBS (pH 7.4) using beads bound to immunoprecipitated Myc-PRMT6 (wild type or E155Q mutant) expressed in mESC stable clones as enzyme source, with 1 μg of recombinant histone H3 (New England Biolabs) as substrate and 0.42 μM S-adenosyl-l-[methyl-^{3}H] methionine (Perkin Elmer) as methyl donor. Reactions were incubated at 30°C for 1 hour, resolved on SDS-PAGE, transferred to PVDF membrane, treated with En^{3}Hance (Perkin Elmer) and exposed to film at −80°C for 4 days.

Quantification of 5mC content by liquid chromatography-tandem mass spectrometry (LC-MS/MS): Quantification of the total levels of 5mC in cancer cells was performed by LC-MS/MS essentially as previously described (63). Briefly, 1 μg of RNA-free genomic DNA was denatured at 95°C for 5 min and then cooled on ice, followed by addition of 0.1 vol of 0.1 M ammonium acetate (pH 5.3) and incubation with 2 units of nuclease P$_1$ (Sigma) for 2 hours at 45°C. Then, 0.1 vol of 1 M ammonium bicarbonate and 0.002 units of phosphodiesterase I (Sigma) were added to the mixture and it was further incubated for 2 hours at 37°C. Finally, 0.5 units of alkaline phosphatase (Sigma) were added and then incubated for 1 additional hour at 37°C. At this point, the solution was ready for immediately analysis by LC-MS/MS. The total deoxycytosine (dC) and 5-methyl-deoxycytosine (5mdC) levels were quantified with an Agilent 1100 liquid chromatograph coupled to a Waters Quattro Premier mass spectrometer. The 5mC total level is expressed as a percentage of the total cytosine pool according to peak areas.

TCGA Bioinformatic and statistical analysis: PRMT6 expression data and DNA methylation data for breast cancer, lung adenocarcinoma and colorectal adenocarcinoma samples in The Cancer Genome Atlas (TCGA) database were analyzed. The mean DNA methylation levels of samples with the highest (top 20%) and lowest (bottom 20%) PRMT6 expression were compared either without taking UHRF1 expression into consideration or by first dividing the samples into UHRF1-high (upper 70%) and UHRF1-low (lower 30%) groups. Wilcoxon rank sum non-parametric test with two-tailed P values was used to determine the significance of differences. Paired t test with a two-tailed p value was used for dot blot data analysis and quantification graphs were generated using GraphPad Prism 6.

CHAPTER 3: Regulation of de novo DNA methylation by DNMT3L in mESCs

3.1 INTRODUCTION

DNA methylation – the addition of a methyl group to the C-5 position of cytosine, forming 5-methylcytosine (5mC) – occurs predominantly in the context of CpG dinucleotides. DNA methylation is essential for mammalian development and plays crucial roles in various biological processes, including regulation of gene expression, maintenance of genomic stability, genomic imprinting, and X chromosome inactivation (3, 164). Aberrant DNA methylation patterns and genetic alterations of the DNA methylation machinery are associated with numerous human diseases, including developmental disorders and cancer (37, 165).

DNA methylation is catalyzed by two families of DNA methyltransferases (Dnmts). Dnmt1 is the major enzyme responsible for maintenance methylation by "copying" the CpG methylation pattern from the parental strand onto the daughter strand during DNA replication. Dnmt3a and Dnmt3b function primarily as *de novo* methyltransferases for the establishment of DNA methylation patterns (3). *Dnmt3c*, a *Dnmt3b* duplicated gene present exclusively in rodents, had been previously annotated as a pseudogene (formerly known as *Gm14490*) but was recently shown to be expressed and play a specific role of *de novo* methylation at retrotransposons during spermatogenesis (9). The Dnmt1 and Dnmt3 enzymes share characteristic catalytic motifs in their C-terminal catalytic domains but have different N-terminal regulatory regions that largely confer functional specificities of these enzymes. For example, Dnmt3a and Dnmt3b contain two chromatin-binding domains in their N-terminal regions that likely play important roles in targeting these enzymes to specific genomic regions – the PWWP domain, which is required for heterochromatin targeting and mediates binding to trimethylated lysine 36 of histone H3 (H3K36me3) marks, and the ADD domain, which interacts with the N-terminal tail of histone H3 with unmethylated lysine 4 (H3K4me0) (20, 21, 23).

Dnmt3L (Dnmt3-like), another member of the Dnmt3 family, shows sequence homology with the Dnmt3 enzymes but lacks the very N terminus, including the PWWP domain, and some essential catalytic motifs in the C-terminal region, including the PC dipeptide at the active site and the sequence motif involved in binding of the methyl donor S-adenosyl-L-methioinine. Therefore, Dnmt3L has no

enzymatic activity (42, 166). However, Dnmt3L has been shown to interact with Dnmt3a and Dnmt3b and significantly stimulates their catalytic activities *in vitro* (166-168). Crystallography evidence reveals that the C-terminal domain of Dnmt3L directly interacts with the C-terminal domain of Dnmt3a to form a heterodimer, which further dimerizes through Dnmt3a-Dnmt3a interaction, resulting in the formation of a tetramer with two Dnmt3a active sites at the center (43, 169, 170). Biochemical and structural data also indicate that Dnmt3L, via its ADD domain, specifically recognizes H3K4me0 and may contribute to the specificity of *de novo* DNA methylation (22). Additionally, the expression pattern of Dnmt3L during development strongly correlates with active *de novo* methylation, with high expression in developing germ cells and early embryos, as well as embryonic stem cells (ESCs), and little to no expression in most somatic tissues. These findings suggest that Dnmt3L is a key regulator of *de novo* DNA methylation.

Genetic evidence supports the role of Dnmt3L as a regulator of *de novo* methylation. *Dnmt3L* knock-out (KO) mice are viable and grossly normal, indicating that zygotic Dnmt3L is not essential for embryonic development (42, 44). However, both male and female *Dnmt3L* KO mice cannot reproduce. Male *Dnmt3L* KO mice show activation of retrotransposons in spermatogonia and spermatocytes, due to failure in *de novo* methylation, resulting in severe spermatogenesis defects (42, 45). Female *Dnmt3L* KO mice also fail to establish DNA methylation, including maternal genomic imprints, in oocytes. They are able to conceive but show maternal-effect lethality – embryos die around mid-gestation – largely due to abnormal expression of imprinted genes (42, 44). The phenotype of *Dnmt3L* KO mice is almost identical to that of mice with conditional *Dnmt3a* deletion in germ cells (35), but different from the embryonic lethal phenotype of *Dnmt3b* KO mice (29).

Although it is generally assumed that Dnmt3L acts as a catalytic cofactor of Dnmt3a and Dnmt3b, the mechanism by which Dnmt3L regulates DNA methylation is not well understood. Also, given that Dnmt3L is capable of interacting with and enhancing the activities of both Dnmt3a and Dnmt3b, it has been puzzling that Dnmt3L is essential for Dnmt3a-mediated *de novo* methylation during gametogenesis but is dispensable for Dnmt3b-mediated *de novo* methylation during embryogenesis. Moreover, contrary to biochemical and genetic evidence that Dnmt3L functions as a positive regulator of DNA methylation, Neri et al. recently showed that Dnmt3L antagonizes DNA methylation in many

promoter regions and favors DNA methylation at gene bodies in mouse ESCs (mESCs) (49). To gain further insights into the role and specificity of Dnmt3L in DNA methylation, we derived mESC lines deficient for maternal Dnmt3L (Dnmt3L mKO), zygotic Dnmt3L (Dnmt3L zKO), or both maternal and zygotic Dnmt3L (Dnmt3L mzKO) from blastocyst-stage embryos. We confirmed that Dnmt3L is a positive regulator of DNA methylation and found no evidence that it antagonizes DNA methylation in mESCs. While Dnmt3L mKO, as expected, mainly affected DNA methylation at imprinting control regions (ICRs), Dnmt3L zKO cell lines showed moderate loss of methylation at many genomic regions that are normally methylated by Dnmt3a. Interestingly, our results showed that Dnmt3L is critical for maintaining the stability of Dnmt3a2, the predominant Dnmt3a protein product in ESCs, and that this new role contributes to the effect of Dnmt3L on Dnmt3a-dependent DNA methylation.

3.2 RESULTS

Dnmt3L deficiency in mESCs results in hypomethylation at specific heterochromatin regions.

Genetic studies in mouse have demonstrated that maternal Dnmt3L is critical for DNA methylation in oocytes, including the establishment of genomic imprints, whereas zygotic Dnmt3L is not essential for mammalian development (42, 44, 171, 172). To better understand the roles of maternal and zygotic Dnmt3L in DNA methylation, we derived mESC lines deficient for maternal Dnmt3L (*Dnmt3L* mKO), zygotic Dnmt3L (*Dnmt3L* zKO, referred to as *Dnmt3L* KO for simplicity), or both maternal and zygotic Dnmt3L (*Dnmt3L* mzKO), as well as wild-type (WT, *Dnmt3L*$^{+/+}$) mESC lines, from blastocyst-stage embryos by breeding *Dnmt3L*-null homozygous (*Dnmt3L*$^{-/-}$) or heterozygous (*Dnmt3L*$^{+/-}$) females with *Dnmt3L*$^{+/-}$ males (Figure 4A). Because female mESCs become hypomethylated in culture due to upregulation of DUSP9, an X-linked MAPK phosphatase (173), we used male mESC lines (determined by PCR amplification of Y-linked *Sry*) for subsequent experiments. The mESC lines were genotyped by PCR and verified by Western blot analysis (Figure 4B).

Mammalian genomes contain different types of repetitive elements, including interspersed transposable elements and tandemly arrayed satellite repeats, that consist of thousands of copies. For instance, in the mouse genome, the major satellite (with a 234-bp unit), located at pericentromeric heterochromatin, reaches up to 6 Mbp, and the minor satellite (with a 120-bp unit), located at centromeric heterochromatin, goes up to 600,000 bp (174, 175). In general, repetitive sequences are heavily methylated, and their methylation status can serve as an indicator of global DNA methylation. To assess the impact of Dnmt3L deficiency on DNA methylation, we first compared the different mESC lines for DNA methylation at the major and minor satellite repeats. Southern blot analysis of genomic DNA digested with methylation-sensitive restriction enzymes revealed that *Dnmt3L* KO and *Dnmt3L* mzKO mESC lines show substantial loss of methylation at the major satellite repeats, but no obvious changes in methylation at the minor satellite repeats (Figure 4C-D). Consistent with previous reports that maternal Dnmt3L is required for global DNA methylation in oocytes (171, 172), the female pronuclei of zygotes derived from Dnmt3L-deficient oocytes were severely hypomethylated (Figure 5). However, *Dnmt3L* mKO mESC lines showed normal levels of DNA methylation at the major satellite repeats (Figure 4C), indicating that *de novo* methylation in *Dnmt3L* mKO embryos largely restored the methylation levels (except special regions such as imprinted loci, see below) during the preimplantation stage or during mESC derivation and culture. Taken together, our results show that zygotic Dnmt3L is required for methylation at specific genomic regions in mESCs.
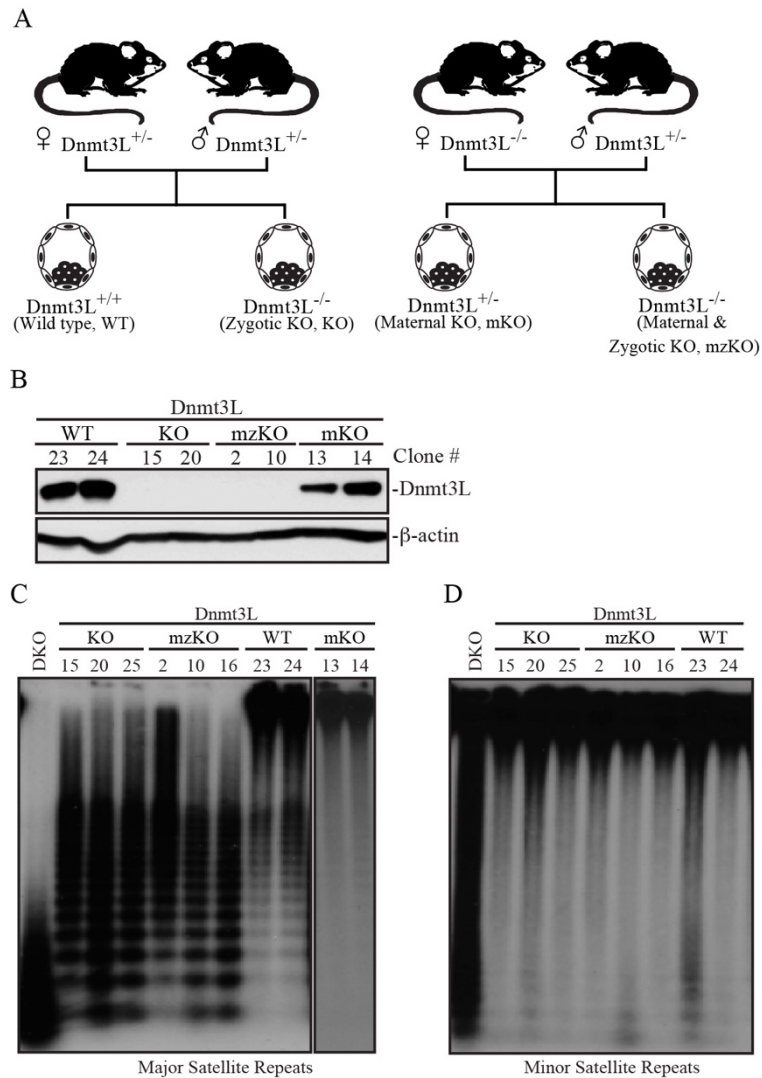
Figure 4: Dnmt3L deficiency in mESCs results in hypomethylation at specific heterochromatin regions.
A. Mice matting strategies to generate mESCs with different genotypes. B. Confirmation of Dnmt3L expression by western blot in different types of Dnmt3L-deficient mESCs, the numbers indicate the clone numbers analyzed in each genotype. C and D. Southern blot analysis using methylation-sensitive restriction enzymes on Dnmt3L-deficient mESCs clones using *Mae*II and major satellite repeat probe (C) or *Hpa*II and minor satellite repeat probe (D). DKO, *Dnmt3a* and *Dnmt3b* double knock-out mESC clone.
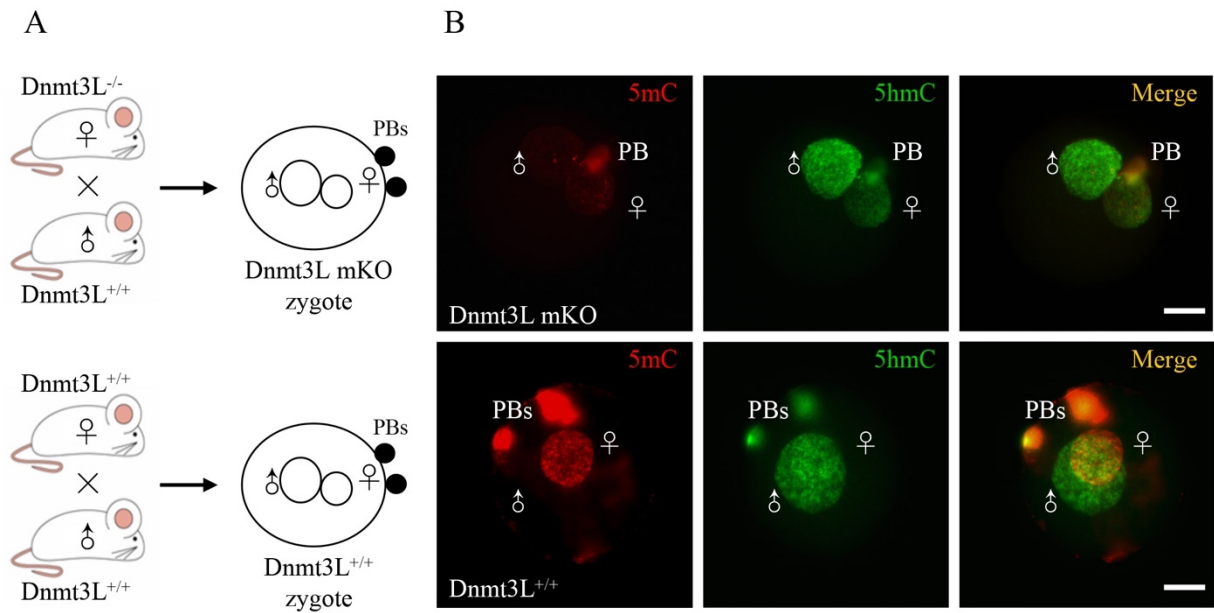
Figure 5: Zygotes derived from Dnmt3L-deficient female mice show global DNA hypomethylation.

A. Mice mating strategies to get Dnmt3L mKO and WT zygotes. PBs, polar bodies. B. 5-methylcytosine (5mC) and 5-hydroxymethylcytosine (5hmC) staining of the zygotes. The male and female pronuclei, as well as PBs, are indicated. Scale bars, 50 μM. This data was generated by Hongbo Zhao and is used with her permission.

Dnmt3L is a positive regulator of DNA methylation in mESCs.

Contrary to biochemical, genetic and genomic evidence that Dnmt3L is a positive regulator of DNA methylation (22, 42, 44, 166, 167, 171, 172, 176), Neri et al. recently reported that Dnmt3L regulates DNA methylation both positively and negatively, depending on genomic regions (49). To further understand the function and specificity of Dnmt3L in DNA methylation, we compared the DNA methylation profiles of the different mESC lines (*Dnmt3L$^{+/+}$*, *Dnmt3L* KO, *Dnmt3L* mKO, and *Dnmt3L* mzKO) by reduced representation bisulfite sequencing (RRBS) analysis (177-179). For each genotype, three independent cell lines (biological replicates) were included. For each cell line, we generated ~12-34 million high quality RRBS reads, of which ~8-23 million were uniquely aligned, containing ~454-679 thousand CpG sites with >=20-fold coverage. Reads from all cell lines showed near complete (>99%) bisulfite conversion of cytosines in non-CpG contexts. In agreement with previous work (178), the methylation levels of CpG sites displayed a bimodal distribution in WT mESCs, as well as in the *Dnmt3L*-mutant cell lines, with most sites being either largely unmethylated (<20% methylation) or largely methylated (>80% methylation) (Figure 6A-C, Figure 7).

We compared the *Dnmt3L*-mutant cell lines with WT mESCs for the methylation levels of CpG sites, with the criteria for differentially methylated CpG sites being methylation difference >= 25% and q value <= 0.01. While the vast majority (>99%) of CpG sites showed no significant changes in methylation in all the *Dnmt3L*-mutant mESC lines, small factions of CpG sites were obviously hypomethylated (Figure 2A-C). The patterns of the hypomethylated sites in *Dnmt3L* mKO and *Dnmt3L* KO mESCs were different. In *Dnmt3L* mKO cells, fewer but more severely hypomethylated CpG sites (387 sites, ~0.07% of all sites analyzed) were observed, most of which were within the imprinting control regions (ICRs) of maternally imprinted genes (as expected, these sites were methylated at ~50% in WT cells) (Figure 6A, D). In *Dnmt3L* KO cells, a larger number of CpG sites were hypomethylated, mostly with moderate loss of methylation (4,281 sites, ~0.78% of all sites analyzed), and none of them were in ICRs (Figure 6B). *Dnmt3L* mzKO cells exhibited combined changes of both *Dnmt3L* mKO and *Dnmt3L* KO cells, with severe loss of methylation in CpG sites in ICRs and moderate hypomethylation of many sites in other regions (Figure 6C). Our results indicate that maternal Dnmt3L is essential for the

46

establishment of genomic imprints, consistent with previous studies (42, 44), but does not play a major role in the methylation of other regions in mESCs, whereas zygotic Dnmt3L affects the methylation of a subset of genomic regions, not including imprinted loci, in mESCs.

In sharp contrast to the report by Neri et al. that nearly 30% of the differentially methylated regions (DMRs) show gain of methylation in shRNA-mediated Dnmt3L knockdown (KD) mESCs (49), we observed only negligible numbers of hypermethylated CpG sites in the *Dnmt3L*-mutant mESC lines (Figure 6A-C). Given that Neri et al. showed that Dnmt3L deficiency-induced gain of methylation occurs mostly at promoter regions, it is unlikely that the discrepancy was due to the restricted coverage of RRBS, as RRBS preferentially captures CG-rich sequences including many CpG islands and promoters. Indeed, our RRBS data had good coverage of promoter regions (Figure 8D). We specifically searched our RRBS data for the five hypermethylated promoter regions (*Rhox5, Hoxa1, Cpne8, Enox1*, and *Zxda*) that Neri and colleagues verified by bisulfite sequencing (49) and found that 9 CpG sites in the Enox1 promoter had sufficient coverage (>=20) in both WT and *Dnmt3L* KO samples. However, our data showed that almost all the sites had lower levels of methylation in *Dnmt3L* KO cells than in WT cells (Figure 9).

Chr #	Start location (bp)	End location (bp)	ICR name
Chr2	152686755	152687275	MCTS2
Chr2	174295707	174300981	NESPAS
Chr2	174326930	174329007	GNAS-EXON1A
Chr6	30736488	30739335	MEST
Chr7	6727576	6732116	ZIM2
Chr7	143295155	143295492	KCNQ1OT1
Chr10	13091144	13091527	ZAC1
Chr11	12025482	12026332	GRB10
Chr11	22971842	22972319	U2AF1-RS1
Chr15	72806335	72811649	PEG13

Figure 6: Dnmt3L is a positive regulator of DNA methylation in mESCs.

Scatter plots showing distribution of genome-wide DNA methylation by RRBS analysis using site resolution in Dnmt3L mKO (A), KO (B) or mzKO (C) compared to WT mESCs. Hypomethylated sites are shown in green, hypermethylated sites in blue, while sites located in ICRs in red. Unchanged sites are in grey. D. ICRs with common hypomethylated sites for Dnmt3L mKO and mzKO mESCs. E. Hypomethylated site overlap between Dnmt3L KO and mzKO mESCs. Panels D and E were prepared with data generated by Sally Gaddis and were used with her permission. Scatter plots panels (A-C) were generated by Sally Gaddis and were used with her permission.
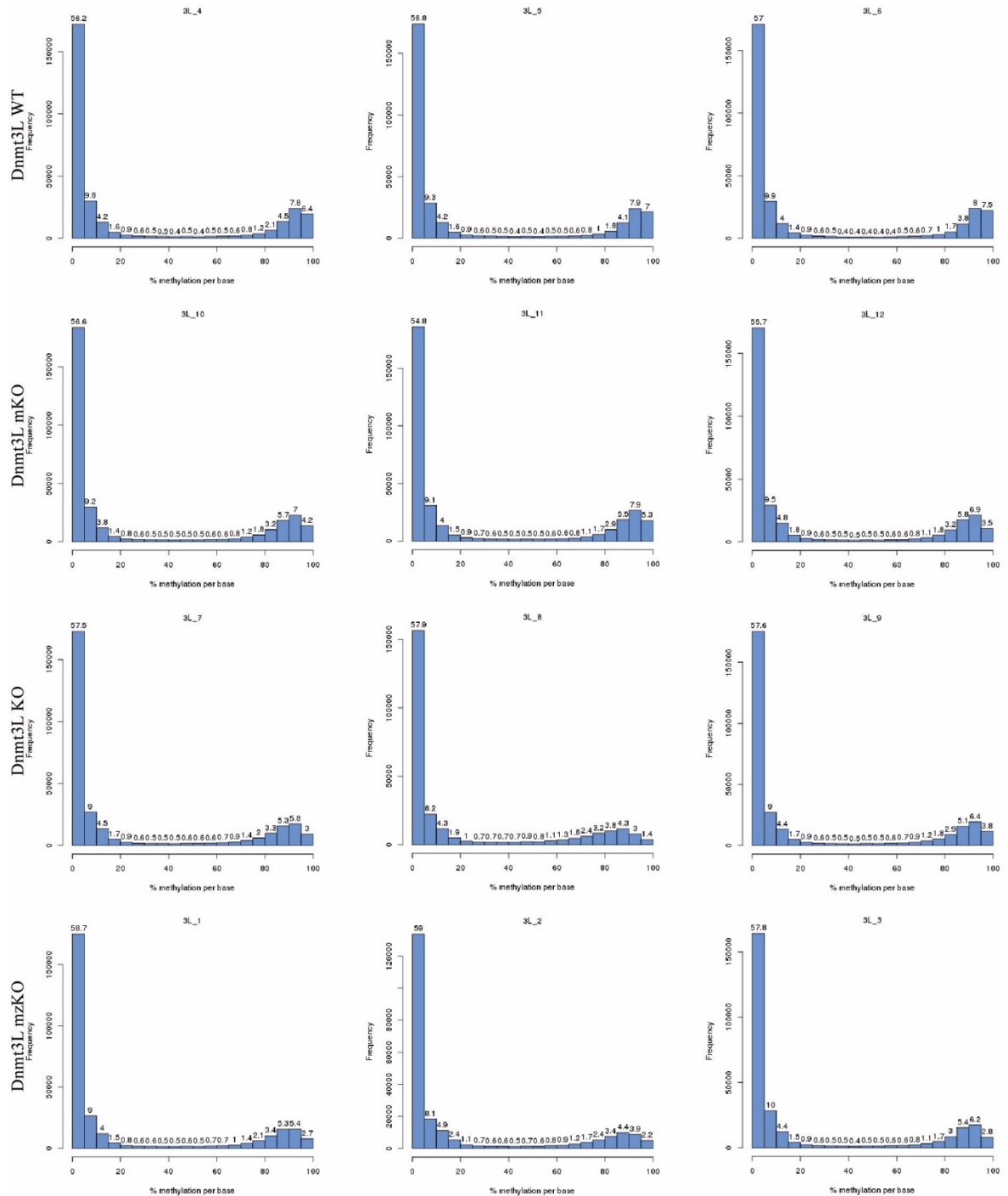
Figure 7. Frequency and percentage of CpG methylation per sample analyzed by RRBS.

Histograms representing the frequency and levels of CpG methylation in percentage per base from the

raw data of the three different biological replicates (mESCs clones) of each of the Dnmt3L genotype (i.e.

Dnmt3L WT, mKO, KO and mzKO) that were analyzed by RRBS. Histograms were generated by Yue

Lu and were used with her permission.
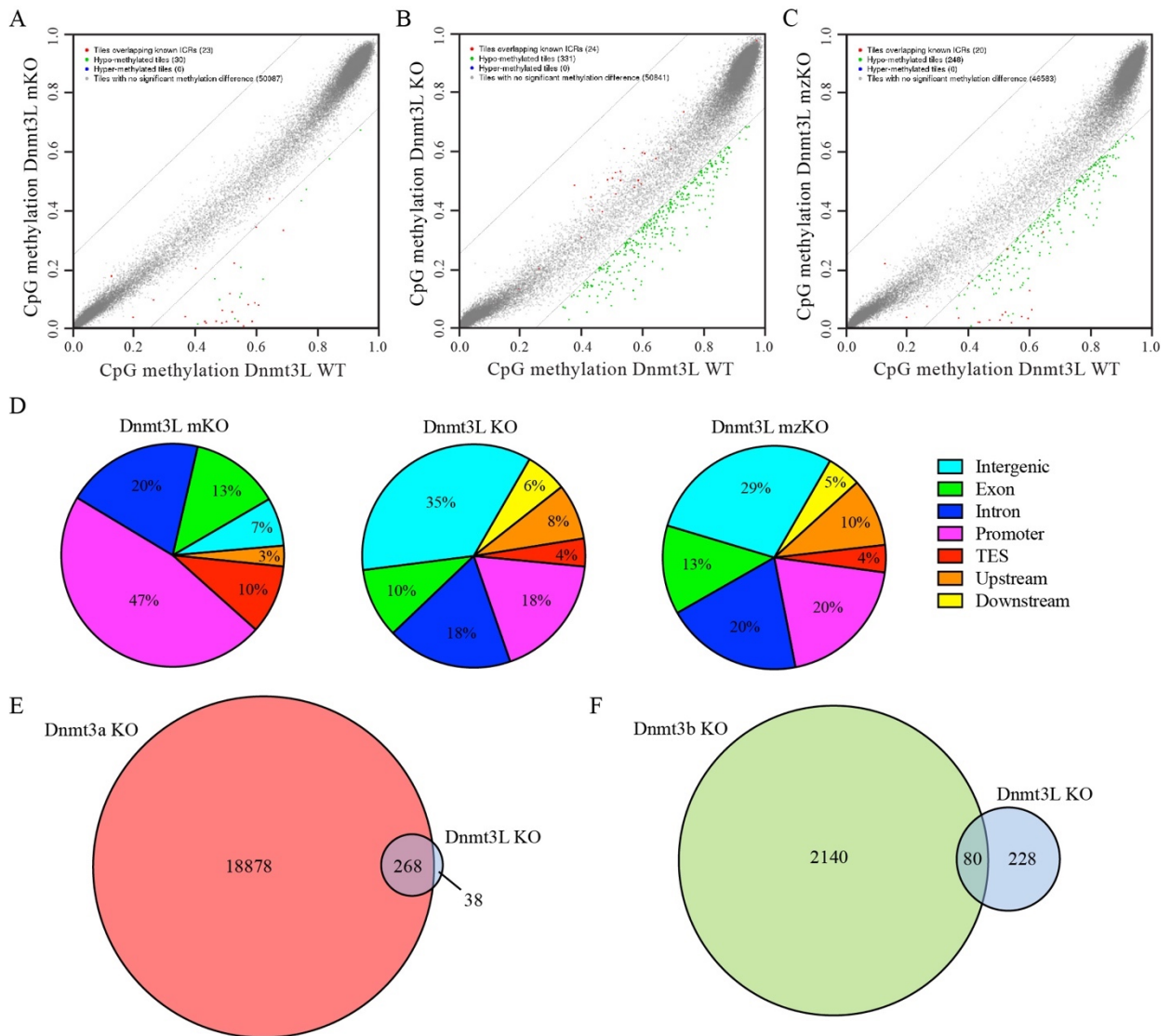
Figure 8: Dnmt3L deficiency mainly affects Dnmt3a-methylated regions.

Scatter plots showing distribution of genome-wide DNA methylation by RRBS analysis using 500 bp tile resolution in Dnmt3L mKO (A), KO (B) or mzKO (C) compared to WT mESCs. Hypomethylated tiles are shown in green, hypermethylated tiles in blue, while tiles located in ICRs in red. Unchanged tiles are in grey. D. Pie charts showing genomic distribution of hypomethylated tiles for Dnmt3L mKO, KO and mzKO mESCs. E. Hypomethylated tile overlap between Dnmt3L KO (blue) and Dnmt3a KO (red) mESCs. F. Hypomethylated tile overlap between Dnmt3L KO (blue) and Dnmt3b KO (green) mESCs. Panels E and F were prepared with data generated by Sally Gaddis and were used with her permission. Scatter plots panels (A-C) pie chart (D) were generated by Sally Gaddis and were used with her permission.
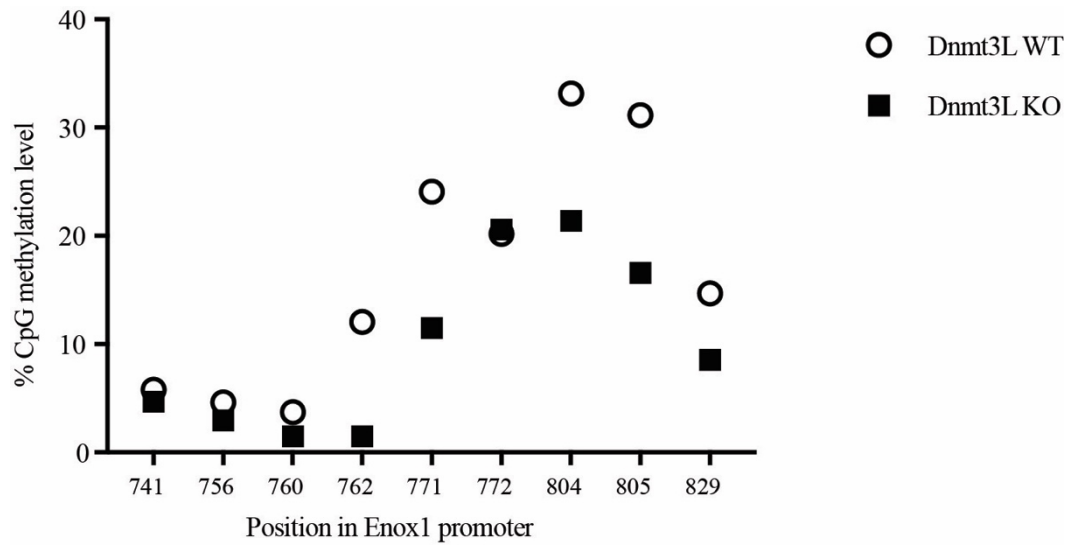
Figure 9. Differential methylation analysis between Dnmt3L KO and WT mESCs of the sites located at the Enox1 promoter using RRBS data.

CpG-containing sites at the Enox1 promoter were found in the RRBS data from both Dnmt3L KO and WT mESCs and their absolute levels of methylation in percentage were plotted. White circles, Dnmt3L WT. Black squares, Dnmt3L KO.

Neri et al. performed MeDIP-seq analysis to compare genome-wide DNA methylation in Dnmt3L KD (shDnmt3L) and control (shGFP) mESCs, with only one sample in each group. By overlap analysis, they designated the peaks unique to shGFP as loss-of-methylation regions (14,107 peaks), the peaks unique to shDnmt3L as gain-of-methylation regions (5,724 peaks), and the overlapped peaks as regions with no change in methylation (41,185 peaks) (49). To determine whether the DMRs are statistically significant, we performed differential analysis of the data deposited by Neri and colleagues, normalizing either by total number of mapped tags or by foreground tags (i.e. the tags in the peaks). At FDR<=0.05 and FC>=2, our analysis confirmed most of the DMRs identified by Neri and colleagues. To our surprise, however, almost all the DMRs turned out to be hypermethylated in Dnmt3L KD cells (including many of the hypermethylated DMRs identified by Neri et al.), and almost none of the hypomethylated DMRs reported by Neri et al. was significant (Figure 10A, B). This outcome is essentially the opposite of our results using Dnmt3L KO mESCs (compare Figure 6B and Figure 10A-C) and contradicts the results of many previous studies (42, 44-48, 171, 172, 180). The result that nearly all DMRs are hypermethylated in Dnmt3L KD cells is also inconsistent with the conclusion of Neri and colleagues that hypomethylated and hypermethylated regions account for ~70% and ~30%, respectively (49). Flaws in their experimental design and data analysis may have contributed to the erroneous conclusion reported by Neri and colleagues. Collectively, our results confirm that Dnmt3L functions as a positive regulator of DNA methylation.
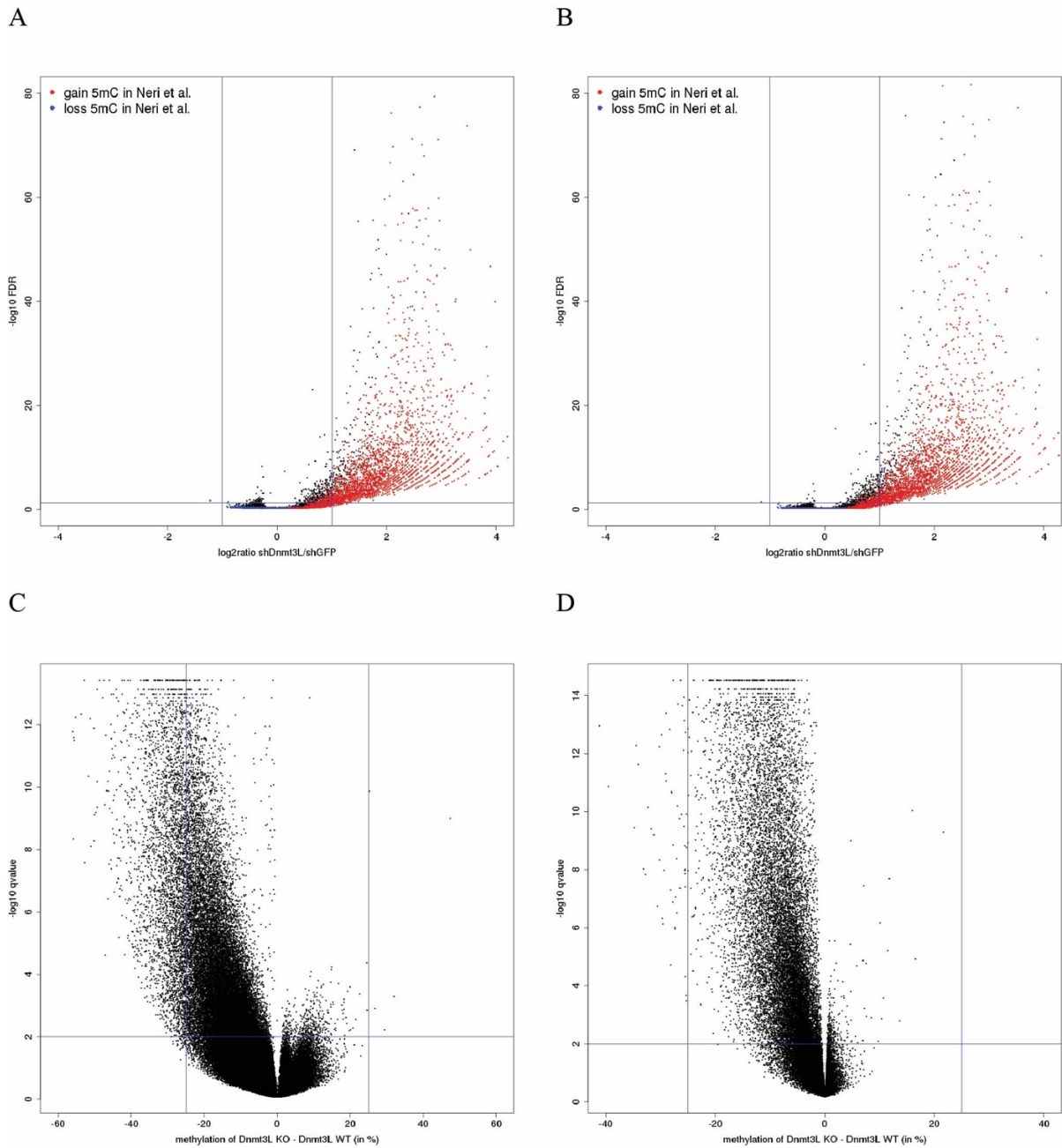
Figure 10. Volcano plots of the MeDIP-Seq data from Neri et al. and the RRBS data from our work.

A. Hypothesized probability of the binomial test is determined by the total number of reads mapped to the shDnmt3L and shGFP samples by Neri et al. B. Hypothesized probability of the binomial test is determined by the number of reads mapped to all the merged peaks in the shDnmt3L and shGFP samples by Neri et al. C. Dnmt3L KO vs WT RRBS by sites from our work. D. Dnmt3L KO vs WT RRBS by 500 bp tiles from our work. Volcano plots were generated by Yue Lu and were used with her permission.

Dnmt3L deficiency mainly affects Dnmt3a-methylated regions.

Our previous work demonstrated that, although Dnmt3a and Dnmt3b redundantly methylate many genomic regions in mESCs, they also have preferred and specific DNA targets. For example, Dnmt3a is more efficient than Dnmt3b in methylating the major satellite repeats, whereas Dnmt3b preferentially methylates the minor satellite repeats (32). Given that *Dnmt3L* KO mESCs showed overt hypomethylation at the major satellite repeats but no changes in methylation at the minor satellite repeats (Figure 4C, D), we postulated that zygotic Dnmt3L preferentially regulates the methylation of Dnmt3a target regions in mESCs.

We recently performed genome-wide DNA methylation analysis of *Dnmt3a* KO mESCs and *Dnmt3b* KO mESCs by whole-genome bisulfite sequencing (WGBS) (manuscript submitted). To test our hypothesis that zygotic Dnmt3L mainly regulates Dnmt3a targets (rather than Dnmt3b targets) in mESCs, we sought to compare the DNA methylation profile of *Dnmt3L* KO mESCs with the WGBS datasets. For the comparisons, the RRBS data were first converted to 500-bp tiles. Again, *Dnmt3L* mKO cells had only a small number of hypomethylated tiles, with the majority (23/30, ~77%) being in ICRs and showing severe loss of methylation, *Dnmt3L* KO cells had ~10 times more hypomethylated tiles (331), mostly with moderate loss of methylation, and *Dnmt3L* mzKO showed the combined changes, whereas none of the cell lines had any hypermethylated tiles (Figure 8A-C). Analysis of the genomic distribution of the hypomethylated tiles revealed that, in *Dnmt3L* mKO cells, nearly half of the them were in promoters, consistent with their enrichment in ICRs, and in *Dnmt3L* KO and *Dnmt3L* mzKO cells, they were mostly located in intergenic regions, gene bodies (introns and exons), and promoters (Figure 8D). Overlap analysis showed that the vast majority (268/306, ~88%) of hypomethylated tiles in *Dnmt3L* KO mESCs overlapped with those in *Dnmt3a* KO mESCs (Figure 8E), whereas a much lower fraction (80/308, ~26%) of hypomethylated tiles in *Dnmt3L* KO cells overlapped with those in *Dnmt3b* KO cells (Figure 8F). These results suggest that Dnmt3L is functionally more important for Dnmt3a than for Dnmt3b in mESCs, in agreement with evidence obtained from genetic studies in mice (29, 35, 42, 44).

Dnmt3a2 is unstable in the absence of Dnmt3L.

Biochemical studies indicate that Dnmt3L interacts with both Dnmt3a and Dnmt3b and stimulates their catalytic activities (166, 167, 176, 181). Why Dnmt3L preferentially regulates Dnmt3a-mediated DNA methylation *in vivo* is an open question. To gain insights into the mechanism underlying the functional specificity of Dnmt3L, we first analyzed the expression of the Dnmt proteins in *Dnmt3L*-deficient mESCs by western blot. As compared to WT mESCs, Dnmt3L KO and mzKO mESCs, but not Dnmt3L mKO mESCs, showed marked decreases in Dnmt3a2 and minor decreases in Dnmt3a1 and Dnmt3b, whereas Dnmt1 was expressed at comparable levels in all the cell lines (Figure 11A). As Dnmt3a2 is the predominant Dnmt3a isoform in mESCs (25), our data raised the possibility that downregulation of Dnmt3a2 could contribute to the preferential effect on Dnmt3a targets observed in *Dnmt3L* KO mESCs.

Transcription of the two *Dnmt3a* isoforms in mESCs - *Dnmt3a1* (minor isoform) and *Dnmt3a2* (major isoform) - was driven by different promoters (25). RT-qPCR analysis using specific primers revealed that *Dnmt3a1, Dnmt3a2* and total *Dnmt3a,* as well as *Dnmt3b,* mRNA levels were not altered in *Dnmt3L* KO mESC lines (Figure 11B). These data suggest that post-transcriptional dysregulation led to the decrease in Dnmt3a2 protein level in *Dnmt3L* KO mESCs.

Next, we examined whether Dnmt3a2 protein stability is affected in the absence of Dnmt3L. To this end, we treated *Dnmt3L* KO and WT mESCs with the protein synthesis inhibitor cycloheximide (CHX) and then monitored the rates of Dnmt3a2 decline over time. p53, a rapidly turning-over protein, was used as a control for the efficacy of CHX treatment, and β-actin, a highly stable protein, was used as a loading control. In the absence of Dnmt3L, Dnmt3a2 declined substantially more rapidly (Figure 11C). By measuring the intensities of the Dnmt3a2 bands, we estimated that the half-life of Dnmt3a2 protein was reduced to ~6 hours in *Dnmt3L* KO mESCs, as opposed to more than 12 hours in WT mESCs (Figure 11D).
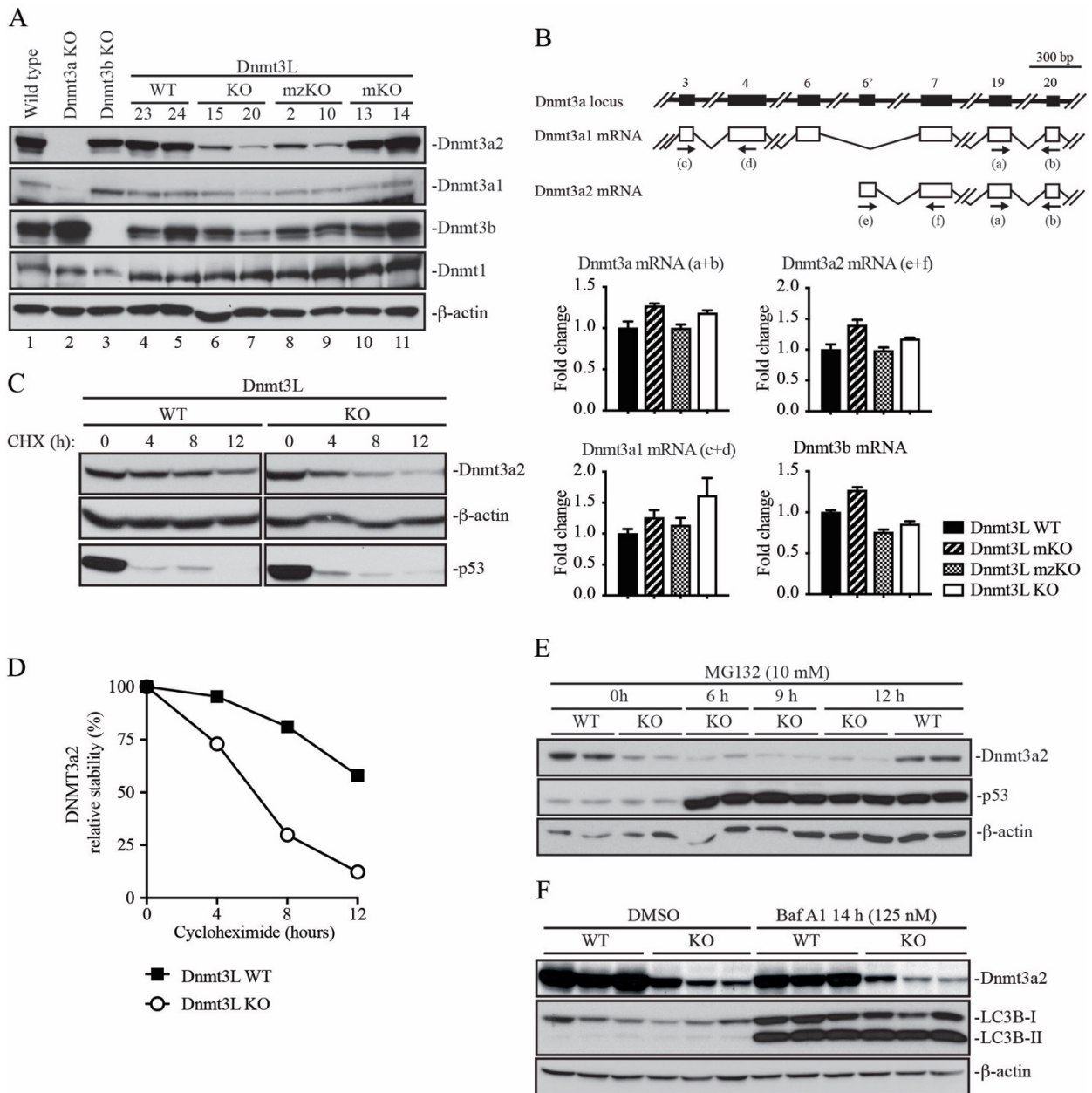
Figure 11: Dnmt3a protein is unstable in the absence of Dnmt3L.

A. Western blot using different types Dnmt3L deficient mESCs, two clones per genotype. B. Upper panel, diagram indicating the Dnmt3a locus (black) and the exons (white) of different Dnmt3a isoforms indicating the position of the primers used for the analysis of mRNA levels by RT-qPCR. C. Analysis of protein stability by treatment with cycloheximide (CHX) for different periods. D. Quantification of the band intensity showed in C. E and F. Western blot results of inhibition of proteosomal (E) or lysosomal (F) protein degradation pathways after treatment with MG132 or Baf-A1, respectively.

Two major pathways - the ubiquitin-proteasome pathway and lysosomal proteolysis - mediate protein degradation in eukaryotic cells. We therefore investigated whether these pathways were involved in Dnmt3a2 degradation in the absence of Dnmt3L. We treated *Dnmt3L* KO and WT mESCs with the proteasome inhibitor MG132 or the lysosome inhibitor Bafilomycin A1 (Baf-A1) for different periods of time and then examined Dnmt3a2 levels by western blot analysis. Although the inhibitors were highly effective, as evidenced by the dramatic accumulation of p53 and LC3B-II, respectively, they failed to recover Dnmt3a2 levels in *Dnmt3L* KO mESCs (Figure 11E, F), suggesting that a different mechanism was responsible for Dnmt3a2 degradation in these cells. Collectively, these results suggest that Dnmt3L is required for Dnmt3a2 protein stability in mESCs.

The ability of Dnmt3L to interact with Dnmt3a is critical for Dnmt3a stability.

Biochemical and structural studies have shown that Dnmt3L and Dnmt3a directly interact via their C-terminal regions (43, 170). We therefore hypothesized that formation of the Dnmt3L-Dnmt3a2 complex could lead to Dnmt3a2 stabilization. To test the hypothesis, we first sought to engineer a Dnmt3L point mutation that abolishes Dnmt3L-Dnmt3a interaction by substituting phenylalanine 297 of mouse Dnmt3L with aspartate (F297D). F297 (equivalent to F261 in human DNMT3L) is a critical residue involved in interacting with Dnmt3a, and replacing this hydrophobic amino acid with the negatively charged aspartate has been shown to abolish the ability of Dnmt3L to stimulate Dnmt3a catalytic activity (43, 170). By co-immunoprecipitation (co-IP) experiments using Myc-tagged Dnmt3L proteins transiently expressed in mESCs, we confirmed that WT Dnmt3L interacted with endogenous Dnmt3a2 and that the F297D mutation disrupted the interaction (Figure 12A). We then performed rescue experiments to compare the effects of WT Dnmt3L and the F297D mutant in restoring Dnmt3a2 levels in *Dnmt3L* KO mESCs. To this end, Myc-tagged Dnmt3L or the F297D mutant was transfected in *Dnmt3L* KO mESCs, and individual stable clones were obtained after 7-10 days of selection with blasticidin. Notably, expression of WT Dnmt3L, but not the F297D mutant, resulted in obvious restoration of Dnmt3a2 levels, as compared to stable clones transfected with the empty vector (Figure 12B). The different effects could not be attributed to differences in expression levels of the Myc-tagged proteins, as

both WT Dnmt3L and the F297D mutant were expressed at similar levels in the clones used in the experiment (Figure 12B). To verify that formation of the Dnmt3L-Dnmt3a2 complex stabilized Dnmt3a2, we again assessed Dnmt3a2 protein stability, as described above (Figure 11C-D), in the stable clones reconstituted with Myc-tagged Dnmt3L proteins. Indeed, Dnmt3a2 stability almost completely recovered in cells expressing WT Dnmt3L (half-life: ~12 hours), and the effect was not observed in cells expressing the F297D mutant (Figure 12C-D). Southern blot analysis also confirmed that the DNA methylation level at the major satellite repeats was rescued to a large extent in *Dnmt3L* KO mESCs reconstituted with WT Dnmt3L, whereas expression of the F297D mutant protein had no effect (Figure 12E). Taken together, these results support our hypothesis that Dnmt3L, by interacting with Dnmt3a2 to form a complex, makes Dnmt3a2 stable.
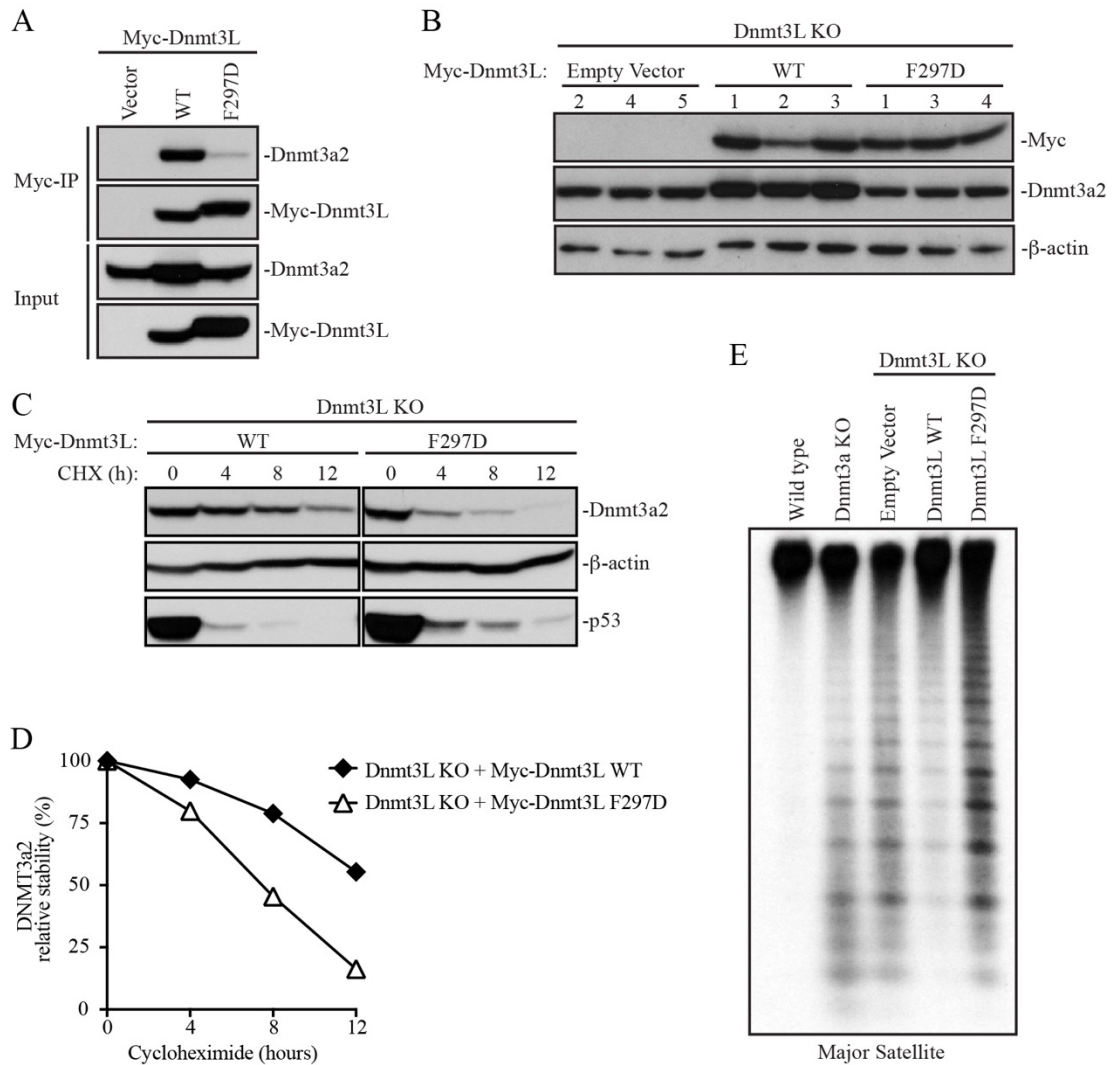
Figure 12: The ability of Dnmt3L to interact with Dnmt3a is critical for Dnmt3a stability.

A. Western blot results of the co-immunoprecipitation experiment of Myc-Dnmt3L WT or F297D mutant with endogenous Dnmt3a2. B. Western blot showing Dnmt3L KO stable rescue clones overexpressing Myc-Dnmt3L WT, Myc-Dnmt3L F297D mutant or empty vector, result of three representative clones per group. C. Analysis of protein stability in Dnmt3L KO stable rescue clones overexpressing Myc-Dnmt3L WT or F297D mutant, by treatment with cycloheximide (CHX) for different periods. D. Quantification of the band intensity showed in C. E. Southern blot results of major satellite repeat with Dnmt3L KO stable rescue clones overexpressing Myc-Dnmt3L WT, Myc-Dnmt3L F297D mutant or empty vector.

Forced expression of Dnmt3a in Dnmt3L KO mESCs rescues DNA methylation.

Our data indicated that Dnmt3L plays a crucial role in maintaining Dnmt3a2 protein stability, in addition to its role in stimulating Dnmt3a catalytic activity (166, 167, 176). The relative contributions of these two regulatory effects of Dnmt3L in Dnmt3a-mediated DNA methylation are unclear. To determine the functional importance of the regulation of Dnmt3a2 stability, we asked whether restoring the Dnmt3a level in the absence of Dnmt3L would be sufficient to rescue DNA methylation. We generated stable clones in *Dnmt3L* KO mESCs expressing Myc-tagged Dnmt3a1 or Dnmt3a2. We were able to obtain Dnmt3a2 clones with expression levels similar to endogenous Dnmt3a2 level in WT mESCs, although the expression levels in the Dnmt3a1 clones were lower (Figure 13A). Southern blot analysis revealed that forced expression of either Dnmt3a1 or Dnmt3a2 substantially restored the methylation levels at the major satellite repeats, although the rescue efficiency appeared to be slightly lower than that of the WT Dnmt3L clone used in the experiment (Figure 13B). Thus, we conclude that regulating Dnmt3a (especially Dnmt3a2) protein stability is an important aspect of Dnmt3L function that significantly contributes to Dnmt3a-dependent DNA methylation in mESCs (Figure 13C).
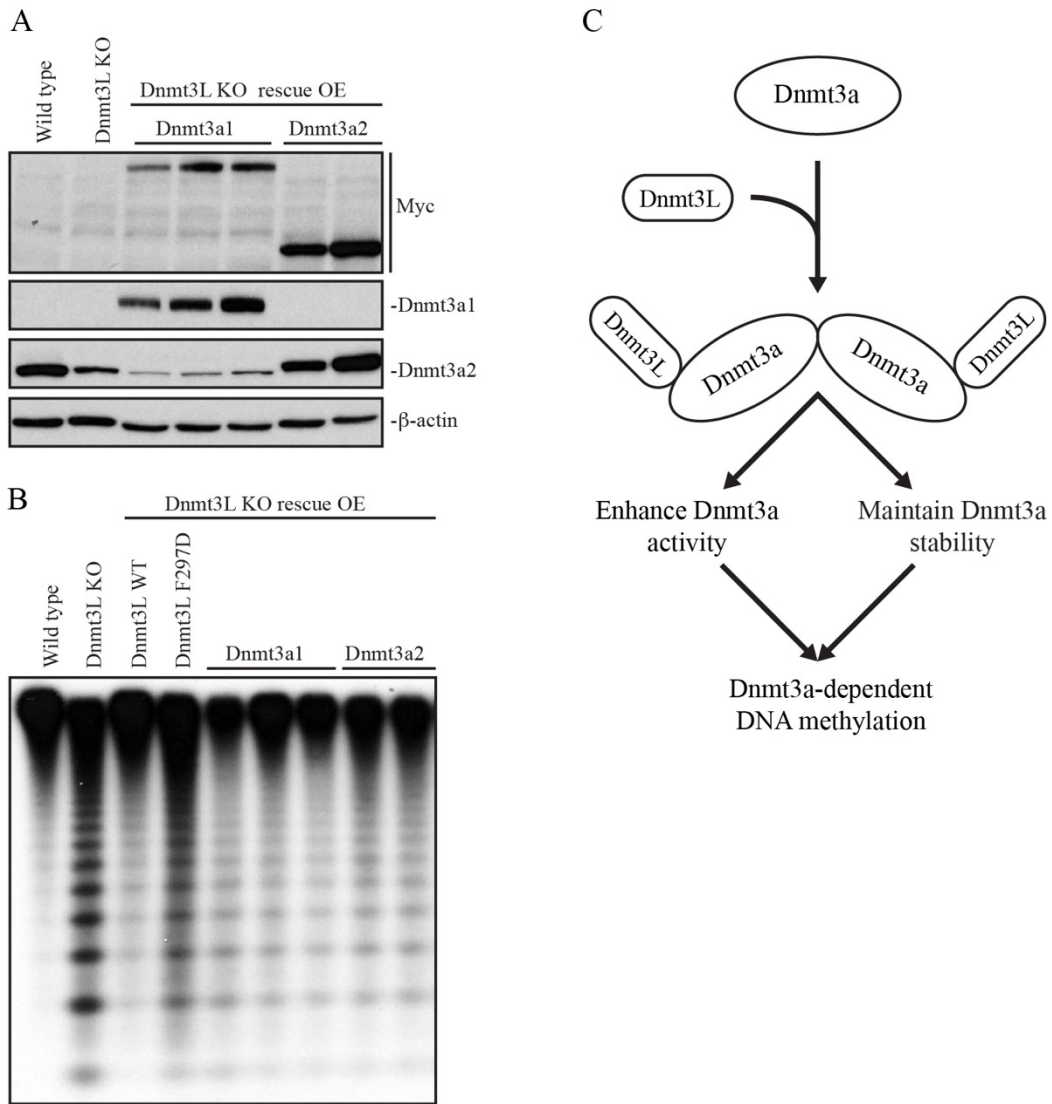
Figure 13: Forced expression of Dnmt3a in Dnmt3L KO mESCs rescues DNA methylation.

A. Western blot results showing Dnmt3L KO stable rescue clones overexpressing Myc-Dnmt3a1 or Myc-Dnmt3a2. B. Southern blot results of major satellite repeat with Dnmt3L KO stable clones overexpressing Myc-Dnmt3L WT, Myc-Dnmt3L F297D mutant, Myc-Dnmt3a1 or Myc-Dnmt3a2. C. Model of the roles of Dnmt3L in the regulation of Dnmt3a activity in mESCs.

3.3 DISCUSSION

Dnmt3L is a key regulator of *de novo* DNA methylation. Based on its ability to stimulate the enzymatic activities of Dnmt3a and Dnmt3b *in vitro* (166, 167, 176), it is generally assumed that Dnmt3L functions primarily as a catalytic cofactor of these enzymes. In the present study, we demonstrate that, in mESCs, Dnmt3L also regulates the abundance of these *de novo* methyltransferases, especially Dnmt3a2, the predominant Dnmt3a protein product in mESCs (25). Our results indicate that Dnmt3L, via interacting with Dnmt3a2 to form a complex, stabilizes Dnmt3a2. Dnmt3L-deficient mESCs show hypomethylation at genomic regions that are mainly Dnmt3a targets, including the major satellite repeats. Restoring Dnmt3a amount (by forced expression of either Dnmt3a1 or Dnmt3a2) in Dnmt3L-deficient mESCs largely rescues DNA methylation levels at the major satellite repeats. These results suggest that Dnmt3L is not absolutely required for Dnmt3a-mediated methylation, at least at some genomic regions, although it seems to enhance the methylation efficiency. Therefore, we conclude that the regulatory roles of Dnmt3L on Dnmt3a activity and stability both contribute to Dnmt3a-dependent DNA methylation and functions (Figure 13C).

During the mammalian life cycle, two waves of *de novo* DNA methylation take place – the first occurring shortly after implantation, which establishes the initial methylation pattern in the embryo, and the second occurring during germ cell maturation, which establishes germ line-specific methylation marks, including genomic imprints (3, 164). Genetic studies and genome-wide DNA methylation analysis suggest that Dnmt3b plays a major role in *de novo* methylation during embryogenesis (first wave) and Dnmt3a is largely responsible for *de novo* methylation in germ cells (second wave) (29, 35, 171, 172, 182). Dnmt3L is essential for Dnmt3a-mediated methylation in germ cells but appears to be dispensable for Dnmt3b-mediated methylation and functions during embryonic development (42, 44, 45, 171, 172). Our finding that Dnmt3L preferentially stabilizes Dnmt3a2 in mESCs provides a plausible explanation for the functional specificity of Dnmt3L *in vivo*. Indeed, Dnmt3a2 and Dnmt3L are highly expressed in prospermatogonia and growing oocytes (183, 184), the stages when active *de novo* DNA

methylation occurs during gametogenesis. Further work is required to confirm the role of Dnmt3L in maintaining Dnmt3a2 stability and the significance of this role in DNA methylation in the germ line.

It remains to be determined why Dnmt3L deficiency has a severe effect on Dnmt3a2 stability, but only minor effects on Dnmt3a1 and Dnmt3b levels. While recombinant or exogenously expressed Dnmt3a, Dnmt3b and Dnmt3L proteins are capable of interacting with each other (38, 166-168), there is evidence that endogenous Dnmt3L physically interacts with Dnmt3a2, but not Dnmt3a1 and Dnmt3b, in mESCs (48). This provides a possible explanation for the preferential effect of Dnmt3L on Dnmt3a2 stability. The full-length Dnmt3a1 and Dnmt3b proteins have high sequence homology except a variable region at their N termini, and this region is absent in the shorter Dnmt3a2 isoform (25). However, this variable region is unlikely to be directly involved in interacting with Dnmt3L, as structural evidence indicates that the Dnmt3L-Dnmt3a2 interaction is mediated by their C-terminal regions (43). One possibility for why endogenous Dnmt3a1 and Dnmt3b fail to form complexes with Dnmt3L in mESCs is that they are less accessible to Dnmt3L. Dnmt3a1 and Dnmt3b are tightly associated with chromatin with significant enrichment in heterochromatin, whereas Dnmt3a2 seems to be more loosely bound to chromatin (25). That Dnmt3a2 is relatively more soluble and more widely distributed perhaps makes it more susceptible to degradation in the absence of Dnmt3L. Alternatively, the extra sequences in the full-length Dnmt3a1 and Dnmt3b proteins may protect them from being degraded by blocking the degradation machinery. While the mechanism by which Dnmt3a2 is degraded remains to be elucidated, our data suggest that it is independent of the ubiquitin-proteasome and lysosomal proteolysis pathways. Another factor that needs to be considered is that, in mESCs, Dnmt3a2 is far more abundant than Dnmt3a1 (25), which may make Dnmt3a2 more sensitive to the effects of Dnmt3L deficiency. Dnmt3b is also abundantly expressed in mESCs. However, Dnmt3b produces multiple alternatively spliced isoforms, some of which have no catalytic activity but may play regulatory roles in Dnmt3b-mediated methylation (185), similar to the effects of Dnmt3L on Dnmt3a.

In agreement with previous studies regarding the role of Dnmt3L in DNA methylation in germ cells, embryos and mESCs (42, 44-48, 171, 172, 180), our work shows that Dnmt3L is a positive regulator of DNA methylation. This is in sharp contrast to a recent report by Neri et al., which concluded

that, in mESCs, Dnmt3L regulates DNA methylation positively or negatively, depending on genomic regions (49). However, their conclusion was not supported by convincing data, as re-analysis of the MeDIP-seq data deposited by Neri and colleagues revealed that, surprisingly, shRNA-mediated Dnmt3L depletion led to gain of methylation at many genomic regions, but almost no region with significant loss of methylation, which would suggest that Dnmt3L functions predominantly as a negative regulator of DNA methylation. Several factors may have contributed to the different conclusion drawn by Neri and colleagues, including the limitations of MeDIP, lack of biological replicates, and flaws in data analysis. Based on the outcome of our analysis of their data, as well as the way some of their data were presented (e.g. Figure 4E in Neri et al.), we also cannot rule out the possibility that their samples or datasets were switched.

In summary, we demonstrate in the present study that Dnmt3L plays a key role in stabilizing Dnmt3a2 protein, in addition to its functions in the regulation of Dnmt3a catalytic activity and chromatin targeting, and this new role likely contributes, to a large extent, to the functional specificity of Dnmt3L *in vivo* (i.e. mainly affecting Dnmt3a-dependent methylation and functions).

CHAPTER 4: Regulation of maintenance DNA methylation by PRMT6 in cancer

This chapter is based upon: Veland, N., Hardikar, S., Zhong, Y., Gayatri, S., Dan, J., Strahl, B.D., Rothbart, S.B., Bedford, M.T. and Chen, T. (2017) The Arginine Methyltransferase PRMT6 Regulates DNA Methylation and Contributes to Global DNA Hypomethylation in Cancer. Cell Rep, 21, 3390-3397.

Used with permission of Elsevier.

4.1 INTRODUCTION

In mammals, DNA methylation (5-methylcytosine, 5mC) is mostly restricted to CpG dinucleotides and plays crucial roles in many biological processes. Aberrant DNA methylation patterns are associated with cancer. Specifically, cancer cells generally exhibit global hypomethylation and loci-specific hypermethylation, which are implicated in genomic instability and tumor suppressor silencing, respectively (4). However, the mechanisms underlying these alterations remain largely unclear.

DNA methylation patterns are established by the de novo DNA methyltransferases DNMT3A and DNMT3B and maintained primarily by the maintenance DNA methyltransferase DNMT1. DNMT1 recruitment to hemi-methylated CpG sites during DNA replication depends on UHRF1, a multi-domain protein (50, 51). The SRA (SET- and RING-associated) domain of UHRF1 preferentially binds hemi-methylated DNA and plays an important role in loading DNMT1 onto newly synthesized DNA (50, 51, 186). The RING domain-mediated ubiquitination of lysine residues in the N-terminal tail of histone H3 promotes DNMT1 association with H3 (67, 187, 188). Moreover, the TTD (tandem Tudor domain) and PHD (plant homeodomain) cooperatively interact with the N-terminal tail of H3 by recognizing a specific histone modification signature. Specifically, the TTD exhibits affinity for di- and tri-methylated lysine 9 (H3K9me2/me3) (66, 186, 189), whereas PHD-mediated binding to H3 is disrupted by arginine 2 (H3R2) methylation (65, 190-192). Recent studies show that the SRA domain interaction with DNA stimulates TTD-PHD-mediated H3 binding and that hemi-methylated DNA recognition allosterically activates RING domain-mediated H3 ubiquitination (188, 193). These data suggest that UHRF1 targets DNMT1 to newly replicated DNA through complex interactions with chromatin.

The observation that the UHRF1 PHD specifically binds unmodified, but not H3R2-methylated, N-terminal tail of H3 suggests that DNA methylation may be modulated by H3R2 methylation. Arginine methylation is carried out by the PRMT family, consisting of nine members (116). PRMT6 is the primary enzyme responsible for asymmetric dimethylation of H3R2 (H3R2me2a) (68-70). Notably, PRMT6 is frequently overexpressed in cancer cells and implicated in tumorigenic functions (113). In this

study, we show that PRMT6 negatively regulates DNA methylation by impairing UHRF1 association with chromatin and that its overexpression contributes to global DNA hypomethylation in cancer.

4.2 RESULTS

PRMT6 overexpression induces global DNA hypomethylation in mESCs

Given that H3R2 methylation disrupts UHRF1-H3 interaction (65, 190-192), we hypothesized that PRMT6, the primary enzyme responsible for H3R2me2a, regulates DNA methylation. To test the hypothesis, we generated mouse embryonic stem cell (mESC) clones overexpressing human PRMT6 by stable transfection of a bicistronic vector expressing Myc-tagged PRMT6 and the blasticidin-resistant gene (Figure 14A). mESCs offer an ideal experimental system for studying DNA methylation regulators, as their survival and proliferation are not affected by DNA methylation loss (194). Western blots detected increases in H3R2me2a that correlated with PRMT6 levels in the stable clones. Consistent with previous reports that H3R2 methylation antagonizes H3K4me3 (68, 69, 135), H3K4me3 levels decreased in clones expressing high levels of PRMT6. As controls, H3K9me3 and total H3 showed no alterations (Figure 14B). Apparently, PRMT6 overexpression also led to increases in arginine methylation of non-histone proteins (Figure 15A). The stable clones maintained the mESC state, as judged by colony morphology, growth rates, and expression of the pluripotency factors Nanog, Sox2 and Oct4 (Figures 15B-D).

To assess the impact of PRMT6 overexpression on DNA methylation, we first analyzed the minor satellite repeats (MSR) and intracisternal A-particle (IAP) retrotransposons. Southern blot analysis of genomic DNA digested with the methylation-sensitive restriction enzyme *Hpa*II revealed that cells expressing Myc-PRMT6 exhibited drastic DNA hypomethylation compared to cells transfected with the empty vector (mock) (Figures 14C and 14D). We then confirmed global DNA hypomethylation in PRMT6-overexpressing mESCs with dot blot and immunofluorescence (IF) analyses using a 5mC antibody (Figures 14E-14G). The effect of PRMT6 on DNA methylation depends on its catalytic

activity, as an inactive PRMT6 mutant (E155Q) failed to induce DNA hypomethylation in mESCs (Figures 16A-C). Together, these results demonstrate that PRMT6 and its methyltransferase activity negatively regulates global DNA methylation, likely by inducing H3R2me2a.

PRMT6 overexpression impairs Uhrf1 association with chromatin

To determine the mechanism by which PRMT6 induces DNA hypomethylation, we first examined the expression of Dnmts, as well as key regulators of DNA methylation, including Uhrf1 (murine Uhrf1 is also known as Np95), PCNA and Usp7. Western blots showed no changes in the levels of these proteins in PRMT6-overexpressing cells (Figure 17A). We then investigated the possibility of increased H3R2me2a affecting Uhrf1 binding to chromatin. Nuclear fractionation experiments revealed that Uhrf1 chromatin association reduced dramatically in PRMT6-overexpressing mESCs compared to mock mESCs (~10% vs. ~60%) (Figures 17B and 17C). Chromatin immunoprecipitation (ChIP) analysis confirmed that increased H3R2me2a levels correlated with decreased Uhrf1 enrichment at MSR and IAP regions in PRMT6-overexpressing mESCs (Figures 17D and 17E). These results support our hypothesis that higher H3R2me2a levels induced by PRMT6 overexpression impair Uhrf1 association with chromatin, resulting in a failure in maintaining DNA methylation.
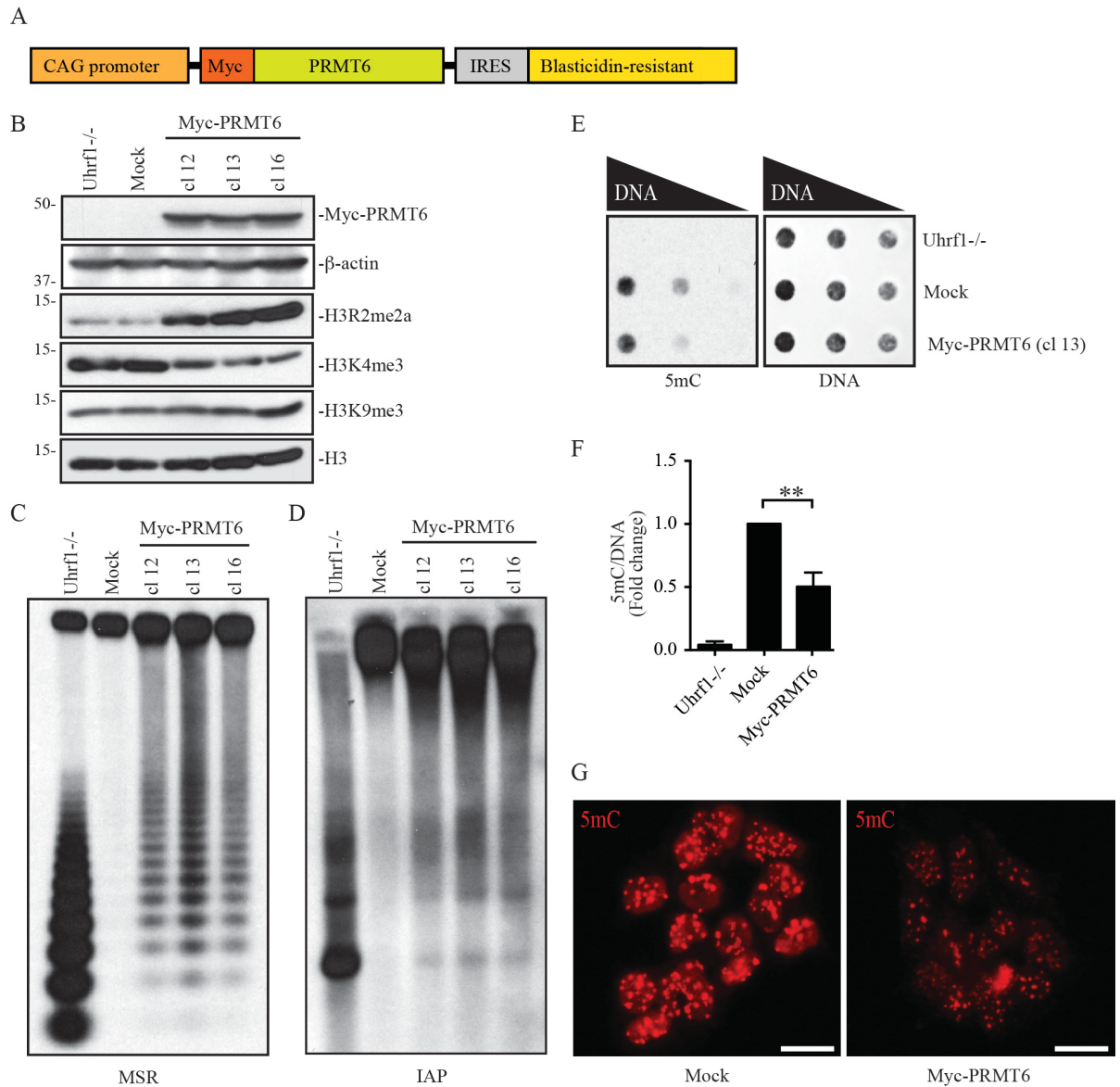
Figure 14. Overexpression of PRMT6 in mESCs induces global DNA hypomethylation.

A. Diagram of *Myc-PRMT6* plasmid. B. Western blots showing the levels of Myc-PRMT6 and histone marks in stable mESC clones. Mock, mESCs transfected with empty vector. Dnmt1-/-, Dnmt1 KO mESCs. C and D. Southern blots showing DNA methylation at MSR (C) and IAP (D) after digestion of genomic DNA with methylation-sensitive restriction enzyme *Hpa*II. Uhrf1-/-, Uhrf1 KO mESCs. E. Dot blot analysis of genomic DNA with 5mC antibody (left). The same membrane was stained with SYTOX Green to verify equal DNA loading (right). F. Quantification of data in (E) by densitometry using Image J. Shown are relative 5mC levels (mean + SD from three independent experiments). Paired t test was used to determine statistical significance. **P < 0.01. G. IF analysis with 5mC antibody.
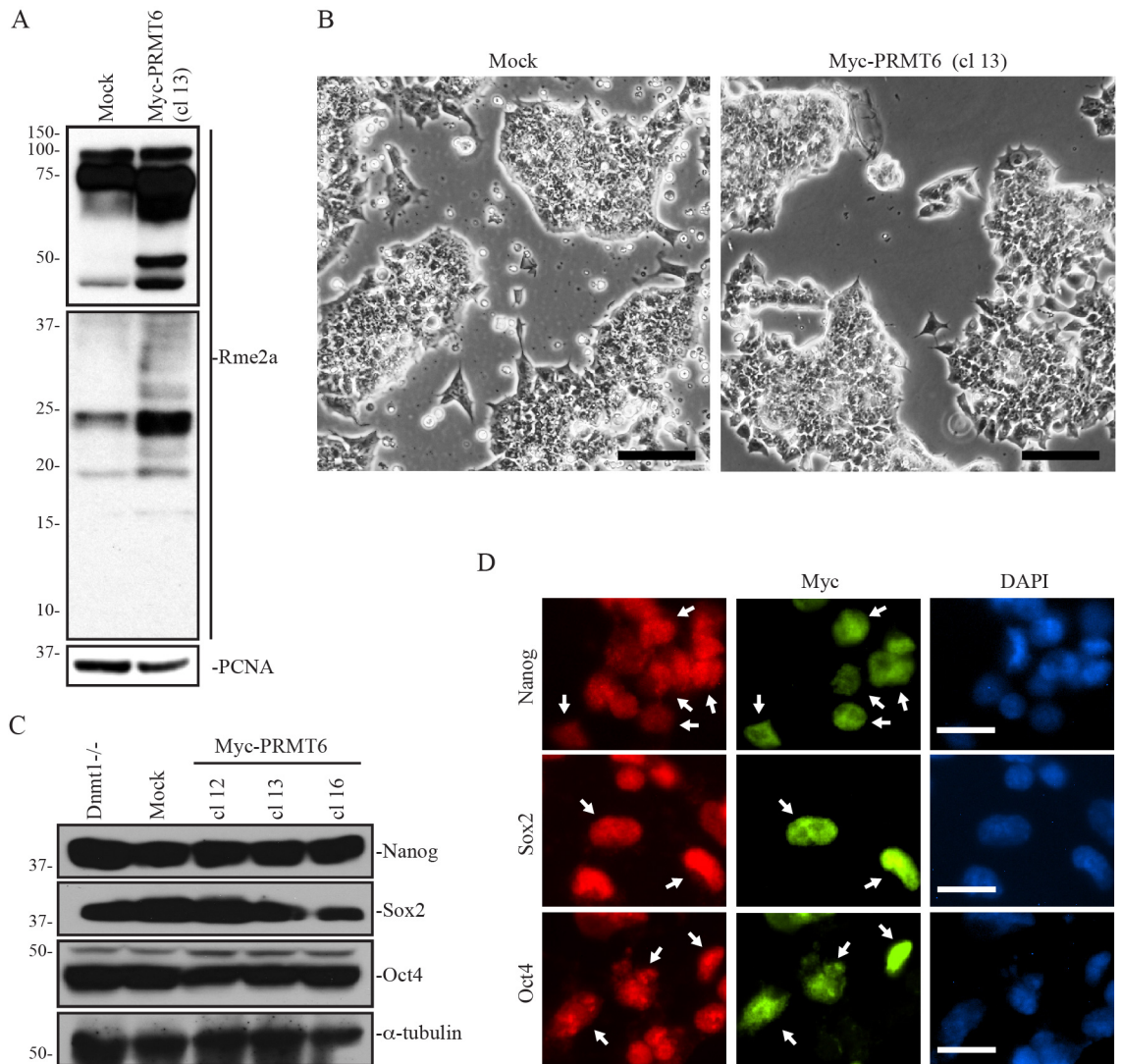
Figure 15. PRMT6 overexpression results in increases in arginine methylation of some non-histone proteins and shows no effect on mESC state.

A. Western blots using a pan-Rme2a antibody showing increases in arginine asymmetric dimethylation of some proteins in mESCs overexpressing Myc-PRMT6. B. Representative images of mock-transfected and Myc-PRMT6-overexpressing mESCs showing similar colony morphology. Scale bars, 50μm. C. Western blots showing no changes in the expression of pluripotency factors Nanog, Sox2 and Oct4 in Myc-PRMT6-overexpressing mESCs. D. IF analysis of co-cultured mock-transfected and Myc-PRMT6 overexpressing (indicated by arrows) mESCs, which confirms no changes in Nanog, Sox2 and Oct4 expression in PRMT6-overexpressing cells. Scale bars, 10μm.
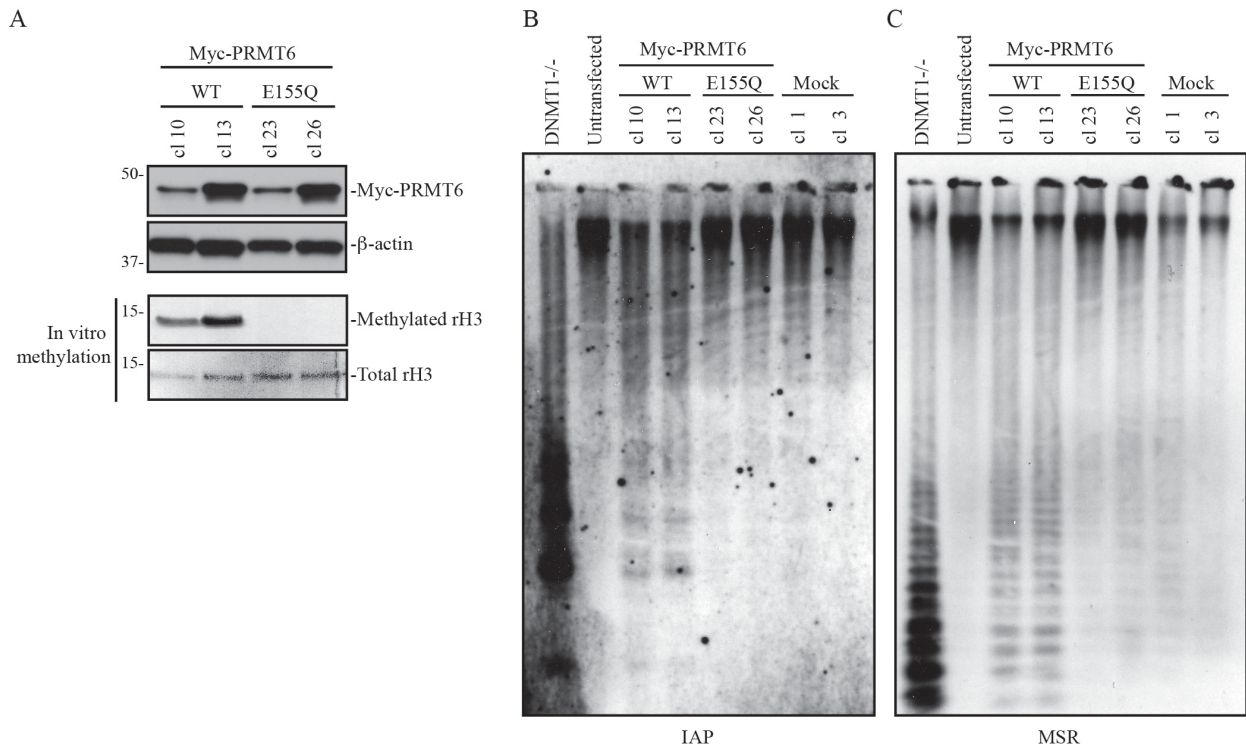
Figure 16. The catalytic activity of PRMT6 is required for its effect on DNA methylation.

A. In vitro methylation assay using PRMT6 proteins immunoprecipitated from mESC stable clones expressing Myc-tagged WT PRMT6 or mutant PRMT6 (E155Q), which demonstrates that the E155Q mutant is catalytically inactive. B and C. Southern blot analysis of IAP retrotransposons (B) or MSR (minor satellite repeats) (C) after digestion of genomic DNA with the DNA methylation-sensitive restriction enzyme HpaII, which shows hypomethylation in mESC clones overexpressing WT PRMT6, but not the inactive E155Q mutant.
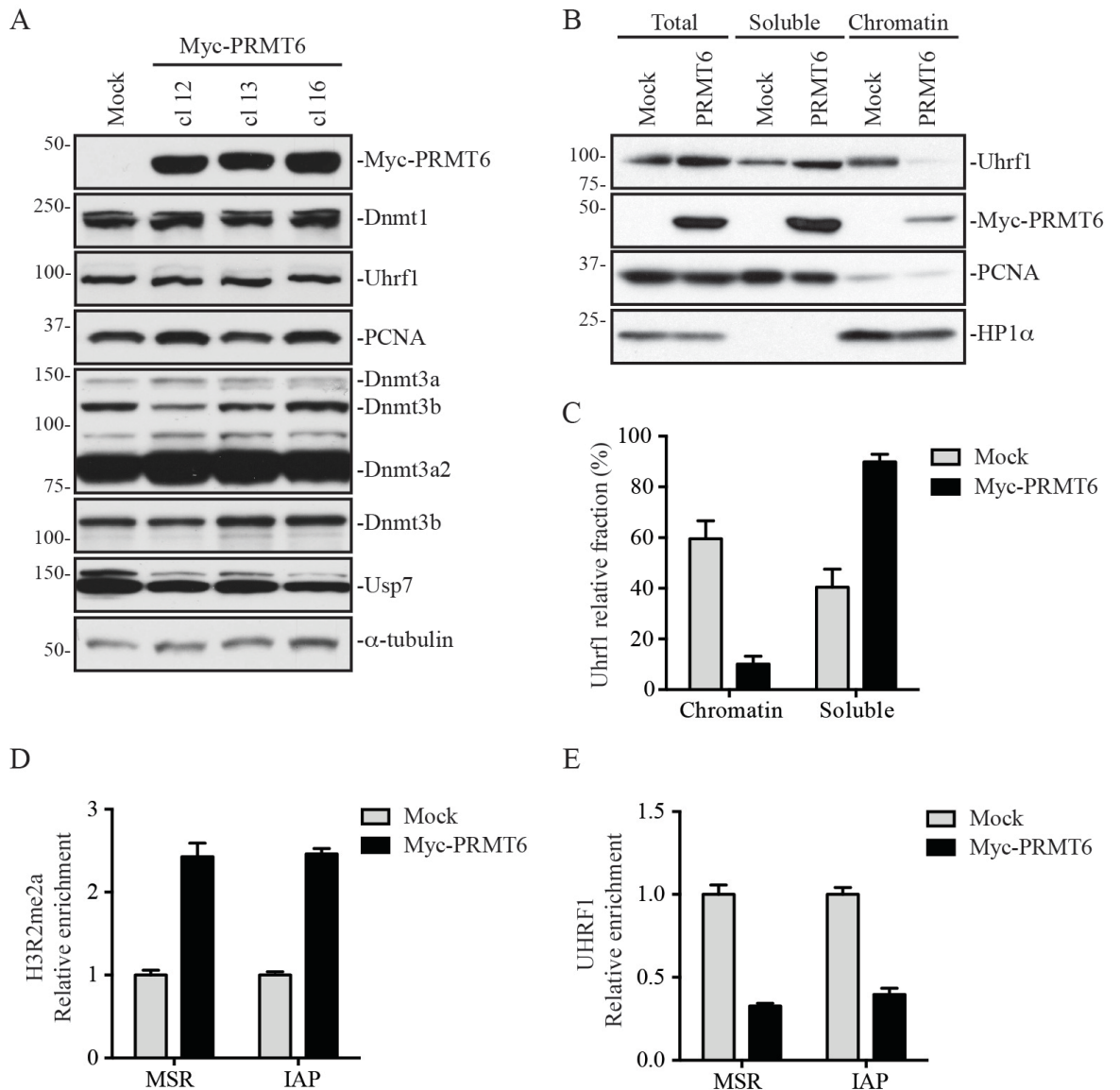
Figure 17. Uhrf1 chromatin association is impaired in mESCs overexpressing PRMT6.

A. Western blots showing the levels of DNA methylation enzymes and regulators. Note that mESCs express two major Dnmt3a isoforms (Dnmt3a and Dnmt3a2) and that the Dnmt3a antibody cross-reacts with Dnmt3b. B. Nuclear fractionation assay showing Uhrf1 chromatin association. PCNA and HP1α were used as controls for soluble and chromatin-associated proteins, respectively. Total, nuclei directly dissolved in 2xSDS loading buffer. C. Quantification of data in (B) by densitometry using Image J. Shown are percentages of soluble and chromatin-associated Uhrf1 in each sample (mean + SD from three independent experiments). D and E. ChIP assays showing relative enrichment of H3R2me2a (D) and Uhrf1 (E) at MSR and IAP regions (mean + SD from three independent experiments).

PRMT6 upregulation correlates with DNA hypomethylation in human cancers

Global DNA hypomethylation is a hallmark of cancer cells (4), but the underlying mechanisms are poorly understood. Given that overexpression of PRMT6 is reported in multiple types of cancer (113), we postulated that PRMT6 upregulation might contribute to global DNA hypomethylation in cancer.

We first assessed the correlation between PRMT6 expression and DNA methylation in a panel of cancer cell lines. Western blots indicated that, compared to non-tumorigenic breast cell lines 76NF2V and MCF 10F, most cancer cell lines examined exhibited upregulation of PRMT6, although the levels varied greatly (Figure 18A). The 5mC content in the cancer cell lines was measured by liquid chromatography and tandem mass spectrometry (LC-MS/MS) (Table 3). Based on the relative levels of PRMT6 (Figure 18A), we divided the cancer cell lines into two groups: the PRMT6-high group had significantly lower levels of 5mC than the PRMT6-low group (Figure 18B).

We next asked whether PRMT6 upregulation correlates with DNA hypomethylation in primary tumor samples by employing The Cancer Genome Atlas (TCGA) database. Data downloaded from the cBioPortal for Cancer Genomics showed wide variations in PRMT6 expression in all cancer types (Figure 19A). We selected three common cancer types, i.e. breast cancer, lung cancer and colorectal cancer, because a large amount of DNA methylation data is available in the TCGA database. When all samples of each cancer type were included in the analyses, no clear correlation was observed between PRMT6 expression and DNA methylation levels, which is not surprising because both PRMT6 and DNA methylation levels are highly variable in different samples. However, comparisons of the samples with the highest 20% and lowest 20% of PRMT6 expression revealed a significant inverse correlation between PRMT6 expression and DNA methylation in lung cancer and colorectal cancer, but not in breast cancer (Figure 18C). Based on our hypothesis, DNA methylation may not be affected by PRMT6 if UHRF1 expression is low. Therefore, we first divided the samples into UHRF1-high (upper 70%) and UHRF1-low (lower 30%) groups and then compared DNA methylation levels in samples with high (top 20%) and low (bottom 20%) PRMT6 expression. Consistent with our hypothesis, we observed a significant inverse correlation between PRMT6 expression and DNA methylation in the UHRF1-high

groups of all three cancer types (Figure 18D upper panel) and no correlations in the UHRF1-low groups (Figure 18D lower panel). Together, these data suggest that PRMT6 upregulation contributes to global DNA hypomethylation in cancer.

PRMT6 depletion or inhibition restores global DNA methylation in MCF7 cells

To validate the significance of PRMT6 upregulation in DNA hypomethylation, we assessed the impact of PRMT6 knockdown (KD) and inhibition in MCF7 cells, a breast cancer cell line with high PRMT6 expression (Figure 18A). Stable expression of PRMT6 shRNAs, which efficiently depleted PRMT6 (Figure 20A), or treatment with MS023, a PRMT inhibitor that is potent for PRMT6 (147), resulted in substantial decreases in H3R2me2a, but no changes in DNMT1 and UHRF1 levels (Figures 20A and 20C). Consistent with previous reports (140-142, 145, 147), PRMT6 KD or MS023 treatment resulted in defects in MCF7 proliferation (Figures 21A-D). Dot blot analysis showed that PRMT6 depletion or inhibition led to increases in global DNA methylation (Figures 20B and 20D). We verified the results by bisulfite sequencing analysis of a region in the 45S ribosomal DNA (rDNA) promoter, which is partially methylated in MCF7 cells (195). Indeed, PRMT6 KD or MS023-treated cells had markedly higher levels of DNA methylation (~90%) than control cells (~60%) (Figure 20E). Both de novo and maintenance methylation probably contributed to the restoration of DNA methylation levels.

In agreement with our hypothesis, UHRF1 chromatin association was substantially enhanced in cells treated with MS023 (as opposed to ~50% chromatin association in cells treated with DMSO) (Figures 20F and 20G). To strengthen the hypothesis, we analyzed the UHRF1 occupancy at the promoter regions of three PRMT6 target genes, HOXA2, CDKN1A and GREB1C (69, 139, 140, 142). ChIP and methylated-DNA immunoprecipitation (MeDIP) analyses confirmed that H3R2me2a reduction induced by MS023 correlated with increases in UHRF1 enrichment and DNA methylation levels at these loci (Figures 20H-20J). Collectively, these results suggest that, in MCF7 cells, increased H3R2me2a due to PRMT6 upregulation plays a critical role in inducing global DNA hypomethylation by impairing UHRF1 chromatin binding.
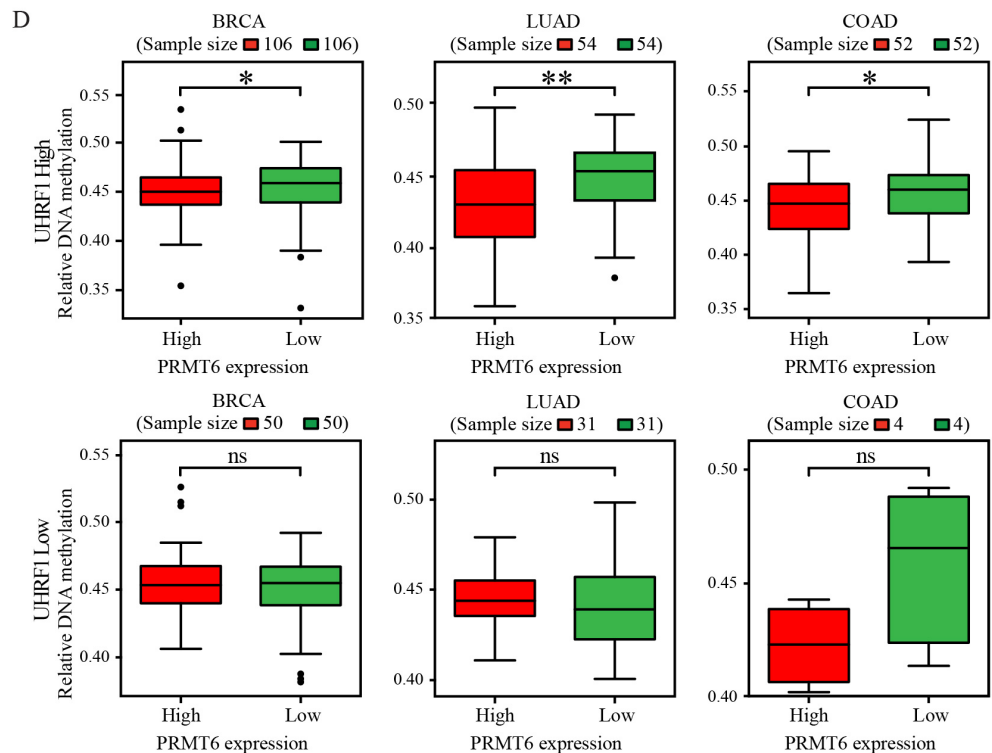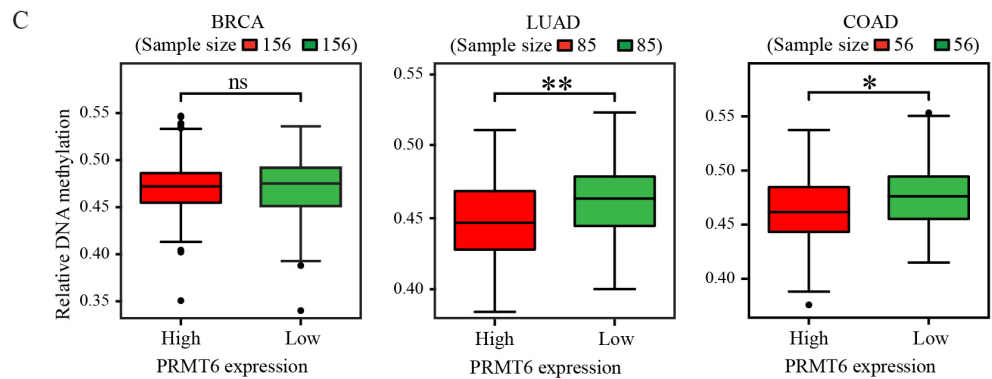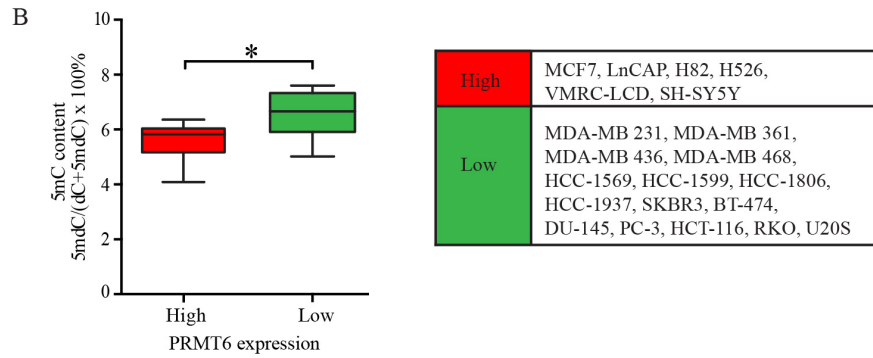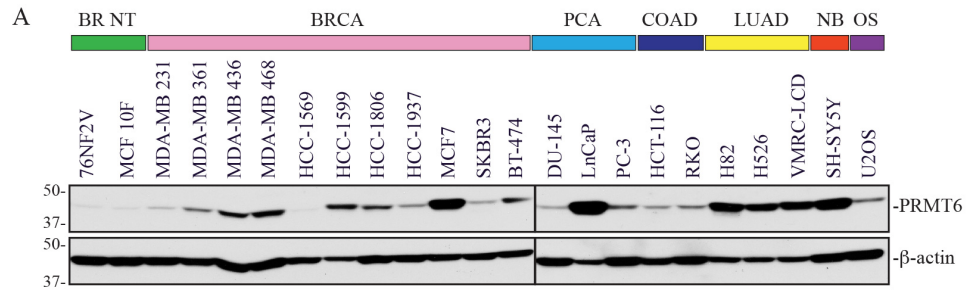
Figure 18. PRMT6 expression inversely correlates with DNA methylation in human cancer cells.

A. Western blots showing PRMT6 levels in human cancer cell lines. BR NT, breast non-tumorigenic; BRCA, breast cancer; PCA, prostate cancer; COAD, colorectal adenocarcinoma; LUAD, lung adenocarcinoma; NB, neuroblastoma; OS, osteosarcoma. B. Comparison between PRMT6-high and PRMT6-low cell lines for total 5mC levels (determined by LC-MS/MS, see Table 3). C and D. Correlation of *PRMT6* expression and DNA methylation data from the TCGA database. The mean DNA methylation levels between cancer samples with the highest (top 20%) and lowest (bottom 20%) *PRMT6* expression in each cancer type were compared, either without considering *UHRF1* expression (C) or by dividing all samples into *UHRF1*-high (upper 70%) and *UHRF1*-low (lower 30%) groups before analysis (D). Note that the 30% cutoff for *UHRF1* expression was based on samples of all three cancer types combined and, therefore, the sample sizes of *UHRF1*-high and *UHRF1*-low groups in each cancer type do not account for precisely 70% and 30%. Wilcoxon rank sum non-parametric test with two-tailed P values was used to determine the significance of differences in (B-D). See also Table 3 and Figure 19.

Table 3: 5mC content in human cancer cell lines.

Cell line	Experiment 1	Experiment 2	Mean	Mean ± SD
	5mdC/(dC+5mdC)			(%)
MDA-MB 231	0.0488	0.0524	0.0506	5.06 ± 0.26
MDA-MB 361	0.0668	0.0721	0.0695	6.95 ± 0.37
MDA-MB 436	0.0721	0.0744	0.0733	7.33 ± 0.16
MDA-MB 468	0.0659	0.0686	0.0672	6.72 ± 0.19
HCC-1569	0.0608	0.0663	0.0636	6.36 ± 0.39
HCC-1599	0.0590	0.0593	0.0592	5.92 ± 0.02
HCC-1806	0.0506	0.0539	0.0523	5.23 ± 0.23
HCC-1937	0.0690	0.0753	0.0722	7.22 ± 0.45
MCF7	0.0548	0.0559	0.0553	5.53 ± 0.07
SKBR3	0.0494	0.0510	0.0502	5.02 ± 0.11
BT-474	0.0730	0.0774	0.0752	7.52 ± 0.31
DU-145	0.0728	0.0775	0.0751	7.51 ± 0.34
LnCaP	0.0403	0.0414	0.0409	4.09 ± 0.08
PC-3	0.0631	0.0659	0.0645	6.45 ± 0.19
HCT-116	0.0736	0.0785	0.0760	7.60 ± 0.34
RKO	0.0657	0.0675	0.0666	6.66 ± 0.13
H82	0.0636	0.0638	0.0637	6.37± 0.02
H526	0.0575	0.0589	0.0582	5.82 ± 0.10
VMRC-LCD	0.0583	0.0587	0.0585	5.85 ± 0.03
SH-SY5Y	0.0584	0.0603	0.0593	5.93 ± 0.13
U2OS	0.0587	0.0618	0.0603	6.03 ± 0.22

The 5mC content in each cell line was quantified by liquid chromatography-tandem mass spectrometry (LC-MS/MS). Shown are results from two independent experiments. The 5mC content is shown as a percentage of the total cytosine pool according to peak areas: 5mdC/(dC+5mdC) x 100%. SD, standard deviation.

A
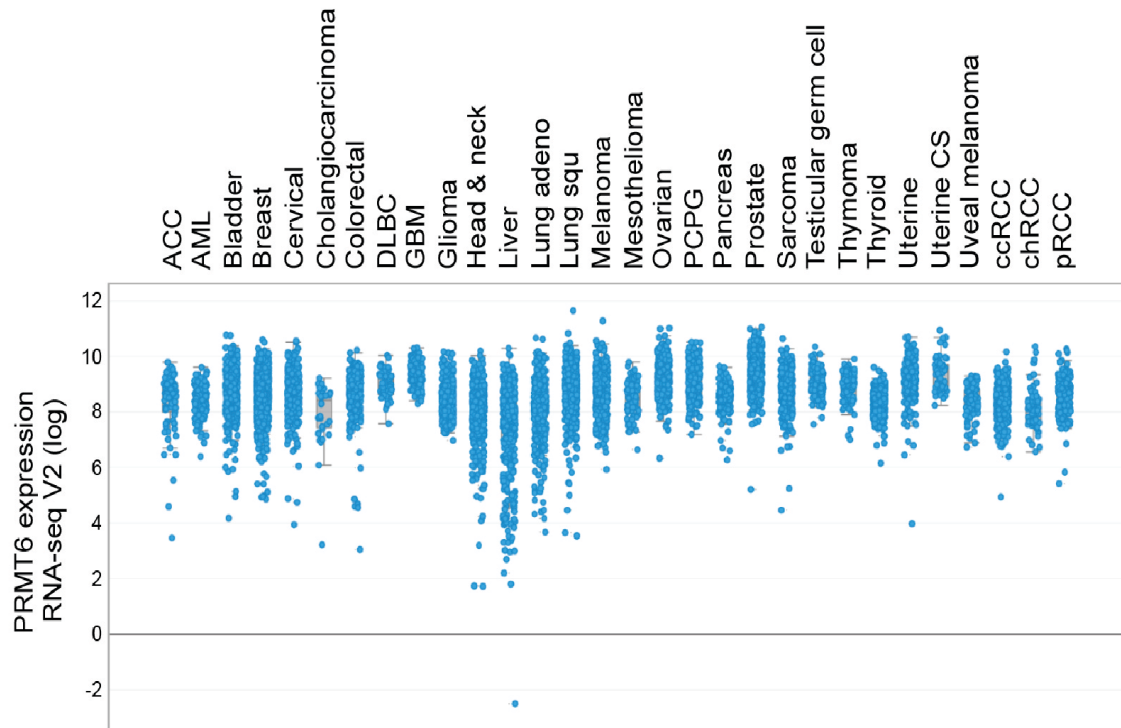
B
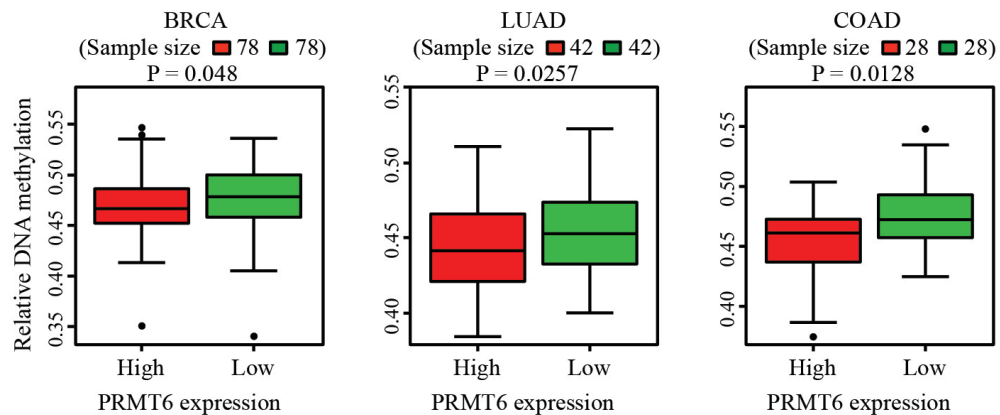
Figure 19. PRMT6 expression and correlation with DNA methylation in cancer samples from TCGA database.

A. Relative expression of PRMT6 in cancer samples in the TCGA database (from cBioPortal for Cancer Genomics). B. Correlation of PRMT6 expression and DNA methylation data in the TCGA database. BRCA, breast cancer; LUAD, lung adenocarcinoma; COAD, colorectal adenocarcinoma. Wilcoxon rank sum non-parametric test with two-tailed P values was used to determine the differences in DNA methylation levels between cancer samples with the highest (top 10%) and lowest (bottom 10%) PRMT6 expression levels in each cancer type.
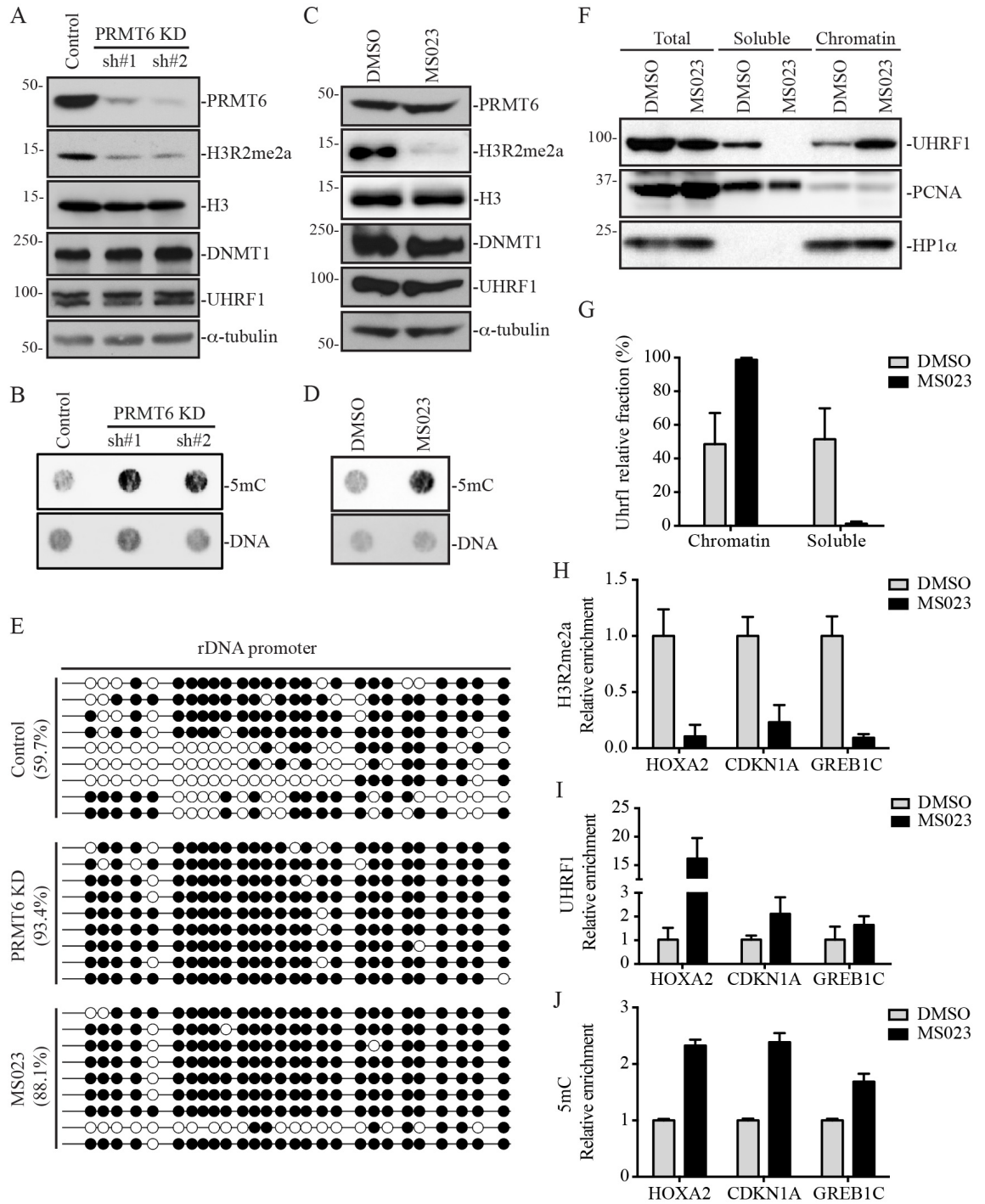
See Figure 20 legend in next page.

Figure 20. PRMT6 depletion or inhibition restores DNA methylation in MCF7 cells.

A and C. Western blot analysis of MCF7 cells stably transfected with PRMT6 shRNAs (A) or treated with MS023 (10 μM for 4 days) (C). B and D. Dot blot analysis of samples in (A) and (C), respectively, with 5mC antibody. DNA loading was verified by SYTOX Green staining. E. Bisulfite sequencing analysis of 45S rDNA promoter region containing 27 CpG sites. Open circles, unmethylated CpGs; Filled circles, methylated CpGs. F. Nuclear fractionation of MCF7 cells treated with MS023 for UHRF1 chromatin association. PCNA and HP1α were used as controls for soluble and chromatin-associated proteins, respectively. G. Quantification of data in (F) by densitometry using Image J. Shown are percentages of soluble and chromatin-associated UHRF1 in each sample (mean + SD from three independent experiments). H-J. ChIP assays or MeDIP assays showing relative enrichment of H3R2me2a (H) and UHRF1 (I) or relative DNA methylation levels (J) at HOXA2, CDKN1A and GREB1C promoter regions (mean + SD from three independent experiments). See also Figure 21.

A

Control (day 10) shRNA #1 (day 10) shRNA #2 (day 10)

B

C

DMSO MS023

Day 4

Day 9

D
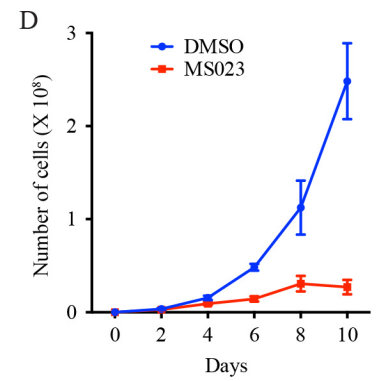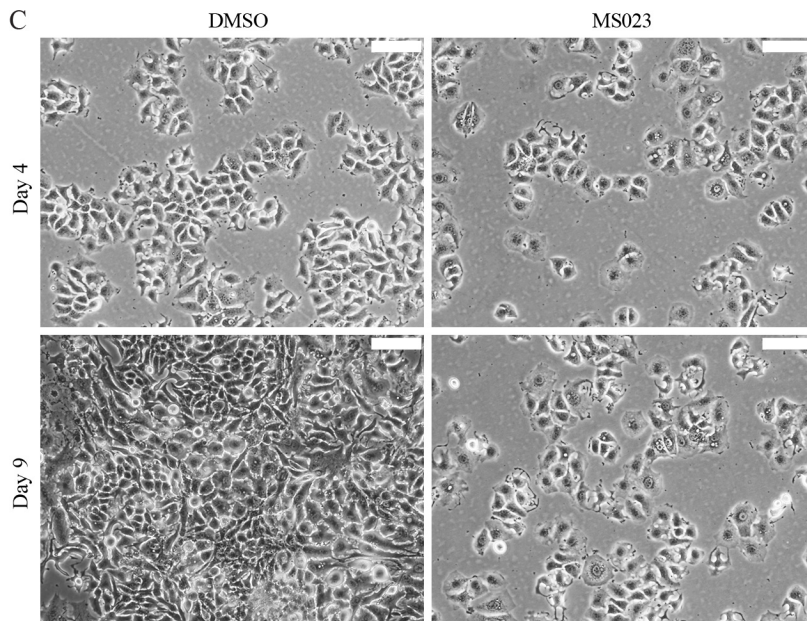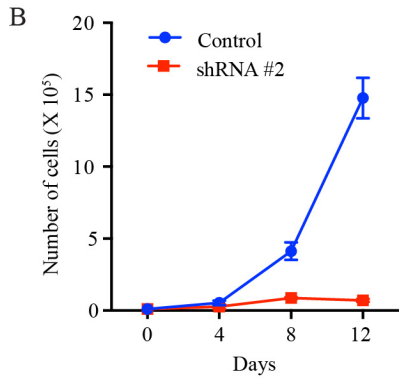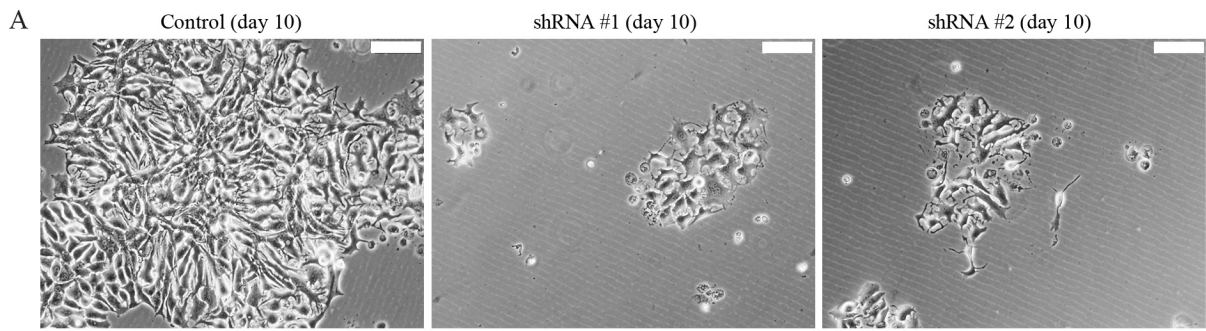
See Figure 21 legend in next page.

Figure 21. PRMT6 knockdown or inhibition in MCF7 cells leads to defects in cell proliferation.

A and B. MCF7 cells stably transfected with control or PRMT6 shRNAs were cultured for 12 days (starting at 10^4 per well), and the cells were visualized daily and counted every 4 days. Shown are representative images on day 10 (A) and the growth curves (B). Scale bars in (A), 50 μm. C and D. MCF7 cells were cultured in the presence of DMSO or MS023 (10 μM) for 10 days (starting at 10^5 per well), and the cells were visualized daily and counted every other day. Shown are representative images on day 4 and day 9 (C) and the growth curves (D). Scale bars in (C), 50 μm.

4.3 DISCUSSION

Various epigenetic mechanisms act cooperatively in regulating chromatin structure and gene activity. While it has been well established that DNA methylation and several histone modifications, notably lysine methylation, are functionally linked (189, 196), much less clear is the crosstalk between DNA methylation and arginine methylation. In this study, we demonstrate that PRMT6 is a negative regulator of DNA methylation. We show that overexpression of PRMT6 in mESCs compromises Uhrf1 association with chromatin. Consistent with biochemical and structural evidence that H3R2 methylation inhibits Uhrf1-H3 interaction (65, 66, 190-192), our results indicate that the catalytic activity of PRMT6 is required for its effect on DNA methylation. Thus, we propose that PRMT6, by generating H3R2me2a, impairs recruitment of the Dnmt1-Uhrf1 complex to newly replicated DNA, resulting in passive DNA demethylation. However, we cannot rule out the possibility that PRMT6-mediated methylation of other arginine residues on histone or non-histone proteins also contributes to DNA methylation changes. Our work uncovers a novel regulatory mechanism involved in the maintenance of DNA methylation.

While the relevance of PRMT6 in regulating DNA methylation in normal developmental and cellular processes remains to be determined, we provide evidence that PRMT6 overexpression contributes to global DNA hypomethylation in cancer cells. We show that PRMT6 expression levels inversely correlate with DNA methylation levels in both cancer cell lines and primary cancer tissues. Moreover, depletion or inhibition of PRMT6 leads to restoration of DNA methylation levels in MCF7 cells, suggesting a causal link between PRMT6 overexpression and DNA hypomethylation. It is worth noting that, while most PRMT6 high-expressing cell lines have relatively low levels of DNA methylation, some cell lines that are severely hypomethylated (e.g., MDA-MB 231, SKBR3) show no obvious PRMT6 upregulation (Figure 18A and Table 3), suggesting that multiple mechanisms are involved in DNA hypomethylation in cancer. Some of the mechanisms likely affect the functionality of the DNMT1-UHRF1 complex. UHRF1 could positively or negatively impact DNA methylation. On the one hand, UHRF1 is essential for DNMT1 recruitment to newly replicated DNA to maintain DNA methylation (50, 51). On the other hand, UHRF1, an E3 ubiquitin ligase, has been shown to ubiquitinate

83

UHRF1 itself, DNMT1 and DNMT3A, leading to their degradation (104, 106-108). UHRF1 is highly expressed in many cancers (113), which likely contributes to DNA methylation changes. Indeed, overexpression of human UHRF1 in zebrafish hepatocytes leads to Dnmt1 mislocalization and degradation, DNA hypomethylation, and hepatocellular carcinoma (109).

PRMT6 is overexpressed in multiple types of cancer. In breast cancer, PRMT6 levels positively correlate with tumor stages, suggesting that PRMT6 may contribute to tumor progression (140). Nevertheless, we observed that the benign breast cancer cell line MCF7 has higher levels of PRMT6 than the aggressive cell line MDA-MB 231 (Figure 18A), indicating that the relationship between PRMT6 expression and cancer invasiveness is complex. These differences could be attributed to the different cancer subtypes that they represent. How PRMT6 overexpression contributes to tumorigenesis remains to be determined. PRMT6 generally functions as a transcriptional repressor, although it has also been shown to act as a co-activator of nuclear receptors such as estrogen receptor (113). In this study, we demonstrate that PRMT6 contributes to DNA hypomethylation, which is another characteristic associated with cancer as it could lead to genomic instability and expression of cancer-promoting genes. Importantly, the effect of PRMT6 on DNA methylation is reversible, as depletion or inhibition of PRMT6 restores DNA methylation levels in MCF7 cells. This raises the possibility of targeting PRMT6 for specific cancer therapy. However, it remains to be determined to what extent PRMT6-dependent DNA hypomethylation contributes to tumorigenesis and maintenance of the tumor phenotype.

CHAPTER 5: Regulation of DNMT1 in intestinal stem cells

5.1 INTRODUCTION

After the establishment of DNA methylation patterns during early embryonic development by *de novo* DNMTs, these patterns are largely maintained by DNMT1 during differentiation of somatic cells, although some loci-specific changes occur in a cell-type specific manner. These DNA methylation changes are important for developmental progression and cell lineage choice, as DNA methylation is a critical component of the regulatory network that controls the gene expression program that drives proper differentiation and maintains the differentiated states (3). In postnatal mammals, DNA methylation is generally stable in most somatic tissues but shows dynamic changes in tissues with high proliferation rates such as the intestine, skin and hematopoietic compartments. In these tissues, somatic or "adult" stem cells are fundamental to maintaining tissue homeostasis, as they undergo constant proliferation, self-renewal and differentiation to give rise to the diverse cell types that form the tissue (197). The balance between adult stem cell self-renewal and differentiation is a complex process that involves various epigenetic mechanisms, including DNA methylation (93, 198-200), and its disruption is associated with development of diseases, including cancer. However, how DNA methylation is regulated in adult stem cells and its roles in self-renewal and differentiation are poorly understood.

The high cell turnover of the intestinal epithelial tissue makes it an ideal system to study adult stem cell functions in tissue regeneration, as well as the molecular mechanisms that regulate their self-renewal and differentiation for the maintenance of tissue homeostasis. This tissue is sustained by the presence of intestinal stem cells (ISCs) that reside at the bottom of the intestinal crypts, which are proliferative units embedded in the wall of the intestine (197, 201). Studies in mouse intestinal epithelium revealed that DNA methylation is required for its development. For example, Dnmt1, the highest expressed DNMT in small intestine, is essential for perinatal development of intestinal epithelial progenitors in mice, as its loss results in impaired proliferation, global DNA hypomethylation, DNA damage and apoptosis, leading to loss of villi and, ultimately, postnatal lethality (202, 203). Similarly, it has been shown that inactivation of the *DNMT1* gene in the human colon cancer cell line HCT116 results in global DNA hypomethylation, increased genomic instability and severe mitotic defects that ultimately

triggers apoptosis (63). In contrast, Dnmt1 function is different in adult small intestine, as its conditional deletion in adult ISCs results in expansion of intestinal crypts and aberrant gene expression (203, 204). Moreover, genome-wide DNA methylation analysis in ISCs showed dynamic DNA methylation at enhancers that regulate critical genes for stem cell self-renewal and differentiation, which is associated with transcription factor binding (204-206). Notably, one study showed that Dnmt1 is required to maintain the gained DNA methylation at specific ISCs enhancers upon differentiation, such as the ones that regulate expression of the genes *Olfm4* and *Hes1* (204). The striking differences observed in the mouse phenotypes after *Dnmt1* deletion in perinatal progenitors compared to adult ISCs are partially due to the compensatory effect of Dnmt3b upregulation after *Dnmt1* deletion in adult crypts (207), as in the absence of Dnmt1, crypts cells require Dnmt3b for their survival. Indeed, combined deficiency of Dnmt1 and Dnmt3b results in increased DNA damage and apoptosis, leading to severe crypt and villi degeneration (207).

Therefore, it is important to understand the role of DNA methylation in the balance between ISCs self-renewal and differentiation, as well as the molecular mechanisms that regulate its function. This is highly relevant to human diseases, as dysregulation of these epigenetic mechanisms contributes to the development of gut disorders, like inflammatory diseases and colon cancer (201). In fact, multiple studies have associated aberrant DNA methylation in ISCs with the development of colon cancer (75, 77, 208, 209). In this study, I discovered that intestinal crypts specifically express a shorter Dnmt1 protein product, which results from an endoproteolytic cleavage event. To our knowledge, this is the first example of a cleavage event as a regulatory mechanism of the DNA methylation machinery. Although the data are preliminary, better understanding of the functional relevance of this particular processing event, as well as the molecular mechanisms involved, could provide important insights into the regulation and functions of DNA methylation in ISCs.

5.2 RESULTS AND DISCUSSION

Mouse intestine express a short Dnmt1 protein product

Other than a few proteins such as Uhrf1 and PCNA, the players that regulate Dnmt1 activity and functions are largely unknown, partly because commercial Dnmt1 antibodies are not specific or not efficient for some applications (e.g. immunoprecipitation). In order to facilitate the study of Dnmt1 regulation in mouse tissues, we generated a Flag-Dnmt1 knock-in (KI) mouse by gene targeting, whereby a 3XFlag tag was introduced in exon 4 of *Dnmt1*, right after the initiation codon of Dnmt1o (Figure 22A). We expected that Dnmt1o would be tagged in oocytes and the full-length Dnmt1 would be tagged in somatic tissues. After obtaining mESC clones containing the correctly targeted allele, they were introduced into receiver blastocysts to derive chimeric mice, which were then crossed with C57BL/6J mice to obtain germline transmission of the targeted allele. Deletion of the floxed IRES-βGeo selection cassette, resulting in the functional Flag-Dnmt1 KI allele, was achieved by crossing with Zp3-Cre mice (Figure 22A).

In order to validate the expression of Flag-Dnmt1 in adult tissues, we performed western blot analysis using Flag antibody on whole protein extracts from different mouse tissues (ovary, liver, brain, colon, small intestine and lung) obtained from heterozygous KI mice and used wild-type mice tissues as controls. Unexpectedly, we were not able to detect Flag-Dnmt1 protein in small intestine (here after referred as intestine for simplicity), although it was detected in the other tissues analyzed (Figure 22B). Surprisingly, when we probed the same membrane with an antibody that recognizes endogenous Dnmt1, we observed a strong band of a significantly smaller size (~160 kDa) in intestine compared to the full-length Dnmt1 protein band (~210 kDa) observed in the rest of the tissues analyzed. Importantly, using the antibody specific for endogenous Dnmt1, we identified the same protein band in intestine obtained from wild-type mouse (Figure 5.1 B). This result indicates that the presence of the smaller Dnmt1 protein band is not an experimental artifact that resulted from the gene-targeting strategy and instead suggests that a smaller Dnmt1 protein product, which lacks part of the N-terminal region including the sequence encoded by exon 4, is specifically present in intestine.
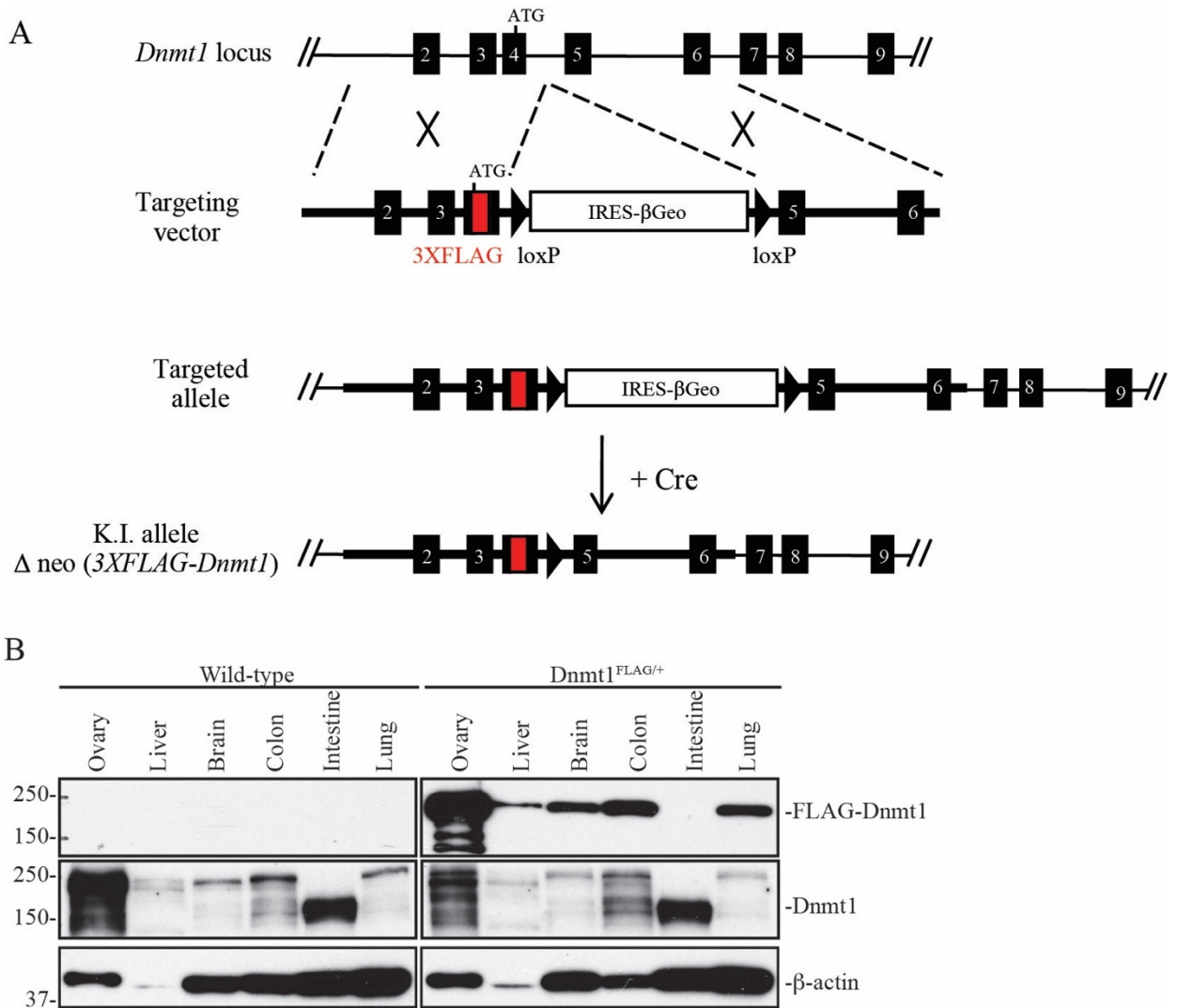
Figure 22: Generation of Flag-Dnmt1 KI allele and detection of a short Dnmt1 protein in small intestine.

A. Gene-targeting strategy for knocking in a 3XFlag tag (in red) in exon 4 of *Dnmt1*, right after the initiation codon (ATG) for Dnmt1o. *Dnmt1* exons are indicated by black boxes. LoxP sites are indicated by black triangles. The IRES-βGeo selection cassette is also shown. Cre-mediated recombination to delete the selection cassette results in the generation of the active KI allele. B. Confirmation of the expression of FLAG-Dnmt1 in different tissues of the KI mouse by western blot using Flag tag antibody. Detection of short Dnmt1 in small intestine is shown using endogenous Dnmt1 antibody, while β-actin is used as loading control.

The short Dnmt1 protein is not due to alternative splicing or different translation start site usage

To determine what level of regulation gives rise to the intestine-specific small Dnmt1 protein product, we first investigate whether the short Dnmt1 results from alternative mRNA splicing. To this end, we isolated total RNA from purified intestinal crypts, as well as from mESCs as a control, and detected by RT-qPCR the presence of transcripts containing different exons encoding amino acids located at the N-terminal region of Dnmt1. We designed primer pairs to amplify fragments covering exons 4 to 6, or 5 to 8, and as control we amplified fragments covering exons 25 and 26 located in the middle of Dnmt1 protein and exons 33 and 34 located at the C-terminal region of the protein (Figure 23A). Our results indicate that all the exons examined were detected in mRNA from intestinal crypts, as well as from mESCs (Figure 23B). We confirmed by sequencing that *Dnmt1* mRNA transcripts from intestinal crypts and mESCs were identical. Together, our data indicates that the short Dnmt1 protein product does not result from alternative mRNA splicing.

Dnmt1o, the oocyte-specific isoform, originates from alternative promoter usage and, as a result, a downstream AUG in exon 4 is used as the translation initiation codon, which results in the lack of 118 amino acids at the N terminus of the full-length DNMT1 (Figure 23A). We therefore investigated whether the usage of a downsteam translation initiation codon would produce the small Dnmt1 protein detected in intestine. To this end, we generated four different constructs using downstream AUG codons with potential Kozak sequences as the translation initiation sites. We expressed these N-terminally truncated Dnmt1 proteins in *Dnmt1* KO mESCs and compared their protein sizes with that of the short Dnmt1 product in intestine by western blot. As shown in Figure 23C, all the constructs generated protein products that were smaller than the short Dnmt1 protein observed in intestinal crypts. These results indicate that it is unlikely that the intestine-specific short Dnmt1 protein product is generated by the usage of an alternative translation initiation codon.

To determine whether the KI allele produces any Flag-tagged protein product in intestine, we performed immunohistochemistry analysis of intestine tissue sections from a Flag-Dnmt1 KI homozygous mouse using a Flag antibody, which detected signal in the intestinal crypts (Figure 23D, left panel). The position of the Flag-positive cells in the crypts indicates that these cells are composed of

90

ISCs (green arrowheads) and transient-amplifying (TA) progenitors (red arrowheads), consistent with the fact these are proliferative populations that express high levels of Dnmt1 (204). Importantly, the cell localization patterns detected with the Flag immunohistochemistry staining was highly similar to the patterns observed in the staining of wild-type intestine with an antibody for endogenous Dnmt1, which recognizes an epitope located at the middle of the protein (Figure 23D, right panel). Together, these results indicates that the missing N-terminal protein fragment from intestinal Dnmt1 is likely present in the intestinal crypts of Flag-Dnmt1 KI mouse, suggesting that the smaller Dnmt1 protein, which lacks this fragment, may result from post-translational processing of the full-length Dnmt1 in these cells.
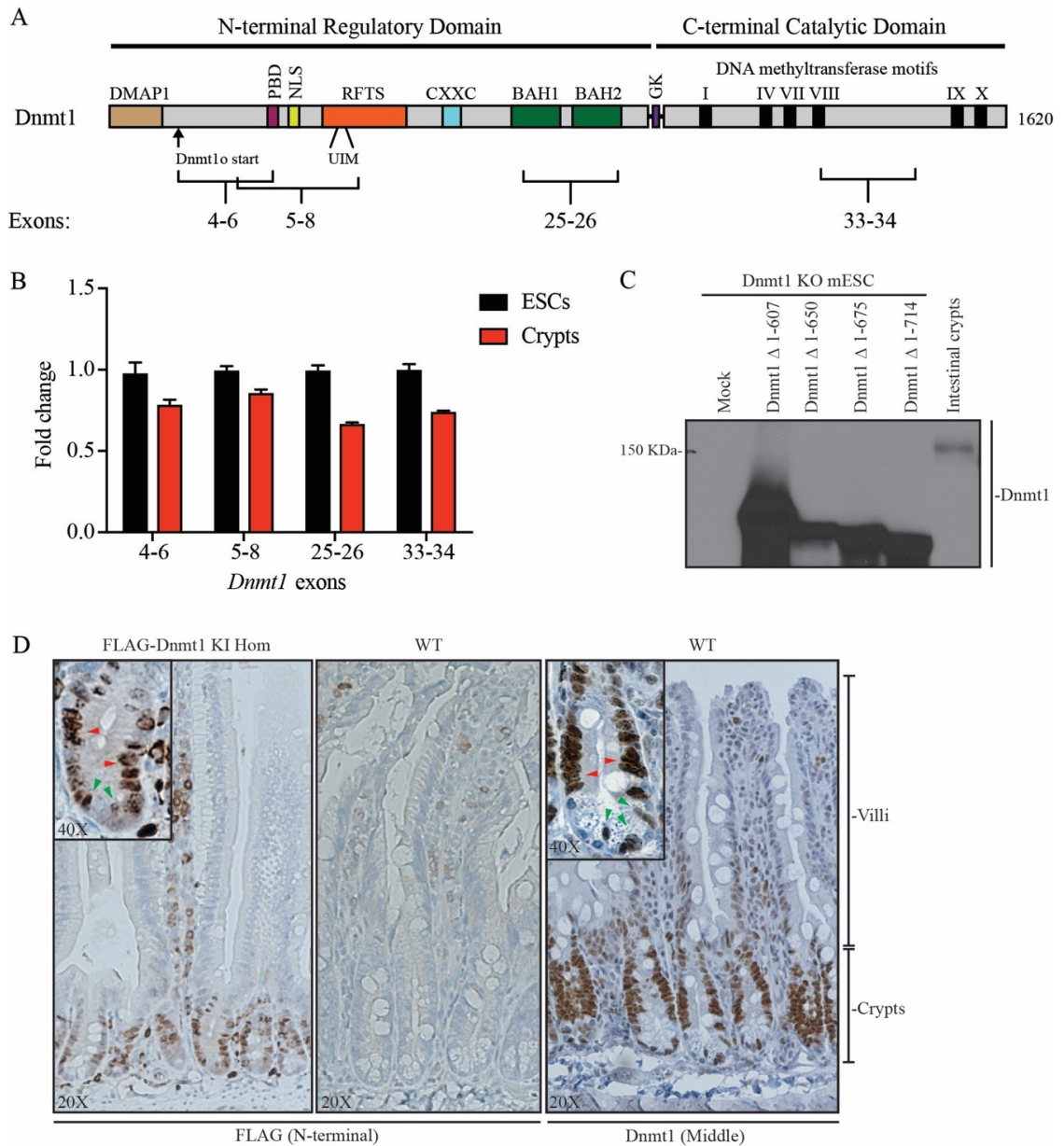
Figure 23: Short intestinal Dnmt1 is not due to alternative splicing or different translation start site usage. A. Diagram of mouse Dnmt1 protein indicating domains and position of exons analyzed by RT-qPCR. B. RT-qPCR results showing the presence of the indicated exons in *Dnmt1* mRNA from intestinal crypts compared to mESCs. C. Western blot indicating that the truncated Dnmt1 proteins generated from potential downstream translation start sites are smaller than the Dnmt1 product detected in intestine. D. Immunohistochemistry analysis of intestine sections with Flag and Dnmt1 antibodies showing both Flag and Dnmt1 signals in intestinal crypts. Green arrowheads, ISCs. Red arrowheads, TA cells.

The intestinal Dnmt1 protein product is generated by an endoproteolytic cleavage event.

Our data indicated that the intestinal short Dnmt1 protein was not produced by alternative mRNA splicing or alternative translation initiation codon usage. Moreover, analysis of Dnmt1 localization in the intestinal crypts suggested that the N-terminal fragment containing the Flag tag was present in cells that express Dnmt1 (Figure 23). Based on these data, we hypothesized that the smaller intestinal Dnmt1 could be caused by a post-translational processing event, such as endoproteolytic cleavage. To test this hypothesis, we examined for the presence of small protein fragments by western blot using different antibodies that recognize epitopes located in the N-terminal or middle region of Dnmt1, as well as Flag antibody. For this analysis, we compared intestinal crypts purified from wild-type mouse, with intestine and colon tissue from a Flag-Dnmt1 KI homozygous mouse. As a control, we used full-length Dnmt1 expressed in *Dnmt1* KO mESCs. Our results confirmed that both purified intestinal crypts and intestine tissue had the short Dnmt1 protein, as the ~160-kDa protein band was detected in both samples using the antibody that recognizes the middle region of Dnmt1 (Figure 24A, left panel). In contrast, colon tissue showed a band of the corresponding size of full-length Dnmt1 (~210 kDa), as observed in mESCs expressing Dnmt1 full-length protein. Notably, western blot analysis using the antibody that recognizes the N-terminal region of the Dnmt1 revealed that the samples corresponding to intestinal crypts and intestine tissue also had the protein band corresponding to the size of full-length Dnmt1, although their levels were lower compared to colon or mESCs (Figure 24A, right panel). Importantly, a small protein fragment of ~50 KDa was detected using this antibody in crypts, intestine and colon samples (Figure 24A, right panel). Similar results were obtained using Flag antibody (Figure 24A, middle panel). Taken together, these results indicate that Dnmt1 undergoes an endoproteolytic cleavage event that results in the short Dnmt1 protein product of ~160 KDa and an N-terminal protein fragment of ~50 KDa in intestine and, to a lesser extent, in colon.

The western blot and immunohistochemistry results suggest that both uncleaved full-length and cleaved Dnmt1 proteins are present in cells at intestinal crypts. Different possibilities can be envisioned regarding the functionality. For example, it is possible that the Dnmt1 protein is not immediately cleaved after protein synthesis and thus it resides in the cells for certain period of time, until the cleavage event

occurs as part of an unknown regulatory mechanism. A second possibility, which is not mutually exclusive from the first possibility, is that the short N-terminal protein fragment that results from the Dnmt1 cleavage event may have its own unidentified biological function. The second possibility is particularly intriguing, given that the small N-terminal fragment is relatively stable rather than being further processed and rapidly degraded. There are some documented examples that protein fragments have independent and different functions from the original protein from where they originate. For example, TET2 has lost its CXXC domain during evolution, as a result of a chromosomal inversion event that has converted a portion of the ancestral *TET2* gene into a separate gene, *IDAX*, which encodes a protein containing the original CXXC domain. IDAX binds unmethylated CpG sequences via its CXXC domain, localizes at CGIs, and physically interacts with TET2, suggesting that it may play a role in recruiting TET2 to its genomic targets (210). Although this is strictly not a similar case as with intestinal Dnmt1, it is possible that evolution has found a different way of generating a protein fragment with possible regulatory functions by cleaving the N-terminal region of Dnmt1. However, the functional significance of this cleavage event requires further investigation.

An important step to determine the functional significance of Dnmt1 cleavage in intestine is to elucidate the molecular mechanism underlying this processing event. To this end, we first aimed to identify the precise site and amino acid motif sequence where the cleavage event occurs. For this purpose, we immunoprecipitated both the full-length Flag-Dnmt1 and the cleaved N-terminal Flag-fragment from intestinal crypts purified from Flag-Dnmt1 KI homozygous mouse (Figure 24B) and submitted the samples for mass spectrometry analysis. Mapping of the peptides identified from the full-length Flag-Dnmt1 indicated that 94 exclusive unique peptides were successfully identified and mapped to the Dnmt1 amino acid sequence accounting for a 54% coverage (Figure 24C-D), while only 9 exclusive unique peptides were successfully identified in the cleaved N-terminal Flag-fragment, which correspond to 8% coverage of Dnmt1 amino acid sequence (Figure 24C and E). The most downstream peptide mapped from the cleaved N-terminal Flag-fragment (SKEDPDREARPE) ended at Glu265 of Dnmt1 (Figure 24E). Based on the sizes of the cleaved N-terminal fragment (~50 kDa) and the remaining Dnmt1 protein product (~160 kDa), we estimated that the cleavage site is around residue 450.

Interestingly, the N-terminal ~450-amino-acid region containing several conserved domains (Figure 23A). For example, this region contains the sequences required for the interaction with DMAP1, Dnmt3a, Dnmt3b and the PRC2/Eed-Ezh2 complex. Of these, it has been suggested that the interaction with DMAP1 regulates Dnmt1 stability, as the DMAP1-interaction domain (residues 1 to 120) is also not present in the more stable DNMT1o isoform (53). Moreover, the missing N-terminal fragment from intestinal Dnmt1 also contains the PBD region (residues 161 to 172), which mediates the interaction between Dnmt1 and PCNA, and the NLS motif (residues 175 to 202) (8). Together, these results suggest that the short intestinal Dnmt1 protein lacks a region that harbors important motifs required for the interaction with proteins that play different regulatory functions such as interaction with the DNA replication machinery, localization and stability.

Furthermore, the cleaved N-terminal fragment of intestinal Dnmt1 contains several sites that are modified by different PTMs, most notably serine phosphorylation. In fact, phosphorylation of one of these serine residues (Ser143 in human DNMT1, equivalent to Ser140 in mouse Dnmt1) by Akt1 has been implicated in Dnmt1 stabilization, while methylation of the adjacent lysine residue (Lys142 in human DNMT1, Lys139 in mouse Dnmt1) by Set7/9 was associated with Dnmt1 degradation (211). In addition, this cleaved fragment might also be required for the homodimerization of Dnmt1, which has been reported to be mediated by head to head interaction of the N-terminal domains (212).

A

Dnmt1 KO mESC | FLAG-Dnmt1 KI Hom | Dnmt1 KO mESC | FLAG-Dnmt1 KI Hom | Dnmt1 KO mESC | FLAG-Dnmt1 KI Hom

Mock | Dnmt1 F.L. | Intest. Crypts (WT) | Intestine | Colon

250 KDa-
150 KDa-
100 KDa-
75 KDa-
50 KDa-
37 KDa-

← Dnmt1 F.L.
← short Dnmt1
← N-terminal protein fragment

WB: Dnmt1 (Middle) CST | FLAG (N-terminal) Sigma | Dnmt1 (N-terminal) Novus Bio.

B

Flag IP

250 KDa-
150 KDa-
100 KDa-
75 KDa-
50 KDa-
37 KDa-

← Flag-Dnmt1 F.L. uncleaved
← Flag-N-terminal cleaved fragment

C

Flag-Dnmt1 F.L. uncleaved (54%)

Flag-N-terminal cleaved fragment (8%)

D

E

See Figure 24 legend in next page.

96

Figure 24: Mouse intestinal Dnmt1 protein product was generated by an endoproteolytic cleavage event.

A. Western blot of Dnmt1 protein products in extracts from purified intestinal crypts, intestine and colon, compared to full-length Dnmt1 transfected into *Dnmt1* KO mESCs as control. Arrows indicate the position of Flag-Dnmt1 full-length (F.L.), short Dnmt1 and the N-terminal protein fragment. B. Flag immunoprecipitation of intestinal Flag-Dnmt1 full-length uncleaved protein and cleaved Flag-N-terminal protein fragment from intestinal crypts purified from Flag-Dnmt1 KI homozygous mouse. Gel was stained with Coomasie Blue and the indicated protein bands were excised and analyzed by mass spectrometry (MS). C. Protein sequence coverage by the MS analysis of both the Flag-Dnmt1 uncleaved protein and the cleaved N-terminal protein fragment. D. Peptides detected in MS analysis (yellow) from the full-length Flag-Dnmt1 uncleaved protein mapped to Flag-Dnmt1 knock-in amino acid sequence. E. Peptides detected in MS analysis (yellow) from the cleaved N-terminal protein fragment mapped to Flag-Dnmt1 knock-in amino acid sequence.

Global DNA methylation in intestine is not significantly different from that in other tissues.

The results described above suggest that the N-terminal cleavage of intestinal Dnmt1 might have regulatory implications, as the cleaved fragment contains important regulatory domains that mediate protein interactions and specific residues that are likely subjected to PTMs with regulatory functions. Therefore, it is reasonable to hypothesize that intestinal short Dnmt1 protein could have different DNA methylation activity. To test this hypothesis, we first analyzed DNA methylation levels using the methylation-sensitive restriction enzymes *Hpa*II and *Mae*II, followed by southern blot hybridization at the centromeric and pericentric heterochromatic regions of minor satellite repeats and major satellite repeats, respectively. We compared DNA purified from intestine, colon, brain and liver tissues and from purified intestinal crypts with *Dnmt1* KO or wild-type mESCs as controls. DNA methylation analysis at minor satellite repeats failed to detect any significant difference in DNA methylation levels in mouse tissues, purified crypts, and mESCs (Figure 25A). In contrast, when DNA methylation levels at major satellite repeats were analyzed, we detected a lower level of DNA methylation in the colon tissue sample, while no difference was observed for the rest of the tissues (Figure 25B). We further analyzed total levels of DNA methylation by dot blot analysis using 5mC specific antibody, in this case comparing DNA samples obtained from brain, lung, liver, intestine, colon and ovary. Our results showed that DNA methylation was slightly higher in intestine compared to the rest of the tissues, and that the lowest levels of DNA methylation were detected in colon (Figure 25C), as similarly observed with major satellite repeats methylation analysis.

Despite this interesting observation, more quantitative and specific experiments, such as quantification of total 5mC by LC-MS/MS and genome-wide DNA methylation analysis by WGBS, would confirm whether DNA methylation is significantly different in intestine compared to other tissues. If this turn out to be the case, it might be possible that intestinal Dnmt1 acquires enhanced stability through the cleavage of its N-terminal, similarly as the more stable Dnmt1o that lacks the first 118 amino acids including the DMAP1 interacting domain (53). However, this hypothesis requires further investigation.

In summary, our finding that Dnmt1 is post-translationally processed in intestine is intriguing but preliminary. Determining the molecular mechanism and biological significance of this cleavage event would contribute to the understanding of the regulation of DNA methylation in intestinal tissue and the role that this plays in maintaining intestinal epithelial homeostasis and regeneration.
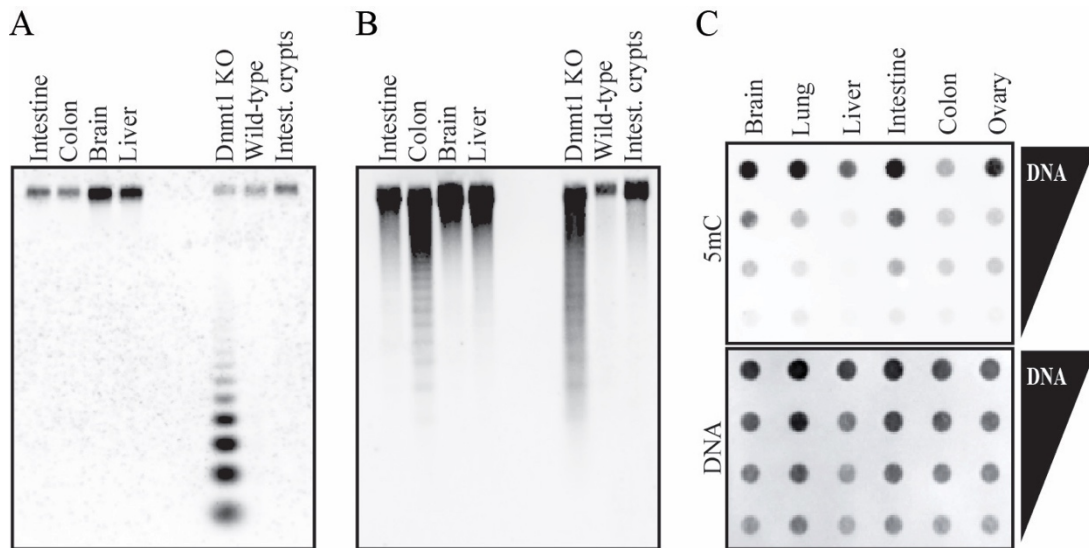
Figure 25: DNA methylation analysis in mouse tissues.

DNA methylation analysis by digestion with methylation-sensitive enzymes and southern blot hybridization for the minor satellite repeats (A) or major satellite repeats (B), in mouse tissues compared to mESCs. *Dnmt1* KO and wild-type mESC were used as controls. C. Analysis of total DNA methylation levels by dot blot using 5mC specific antibody in different mouse tissues. Total DNA was stained with Sytox Green Dye as loading control.

CHAPTER 6: DISCUSSION

A complex network of different types of epigenetic mechanisms control the structure and functions of chromatin that is fundamental for multiple biological processes. DNA methylation, which is present in many eukaryotic organisms, is an important component of the network (196). In mammals, DNA methylation is essential for a variety of biological functions, and its dysregulation plays major roles in the development of multiple human diseases (3, 165). Since the discovery of DNA methylation more than 60 years ago (1), extensive research in this epigenetic modification has elucidated most of its functions (5). However, many aspects of the regulation of DNA methylation remain poorly understood.

The regulation of DNA methylation is complex, which occurs at different levels, including the production of multiple DNMT isoforms. For example, as described earlier in section 1.2, DNMT3A has two major isoforms, the full-length DNMT3A1 that is ubiquitously expressed at low levels in most somatic cells, and a shorter isoform known as DNMT3A2 (Figure 2), which is highly expressed in mESCs and germ cells. DNMT3A1 is highly enriched and tightly associated with heterochromatin, and DNMT3A2 is more widely distributed on and less tightly bound to chromatin (213). In the case of the DNMT3B, alternative splicing generates more than 30 isoforms, many of which lack catalytic activity but might play regulatory roles (26). For instance, mESCs mainly express the full-length catalytically active isoform DNMT3B1 and the inactive DNMT3B6, while somatic cells mainly express DNMT3B2 and DNMT3B3, which are active and inactive isoforms, respectively (18, 213). In addition, three different isoforms of DNMT3L are expressed from cell-specific promoters at different developmental stages (180). Similarly, as described in detail in section 1.3, DNMT1 also express two major cell-specific isoforms, the full-length DNMT1 is expressed in somatic cells, while the shorter isoform DNMT1o is produced exclusively in oocytes (Figure 2) (8). In **Chapter 5** of this dissertation, I described the identification of a new DNMT1 protein product, which is specifically present in mouse intestine. In clear contrast to the other known DNMTs isoforms that are generated by alternative splicing or different promoter usage, this new DNMT1 protein is generated by cleavage of the N-terminal region of the full-length DNMT1 in intestinal stem cells (ISCs) (Figure 24). Endoproteolytic cleavage is a posttranslational

processing event that regulates the activity of a great number of proteins involved in multiple physiological functions, including signal transduction pathways or activation of apoptosis (214, 215). For example, in the Notch signaling pathway, the cleavage of the intracellular domain of the receptor is required for its nuclear translocation, where it binds to transcription factors and activates gene expression (214). In addition, proteolytic cleavage is also used to activate caspases from its pro-caspase inactive form, which in turn are responsible for the cleavage of multiple substrates to trigger apoptosis (215). To the best of my knowledge, the cleavage of the N-terminal region of DNMT1 is the first example of this kind of processing occurring in proteins involved in DNA methylation. Although the precise point of cleavage remains to be determined, the size of the cleaved fragment suggests that the resultant DNMT1 protein product, like Dnmt1o, would lack the functional domain that mediates the interaction with DMAP1. Dnmt1o has been shown to be more stable than the full-length Dnmt1 (53). It is therefore possible that this cleavage event is functionally important for ISCs, which are actively proliferating, unlike most adult stem cells that are generally quiescent. However, further biochemical, cellular and genetic studies are required to determine the biological role and functional significance of this event.

DNA methylation can also be regulated by DNMT-interacting proteins and cofactors. For instance, as described in section 1.2, *in vitro* studies demonstrate that DNMT3L serves as a cofactor for both DNMT3A and DNMT3B, as it enhances their catalytic activity to similar extent (166-168). However, the *in vivo* function of DNMT3L seems to be very different, as genetic studies in mice showed that *Dnmt3L* deletion results in infertility (42, 44, 45), while this phenotype was only recapitulated by the conditional deletion of *Dnmt3a*, but not *Dnmt3b*, in the germ line (35). These genetic evidences suggest that the functions of DNMT3L *in vivo* are more likely associated with DNMT3A activity, rather than DNMT3B activity. What determines the functional specificity of Dnmt3L is not well understood. In **Chapter 3** of this dissertation, I addressed this issue using mESCs, which express high levels of DNMT3A, DNMT3B and DNMT3L, consistent with the high rate of *de novo* DNA methylation observed in these cells (32). By genome-wide DNA methylation analysis, I found that a significant fraction of the genome is hypomethylated in DNMT3L-deficient mESCs, with the majority of hypomethylated CpG sites being DNMT3A targets (Figure 8). Importantly, I found that DNMT3L is

critical for DNMT3A (especially DNMT3A2) protein stability through direct interaction and the formation of the DNMT3L-DNMT3A2 complex (Figure 12). Therefore, in the absence of DNMT3L, DNMT3A2 protein becomes unstable and is rapidly degraded, leading to DNA hypomethylation at DNMT3A-specific loci. These findings, described in **Chapter 3,** uncover a new role for DNMT3L in the regulation of DNMT3A function, which provides a plausible explanation for the functional specificity of DNMT3L *in vivo* (Figure 13C). My results also confirmed that DNMT3L is predominantly a positive regulator of *de novo* methylation, contrary to a recent report showing that DNMT3L regulates DNA methylation positively or negatively, depending on genomic regions, in mESCs (49).

While DNMT3L is an important regulator of *de novo* DNA methylation, UHRF1 is essential for maintenance DNA methylation by directing DNMT1 to hemi-methylated CpG sites generated during DNA replication (50, 51). Multiple studies have explored the regulation of UHRF1 functions in the modulation of DNA methylation using mESCs as a model system. For example, a recent study from our laboratory, which I contributed to, showed that UHRF1 degradation is responsible for global DNA hypomethylation in a small population, known as 2C-like mESCs, and that this event is essential for the maintenance of telomere homeostasis and long-term self-renewal of mESCs (148). Another study showed that mESCs cultured in 2i medium, which maintains mESCs in the ground naïve state (216), show global DNA hypomethylation due, at least in part, to reduction of UHRF1 at the protein level (217). The role of UHRF1 in DNA methylation is complex, as it can act either as a positive regulator by serving as a DNMT1 cofactor or as a negative regulator through its E3 ligase-mediated degradation of UHRF1 itself and DNMT1. For instance, UHRF1 is frequently upregulated in cancer, and overexpression of UHRF1 experimentally can induce global DNA hypomethylation and tumorigenesis (109). Together, all these findings indicate that UHRF1 is a major point of regulation in inducing changes in global DNA methylation during normal development and in diseases.

In **Chapter 4** of this dissertation, I provided evidence that global DNA methylation can also be altered by regulating UHRF1 chromatin association. UHRF1 has different domains that recognize epigenetic modifications, which play critical roles in its regulation through a complex crosstalk between DNA methylation and different histone modifications (196). Previous biochemical studies showed that

the PHD finger of URHF1, which is slightly different from other PHD fingers that usually bind to trimethylated lysine residues in histones (e.g. H3K4me3) (218), instead binds to unmodified H3R2, but not methylated H3R2 (65). My work, described in **Chapter 4**, extended the previous finding by demonstrating that H3R2 methylation has a major effect on DNA methylation. Specifically, I showed that PRMT6, an enzyme responsible for H3R2me2a, negatively regulates global DNA methylation by impairing the recruitment of UHRF1 to chromatin. My finding uncovers a functional and mechanistic link between histone arginine methylation and DNA methylation, an area we are largely ignorant about, unlike the crosstalk between histone lysine methylation and DNA methylation, which has been well established (196). Notably, PRMT6 is highly overexpressed in cancer cells, which also exhibit global DNA hypomethylation as a characteristic epigenetic feature (4, 113). Based on the evidence, I further explored the connection between these two molecular alterations in cancer cells. The results obtained indicate that PRMT6 is indeed upregulated in both cancer cell lines and in many primary tumor samples, and that this upregulation correlates with global DNA hypomethylation in cancer (Figure 18). Importantly, I was also able to demonstrate that the effect of PRMT6 on DNA methylation is reversible in cancer cells, as depletion of PRMT6 protein or inhibition of its enzymatic activity leads to restoration of DNA methylation levels in MCF7 cells, a breast cancer cell line with high expression of PRMT6 (Figure 20). This finding has important translational implications, as it raises the possibility of targeting PRMT6 for cancer therapy. In addition, recent studies showed that the combination of the DNMT inhibitor 5-azacitidine (5-Aza) with immune checkpoint blockade therapy (anti-CTLA-4 and anti-PD-L1) have important synergistic anti-tumor effects (219-226). My findings demonstrate that similarly to 5-aza, PRMT6 overexpression causes global DNA hypomethylation in cancer cells. This can be advantageous to clinicians, as the effect of DNA hypomethylation is specifically restricted to cancer cells, unlike 5-aza that is delivered systemically and has important side effects. It will be interesting to explore whether tumors with PRMT6 upregulation are more sensitive to immune checkpoint therapy and whether PRMT6 levels can be used for patient stratification for the choice of therapies.

In summary, my work led to the following key conclusions: i. DNMT3L is a positive regulator of *de novo* DNA methylation in mESCs that mainly affects DNMT3A target regions; ii. The functional specificity of DNMT3L is largely conferred by its role in stabilizing DNMT3A2 protein; iii. PRMT6 negatively regulates maintenance DNA methylation by impairing the recruitment of the UHRF1-DNMT1 complex to chromatin; iv. PRMT6 upregulation contributes to global DNA hypomethylation in cancer cells; v. PRMT6-induced DNA hypomethylation is reversible in cancer cells; and vi. Intestinal stem cells produce a shorter DNMT1 protein due to endoproteolytic cleavage. These findings expand the knowledge on the regulation of DNA methylation in mammalian development and cancer.

Future directions

The research findings described in this dissertation suggest important potential avenues for further research in the future. For instance, the presence of DNMT3L and DNMT3A is essential for the establishment of genomic imprints in germ cells, as their deletion in these cells show almost identical phenotypes (35, 42, 44, 45). Given its ability to stimulate DNMT3A activity *in vitro*, DNMT3L is generally assumed to function primarily as a catalytic cofactor of DNMT3A. Based on my findings reported in **Chapter 3**, it is likely that DNMT3L plays a critical role in stabilizing DNMT3A2 in germ cells as well (DNMT3A2 is the major DNMT3A isoform in the germ line). It will be interesting to examine the levels of DNMT3A2 in prospermatogonia and growing oocytes in DNMT3L KO mice and determine the significance of DNMT3A2 degradation (if proved true) in the phenotypes associated with DNMT3L deficiency, including the failure to establish germ line imprints.

It is well established that various epigenetic mechanisms function cooperatively in regulating chromatin structure and functions. The crosstalk between arginine methylation and DNA methylation has been an understudied area. My work described in **Chapter 4** indicates that PRMT6-mediated H3R2me2a is an epigenetic modification that negatively regulates DNA methylation and that dysregulation of this mechanism contributes to global DNA hypomethylation in cancer cells. Many questions remain to be answered. For example, it will be important to determine whether the mechanism is relevant in the regulation of DNA methylation in normal developmental and cellular processes. Given its dramatic

105

effect on global DNA methylation, it will be particularly interesting to investigate whether PRMT6 expression and function are dynamically regulated and whether it plays a critical role in epigenetic reprogramming events during early embryogenesis and in germ cells.

Moreover, global DNA hypomethylation is a common epigenetic alteration observed in cancer cells that has been associated with tumorigenesis (4). In addition, PRMT6 is frequently overexpressed in cancer cells, and several studies propose multiple roles implicating it in malignant transformation (113). In **Chapter 4**, I described the identification of a correlation between PRMT6 upregulation and global DNA hypomethylation in cancer cells, and provided evidence for the molecular mechanism involved. However, it remains to be investigated whether PRMT6-dependent DNA hypomethylation plays a major role in the formation and/or progression of tumors. The answer to this question could advance our understanding of the importance of DNA methylation in oncogenesis and provide further information regarding the relevance of targeting this mechanism for therapeutic purposes.

Finally, in **Chapter 5** of this dissertation, I described the finding of a short DNMT1 protein product present specifically in intestinal stem cells, which results from an endoproteolytic cleavage event. However, multiple issues remain to be addressed. The most important is to elucidate the biological significance of this event, together with the elucidation of the molecular mechanisms underlying this process (e.g. the enzyme(s) involved). Intestinal stem cells are very important to maintain tissue homeostasis in the gut, and they have been implicated in the development of colon cancer. Determining the function, mechanism and significance of this unique DNMT1 protein product could shed light on the functions of intestinal stem cells.

Exploration of these research questions would further contribute to our understanding of the regulation of DNA methylation in mammalian development and human diseases.

BIBLIOGRAPHY

1.   Hotchkiss, R. D. 1948. The quantitative separation of purines, pyrimidines, and nucleosides by paper chromatography. *J Biol Chem* 175: 315-332.

2.   Patil, V., R. L. Ward, and L. B. Hesson. 2014. The evidence for functional non-CpG methylation in mammalian cells. *Epigenetics* 9: 823-828.

3.   Smith, Z. D., and A. Meissner. 2013. DNA methylation: roles in mammalian development. *Nat Rev Genet* 14: 204-220.

4.   Baylin, S. B., and P. A. Jones. 2016. Epigenetic Determinants of Cancer. *Cold Spring Harb Perspect Biol* 8.

5.   Jones, P. A. 2012. Functions of DNA methylation: islands, start sites, gene bodies and beyond. *Nat Rev Genet* 13: 484-492.

6.   Holliday, R., and J. E. Pugh. 1975. DNA modification mechanisms and gene activity during development. *Science* 187: 226-232.

7.   Riggs, A. D. 1975. X inactivation, differentiation, and DNA methylation. *Cytogenetics and cell genetics* 14: 9-25.

8.   Chen, T., and E. Li. 2004. Structure and function of eukaryotic DNA methyltransferases. *Curr Top Dev Biol* 60: 55-89.

9.   Barau, J., A. Teissandier, N. Zamudio, S. Roy, V. Nalesso, Y. Herault, F. Guillou, and D. Bourc'his. 2016. The DNA methyltransferase DNMT3C protects male germ cells from transposon activity. *Science* 354: 909-912.

10.   Goll, M. G., F. Kirpekar, K. A. Maggert, J. A. Yoder, C. L. Hsieh, X. Zhang, K. G. Golic, S. E. Jacobsen, and T. H. Bestor. 2006. Methylation of tRNAAsp by the DNA methyltransferase homolog Dnmt2. *Science* 311: 395-398.

11.   Zhao, H., and T. Chen. 2013. Tet family of 5-methylcytosine dioxygenases in mammalian development. *J Hum Genet* 58: 421-427.

12.   Wu, H., and Y. Zhang. 2014. Reversing DNA methylation: mechanisms, genomics, and biological functions. *Cell* 156: 45-68.

13.   Tahiliani, M., K. P. Koh, Y. Shen, W. A. Pastor, H. Bandukwala, Y. Brudno, S. Agarwal, L. M. Iyer, D. R. Liu, L. Aravind, and A. Rao. 2009. Conversion of 5-methylcytosine to 5-hydroxymethylcytosine in mammalian DNA by MLL partner TET1. *Science* 324: 930-935.

14.   Ito, S., A. C. D'Alessio, O. V. Taranova, K. Hong, L. C. Sowers, and Y. Zhang. 2010. Role of Tet proteins in 5mC to 5hmC conversion, ES-cell self-renewal and inner cell mass specification. *Nature* 466: 1129-1133.

15.   Ito, S., L. Shen, Q. Dai, S. C. Wu, L. B. Collins, J. A. Swenberg, C. He, and Y. Zhang. 2011. Tet proteins can convert 5-methylcytosine to 5-formylcytosine and 5-carboxylcytosine. *Science* 333: 1300-1303.

16.   He, Y. F., B. Z. Li, Z. Li, P. Liu, Y. Wang, Q. Tang, J. Ding, Y. Jia, Z. Chen, L. Li, Y. Sun, X. Li, Q. Dai, C. X. Song, K. Zhang, C. He, and G. L. Xu. 2011. Tet-mediated formation of 5-carboxylcytosine and its excision by TDG in mammalian DNA. *Science* 333: 1303-1307.

17.   Smallwood, S. A., and G. Kelsey. 2012. De novo DNA methylation: a germ cell perspective. *Trends Genet* 28: 33-42.

18.   Okano, M., S. Xie, and E. Li. 1998. Cloning and characterization of a family of novel mammalian DNA (cytosine-5) methyltransferases. *Nat Genet* 19: 219-220.

19.   Baubec, T., D. F. Colombo, C. Wirbelauer, J. Schmidt, L. Burger, A. R. Krebs, A. Akalin, and D. Schubeler. 2015. Genomic profiling of DNA methyltransferases reveals a role for DNMT3B in genic methylation. *Nature* 520: 243-247.

20.   Chen, T., N. Tsujimoto, and E. Li. 2004. The PWWP domain of Dnmt3a and Dnmt3b is required for directing DNA methylation to the major satellite repeats at pericentric heterochromatin. *Mol Cell Biol* 24: 9048-9058.

21.   Dhayalan, A., A. Rajavelu, P. Rathert, R. Tamas, R. Z. Jurkowska, S. Ragozin, and A. Jeltsch. 2010. The Dnmt3a PWWP domain reads histone 3 lysine 36 trimethylation and guides DNA methylation. *J Biol Chem* 285: 26114-26120.

22.   Ooi, S. K., C. Qiu, E. Bernstein, K. Li, D. Jia, Z. Yang, H. Erdjument-Bromage, P. Tempst, S. P. Lin, C. D. Allis, X. Cheng, and T. H. Bestor. 2007. DNMT3L connects unmethylated lysine 4 of histone H3 to de novo methylation of DNA. *Nature* 448: 714-717.

23.   Otani, J., T. Nankumo, K. Arita, S. Inamoto, M. Ariyoshi, and M. Shirakawa. 2009. Structural basis for recognition of H3K4 methylation status by the DNA methyltransferase 3A ATRX-DNMT3-DNMT3L domain. *EMBO Rep* 10: 1235-1241.

24.   Guo, X., L. Wang, J. Li, Z. Ding, J. Xiao, X. Yin, S. He, P. Shi, L. Dong, G. Li, C. Tian, J. Wang, Y. Cong, and Y. Xu. 2015. Structural insight into autoinhibition and histone H3-induced activation of DNMT3A. *Nature* 517: 640-644.

25.   Chen, T., Y. Ueda, S. Xie, and E. Li. 2002. A novel Dnmt3a isoform produced from an alternative promoter localizes to euchromatin and its expression correlates with active de novo methylation. *J Biol Chem* 277: 38746-38754.

26.   Duymich, C. E., J. Charlet, X. Yang, P. A. Jones, and G. Liang. 2016. DNMT3B isoforms without catalytic activity stimulate gene body methylation as accessory proteins in somatic cells. *Nat Commun* 7: 11453.

27.   Pradhan, S., A. Bacolla, R. D. Wells, and R. J. Roberts. 1999. Recombinant human DNA (cytosine-5) methyltransferase. I. Expression, purification, and comparison of de novo and maintenance methylation. *J Biol Chem* 274: 33002-33010.

28.   Chedin, F. 2011. The DNMT3 family of mammalian de novo DNA methyltransferases. *Progress in molecular biology and translational science* 101: 255-285.

29.   Okano, M., D. W. Bell, D. A. Haber, and E. Li. 1999. DNA methyltransferases Dnmt3a and Dnmt3b are essential for de novo methylation and mammalian development. *Cell* 99: 247-257.

30.   Hsieh, C. L. 1999. In vivo activity of murine de novo methyltransferases, Dnmt3a and Dnmt3b. *Mol Cell Biol* 19: 8211-8218.

31.   Lyko, F., B. H. Ramsahoye, H. Kashevsky, M. Tudor, M. A. Mastrangelo, T. L. Orr-Weaver, and R. Jaenisch. 1999. Mammalian (cytosine-5) methyltransferases cause genomic DNA methylation and lethality in Drosophila. *Nat Genet* 23: 363-366.

32. Chen, T., Y. Ueda, J. E. Dodge, Z. Wang, and E. Li. 2003. Establishment and maintenance of genomic methylation patterns in mouse embryonic stem cells by Dnmt3a and Dnmt3b. *Mol Cell Biol* 23: 5594-5605.

33. Hu, J. L., B. O. Zhou, R. R. Zhang, K. L. Zhang, J. Q. Zhou, and G. L. Xu. 2009. The N-terminus of histone H3 is required for de novo DNA methylation in chromatin. *Proc Natl Acad Sci U S A* 106: 22187-22192.

34. Borgel, J., S. Guibert, Y. Li, H. Chiba, D. Schubeler, H. Sasaki, T. Forne, and M. Weber. 2010. Targets and dynamics of promoter DNA methylation during early mouse development. *Nat Genet* 42: 1093-1100.

35. Kaneda, M., M. Okano, K. Hata, T. Sado, N. Tsujimoto, E. Li, and H. Sasaki. 2004. Essential role for de novo DNA methyltransferase Dnmt3a in paternal and maternal imprinting. *Nature* 429: 900-903.

36. Hirasawa, R., H. Chiba, M. Kaneda, S. Tajima, E. Li, R. Jaenisch, and H. Sasaki. 2008. Maternal and zygotic Dnmt1 are necessary and sufficient for the maintenance of DNA methylation imprints during preimplantation development. *Genes Dev* 22: 1607-1616.

37. Hamidi, T., A. K. Singh, and T. Chen. 2015. Genetic alterations of DNA methylation machinery in human diseases. *Epigenomics* 7: 247-265.

38. Kim, S. J., H. Zhao, S. Hardikar, A. K. Singh, M. A. Goodell, and T. Chen. 2013. A DNMT3A mutation common in AML exhibits dominant-negative effects in murine ES cells. *Blood* 122: 4086-4089.

39. de Greef, J. C., J. Wang, J. Balog, J. T. den Dunnen, R. R. Frants, K. R. Straasheijm, C. Aytekin, M. van der Burg, L. Duprez, A. Ferster, A. R. Gennery, G. Gimelli, I. Reisli, C. Schuetz, A. Schulz, D. F. Smeets, Y. Sznajer, C. Wijmenga, M. C. van Eggermond, M. M. van Ostaijen-Ten Dam, A. C. Lankester, M. J. van Tol, P. J. van den Elsen, C. M. Weemaes, and S. M. van der Maarel. 2011. Mutations in ZBTB24 are associated with immunodeficiency, centromeric instability, and facial anomalies syndrome type 2. *American journal of human genetics* 88: 796-804.

40.   Thijssen, P. E., Y. Ito, G. Grillo, J. Wang, G. Velasco, H. Nitta, M. Unoki, M. Yoshihara, M. Suyama, Y. Sun, R. J. Lemmers, J. C. de Greef, A. Gennery, P. Picco, B. Kloeckener-Gruissem, T. Gungor, I. Reisli, C. Picard, K. Kebaili, B. Roquelaure, T. Iwai, I. Kondo, T. Kubota, M. M. van Ostaijen-Ten Dam, M. J. van Tol, C. Weemaes, C. Francastel, S. M. van der Maarel, and H. Sasaki. 2015. Mutations in CDCA7 and HELLS cause immunodeficiency-centromeric instability-facial anomalies syndrome. *Nat Commun* 6: 7870.

41.   Zhu, H., T. M. Geiman, S. Xi, Q. Jiang, A. Schmidtmann, T. Chen, E. Li, and K. Muegge. 2006. Lsh is involved in de novo methylation of DNA. *Embo J* 25: 335-345.

42.   Hata, K., M. Okano, H. Lei, and E. Li. 2002. Dnmt3L cooperates with the Dnmt3 family of de novo DNA methyltransferases to establish maternal imprints in mice. *Development* 129: 1983-1993.

43.   Jia, D., R. Z. Jurkowska, X. Zhang, A. Jeltsch, and X. Cheng. 2007. Structure of Dnmt3a bound to Dnmt3L suggests a model for de novo DNA methylation. *Nature* 449: 248-251.

44.   Bourc'his, D., G. L. Xu, C. S. Lin, B. Bollman, and T. H. Bestor. 2001. Dnmt3L and the establishment of maternal genomic imprints. *Science* 294: 2536-2539.

45.   Bourc'his, D., and T. H. Bestor. 2004. Meiotic catastrophe and retrotransposon reactivation in male germ cells lacking Dnmt3L. *Nature* 431: 96-99.

46.   Ooi, S. K., D. Wolf, O. Hartung, S. Agarwal, G. Q. Daley, S. P. Goff, and T. H. Bestor. 2010. Dynamic instability of genomic methylation patterns in pluripotent stem cells. *Epigenetics Chromatin* 3: 17.

47.   Kao, T. H., H. F. Liao, D. Wolf, K. Y. Tai, C. Y. Chuang, H. S. Lee, H. C. Kuo, K. Hata, X. Zhang, X. Cheng, S. P. Goff, S. K. Ooi, T. H. Bestor, and S. P. Lin. 2014. Ectopic DNMT3L triggers assembly of a repressive complex for retroviral silencing in somatic cells. *J Virol* 88: 10680-10695.

48.   Nimura, K., C. Ishida, H. Koriyama, K. Hata, S. Yamanaka, E. Li, K. Ura, and Y. Kaneda. 2006. Dnmt3a2 targets endogenous Dnmt3L to ES cell chromatin and induces regional DNA methylation. *Genes Cells* 11: 1225-1237.

49. Neri, F., A. Krepelova, D. Incarnato, M. Maldotti, C. Parlato, F. Galvagni, F. Matarese, H. G. Stunnenberg, and S. Oliviero. 2013. Dnmt3L antagonizes DNA methylation at bivalent promoters and favors DNA methylation at gene bodies in ESCs. *Cell* 155: 121-134.

50. Bostick, M., J. K. Kim, P. O. Esteve, A. Clark, S. Pradhan, and S. E. Jacobsen. 2007. UHRF1 plays a role in maintaining DNA methylation in mammalian cells. *Science* 317: 1760-1764.

51. Sharif, J., M. Muto, S. Takebayashi, I. Suetake, A. Iwamatsu, T. A. Endo, J. Shinga, Y. Mizutani-Koseki, T. Toyoda, K. Okamura, S. Tajima, K. Mitsuya, M. Okano, and H. Koseki. 2007. The SRA protein Np95 mediates epigenetic inheritance by recruiting Dnmt1 to methylated DNA. *Nature* 450: 908-912.

52. Bestor, T., A. Laudano, R. Mattaliano, and V. Ingram. 1988. Cloning and sequencing of a cDNA encoding DNA methyltransferase of mouse cells. The carboxyl-terminal domain of the mammalian enzymes is related to bacterial restriction methyltransferases. *J Mol Biol* 203: 971-983.

53. Ding, F., and J. R. Chaillet. 2002. In vivo stabilization of the Dnmt1 (cytosine-5)-methyltransferase protein. *Proceedings of the National Academy of Sciences of the United States of America* 99: 14861-14866.

54. Qin, W., P. Wolf, N. Liu, S. Link, M. Smets, F. La Mastra, I. Forne, G. Pichler, D. Horl, K. Fellinger, F. Spada, I. M. Bonapace, A. Imhof, H. Harz, and H. Leonhardt. 2015. DNA methylation requires a DNMT1 ubiquitin interacting motif (UIM) and histone ubiquitination. *Cell Res* 25: 911-929.

55. Takeshita, K., I. Suetake, E. Yamashita, M. Suga, H. Narita, A. Nakagawa, and S. Tajima. 2011. Structural insight into maintenance methylation by mouse DNA methyltransferase 1 (Dnmt1). *Proc Natl Acad Sci U S A* 108: 9055-9059.

56. Leonhardt, H., A. W. Page, H. U. Weier, and T. H. Bestor. 1992. A targeting sequence directs DNA methyltransferase to sites of DNA replication in mammalian nuclei. *Cell* 71: 865-873.

57. Li, E., T. H. Bestor, and R. Jaenisch. 1992. Targeted mutation of the DNA methyltransferase gene results in embryonic lethality. *Cell* 69: 915-926.

58.   Lei, H., S. P. Oh, M. Okano, R. Juttermann, K. A. Goss, R. Jaenisch, and E. Li. 1996. De novo DNA cytosine methyltransferase activities in mouse embryonic stem cells. *Development* 122: 3195-3205.

59.   Tucker, K. L., D. Talbot, M. A. Lee, H. Leonhardt, and R. Jaenisch. 1996. Complementation of methylation deficiency in embryonic stem cells by a DNA methyltransferase minigene. *Proc Natl Acad Sci U S A* 93: 12920-12925.

60.   Tsumura, A., T. Hayakawa, Y. Kumaki, S. Takebayashi, M. Sakaue, C. Matsuoka, K. Shimotohno, F. Ishikawa, E. Li, H. R. Ueda, J. Nakayama, and M. Okano. 2006. Maintenance of self-renewal ability of mouse embryonic stem cells in the absence of DNA methyltransferases Dnmt1, Dnmt3a and Dnmt3b. *Genes Cells* 11: 805-814.

61.   Liao, J., R. Karnik, H. Gu, M. J. Ziller, K. Clement, A. M. Tsankov, V. Akopian, C. A. Gifford, J. Donaghey, C. Galonska, R. Pop, D. Reyon, S. Q. Tsai, W. Mallard, J. K. Joung, J. L. Rinn, A. Gnirke, and A. Meissner. 2015. Targeted disruption of DNMT1, DNMT3A and DNMT3B in human embryonic stem cells. *Nat Genet* 47: 469-478.

62.   Jackson-Grusby, L., C. Beard, R. Possemato, M. Tudor, D. Fambrough, G. Csankovszki, J. Dausman, P. Lee, C. Wilson, E. Lander, and R. Jaenisch. 2001. Loss of genomic methylation causes p53-dependent apoptosis and epigenetic deregulation. *Nat Genet* 27: 31-39.

63.   Chen, T., S. Hevi, F. Gay, N. Tsujimoto, T. He, B. Zhang, Y. Ueda, and E. Li. 2007. Complete inactivation of DNMT1 leads to mitotic catastrophe in human cancer cells. *Nat Genet* 39: 391-396.

64.   Muto, M., Y. Kanari, E. Kubo, T. Takabe, T. Kurihara, A. Fujimori, and K. Tatsumi. 2002. Targeted disruption of Np95 gene renders murine embryonic stem cells hypersensitive to DNA damaging agents and DNA replication blocks. *J Biol Chem* 277: 34549-34555.

65.   Rajakumara, E., Z. Wang, H. Ma, L. Hu, H. Chen, Y. Lin, R. Guo, F. Wu, H. Li, F. Lan, Y. G. Shi, Y. Xu, D. J. Patel, and Y. Shi. 2011. PHD finger recognition of unmodified histone H3R2 links UHRF1 to regulation of euchromatic gene expression. *Mol Cell* 43: 275-284.

66. Rothbart, S. B., B. M. Dickson, M. S. Ong, K. Krajewski, S. Houliston, D. B. Kireev, C. H. Arrowsmith, and B. D. Strahl. 2013. Multivalent histone engagement by the linked tandem Tudor and PHD domains of UHRF1 is required for the epigenetic inheritance of DNA methylation. *Genes Dev* 27: 1288-1298.

67. Nishiyama, A., L. Yamaguchi, J. Sharif, Y. Johmura, T. Kawamura, K. Nakanishi, S. Shimamura, K. Arita, T. Kodama, F. Ishikawa, H. Koseki, and M. Nakanishi. 2013. Uhrf1-dependent H3K23 ubiquitylation couples maintenance DNA methylation and replication. *Nature* 502: 249-253.

68. Guccione, E., C. Bassi, F. Casadio, F. Martinato, M. Cesaroni, H. Schuchlautz, B. Luscher, and B. Amati. 2007. Methylation of histone H3R2 by PRMT6 and H3K4 by an MLL complex are mutually exclusive. *Nature* 449: 933-937.

69. Hyllus, D., C. Stein, K. Schnabel, E. Schiltz, A. Imhof, Y. Dou, J. Hsieh, and U. M. Bauer. 2007. PRMT6-mediated methylation of R2 in histone H3 antagonizes H3 K4 trimethylation. *Genes Dev* 21: 3369-3380.

70. Iberg, A. N., A. Espejo, D. Cheng, D. Kim, J. Michaud-Levesque, S. Richard, and M. T. Bedford. 2008. Arginine methylation of the histone H3 tail impedes effector binding. *J Biol Chem* 283: 3006-3010.

71. Baylin, S. B., and P. A. Jones. 2011. A decade of exploring the cancer epigenome - biological and translational implications. *Nat Rev Cancer* 11: 726-734.

72. Esteller, M. 2007. Cancer epigenomics: DNA methylomes and histone-modification maps. *Nat Rev Genet* 8: 286-298.

73. Kulis, M., and M. Esteller. 2010. DNA methylation and cancer. *Adv Genet* 70: 27-56.

74. Jones, P. A., and S. B. Baylin. 2002. The fundamental role of epigenetic events in cancer. *Nat Rev Genet* 3: 415-428.

75. Cui, H., I. L. Horon, R. Ohlsson, S. R. Hamilton, and A. P. Feinberg. 1998. Loss of imprinting in normal tissue of colorectal cancer patients with microsatellite instability. *Nat Med* 4: 1276-1280.

76.   Bell, A. C., and G. Felsenfeld. 2000. Methylation of a CTCF-dependent boundary controls imprinted expression of the Igf2 gene. *Nature* 405: 482-485.

77.   Sakatani, T., A. Kaneda, C. A. Iacobuzio-Donahue, M. G. Carter, S. de Boom Witzel, H. Okano, M. S. Ko, R. Ohlsson, D. L. Longo, and A. P. Feinberg. 2005. Loss of imprinting of Igf2 alters intestinal maturation and tumorigenesis in mice. *Science* 307: 1976-1978.

78.   Rasmussen, K. D., and K. Helin. 2016. Role of TET enzymes in DNA methylation, development, and cancer. *Genes Dev* 30: 733-750.

79.   Shih, A. H., O. Abdel-Wahab, J. P. Patel, and R. L. Levine. 2012. The role of mutations in epigenetic regulators in myeloid malignancies. *Nat Rev Cancer* 12: 599-612.

80.   Pastor, W. A., L. Aravind, and A. Rao. 2013. TETonic shift: biological roles of TET proteins in DNA demethylation and transcription. *Nat Rev Mol Cell Biol* 14: 341-356.

81.   Hon, G. C., C. X. Song, T. Du, F. Jin, S. Selvaraj, A. Y. Lee, C. A. Yen, Z. Ye, S. Q. Mao, B. A. Wang, S. Kuan, L. E. Edsall, B. S. Zhao, G. L. Xu, C. He, and B. Ren. 2014. 5mC oxidation by Tet2 modulates enhancer activity and timing of transcriptome reprogramming during differentiation. *Mol Cell* 56: 286-297.

82.   Rasmussen, K. D., G. Jia, J. V. Johansen, M. T. Pedersen, N. Rapin, F. O. Bagger, B. T. Porse, O. A. Bernard, J. Christensen, and K. Helin. 2015. Loss of TET2 in hematopoietic cells leads to DNA hypermethylation of active enhancers and induction of leukemogenesis. *Genes Dev* 29: 910-922.

83.   Uribe-Lewis, S., R. Stark, T. Carroll, M. J. Dunning, M. Bachman, Y. Ito, L. Stojic, S. Halim, S. L. Vowler, A. G. Lynch, B. Delatte, E. J. de Bony, L. Colin, M. Defrance, F. Krueger, A. L. Silva, R. Ten Hoopen, A. E. Ibrahim, F. Fuks, and A. Murrell. 2015. 5-hydroxymethylcytosine marks promoters in colon that resist DNA hypermethylation in cancer. *Genome Biol* 16: 69.

84.   Verma, N., H. Pan, L. C. Dore, A. Shukla, Q. V. Li, B. Pelham-Webb, V. Teijeiro, F. Gonzalez, A. Krivtsov, C. J. Chang, E. P. Papapetrou, C. He, O. Elemento, and D. Huangfu. 2018. TET proteins safeguard bivalent promoters from de novo methylation in human embryonic stem cells. *Nat Genet* 50: 83-95.

85. Chen, T., and S. Y. Dent. 2014. Chromatin modifiers and remodellers: regulators of cellular differentiation. *Nat Rev Genet* 15: 93-106.

86. Feinberg, A. P., and B. Vogelstein. 1983. Hypomethylation distinguishes genes of some human cancers from their normal counterparts. *Nature* 301: 89-92.

87. Feinberg, A. P., and B. Vogelstein. 1983. Hypomethylation of ras oncogenes in primary human cancers. *Biochem Biophys Res Commun* 111: 47-54.

88. Bedford, M. T., and P. D. van Helden. 1987. Hypomethylation of DNA in pathological conditions of the human prostate. *Cancer Res* 47: 5274-5276.

89. Ehrlich, M. 2002. DNA methylation in cancer: too much, but also too little. *Oncogene* 21: 5400-5413.

90. Gaudet, F., J. G. Hodgson, A. Eden, L. Jackson-Grusby, J. Dausman, J. W. Gray, H. Leonhardt, and R. Jaenisch. 2003. Induction of tumors in mice by genomic hypomethylation. *Science* 300: 489-492.

91. Eden, A., F. Gaudet, A. Waghmare, and R. Jaenisch. 2003. Chromosomal instability and tumors promoted by DNA hypomethylation. *Science* 300: 455.

92. Holm, T. M., L. Jackson-Grusby, T. Brambrink, Y. Yamada, W. M. Rideout, 3rd, and R. Jaenisch. 2005. Global loss of imprinting leads to widespread tumorigenesis in adult mice. *Cancer Cell* 8: 275-285.

93. Brunetti, L., M. C. Gundry, and M. A. Goodell. 2017. DNMT3A in Leukemia. *Cold Spring Harb Perspect Med* 7.

94. Jeong, M., D. Sun, M. Luo, Y. Huang, G. A. Challen, B. Rodriguez, X. Zhang, L. Chavez, H. Wang, R. Hannah, S. B. Kim, L. Yang, M. Ko, R. Chen, B. Gottgens, J. S. Lee, P. Gunaratne, L. A. Godley, G. J. Darlington, A. Rao, W. Li, and M. A. Goodell. 2014. Large conserved domains of low DNA methylation maintained by Dnmt3a. *Nat Genet* 46: 17-23.

95. Celik, H., C. Mallaney, A. Kothari, E. L. Ostrander, E. Eultgen, A. Martens, C. A. Miller, J. Hundal, J. M. Klco, and G. A. Challen. 2015. Enforced differentiation of Dnmt3a-null bone

marrow leads to failure with c-Kit mutations driving leukemic transformation. *Blood* 125: 619-628.

96.   Mayle, A., L. Yang, B. Rodriguez, T. Zhou, E. Chang, C. V. Curry, G. A. Challen, W. Li, D. Wheeler, V. I. Rebel, and M. A. Goodell. 2015. Dnmt3a loss predisposes murine hematopoietic stem cells to malignant transformation. *Blood* 125: 629-638.

97.   Yang, L., B. Rodriguez, A. Mayle, H. J. Park, X. Lin, M. Luo, M. Jeong, C. V. Curry, S. B. Kim, D. Ruau, X. Zhang, T. Zhou, M. Zhou, V. I. Rebel, G. A. Challen, B. Gottgens, J. S. Lee, R. Rau, W. Li, and M. A. Goodell. 2016. DNMT3A Loss Drives Enhancer Hypomethylation in FLT3-ITD-Associated Leukemias. *Cancer Cell* 30: 363-365.

98.   Meyer, S. E., T. Qin, D. E. Muench, K. Masuda, M. Venkatasubramanian, E. Orr, L. Suarez, S. D. Gore, R. Delwel, E. Paietta, M. S. Tallman, H. Fernandez, A. Melnick, M. M. Le Beau, S. Kogan, N. Salomonis, M. E. Figueroa, and H. L. Grimes. 2016. DNMT3A Haploinsufficiency Transforms FLT3ITD Myeloproliferative Disease into a Rapid, Spontaneous, and Fully Penetrant Acute Myeloid Leukemia. *Cancer Discov* 6: 501-515.

99.   Qu, Y., A. Lennartsson, V. I. Gaidzik, S. Deneberg, M. Karimi, S. Bengtzen, M. Hoglund, L. Bullinger, K. Dohner, and S. Lehmann. 2014. Differential methylation in CN-AML preferentially targets non-CGI regions and is dictated by DNMT3A mutational status and associated with predominant hypomethylation of HOX genes. *Epigenetics* 9: 1108-1119.

100.   Jin, W., L. Chen, Y. Chen, S. G. Xu, G. H. Di, W. J. Yin, J. Wu, and Z. M. Shao. 2010. UHRF1 is associated with epigenetic silencing of BRCA1 in sporadic breast cancer. *Breast Cancer Res Treat* 123: 359-373.

101.   Unoki, M., Y. Daigo, J. Koinuma, E. Tsuchiya, R. Hamamoto, and Y. Nakamura. 2010. UHRF1 is a novel diagnostic marker of lung cancer. *Br J Cancer* 103: 217-222.

102.   Babbio, F., C. Pistore, L. Curti, I. Castiglioni, P. Kunderfranco, L. Brino, P. Oudet, R. Seiler, G. N. Thalman, E. Roggero, M. Sarti, S. Pinton, M. Mello-Grand, G. Chiorino, C. V. Catapano, G. M. Carbone, and I. M. Bonapace. 2012. The SRA protein UHRF1 promotes epigenetic crosstalks and is involved in prostate cancer progression. *Oncogene* 31: 4878-4887.

103. Wang, F., Y. Z. Yang, C. Z. Shi, P. Zhang, M. P. Moyer, H. Z. Zhang, Y. Zou, and H. L. Qin. 2012. UHRF1 promotes cell growth and metastasis through repression of p16(ink(4)a) in colorectal cancer. *Ann Surg Oncol* 19: 2753-2762.

104. Jia, Y., P. Li, L. Fang, H. Zhu, L. Xu, H. Cheng, J. Zhang, F. Li, Y. Feng, Y. Li, J. Li, R. Wang, J. X. Du, J. Li, T. Chen, H. Ji, J. Han, W. Yu, Q. Wu, and J. Wong. 2016. Negative regulation of DNMT3A de novo DNA methylation by frequently overexpressed UHRF family proteins as a mechanism for widespread DNA hypomethylation in cancer. *Cell Discov* 2: 16007.

105. Ashraf, W., A. Ibrahim, M. Alhosin, L. Zaayter, K. Ouararhni, C. Papin, T. Ahmad, A. Hamiche, Y. Mely, C. Bronner, and M. Mousli. 2017. The epigenetic integrator UHRF1: on the road to become a universal biomarker for cancer. *Oncotarget* 8: 51946-51962.

106. Jenkins, Y., V. Markovtsov, W. Lang, P. Sharma, D. Pearsall, J. Warner, C. Franci, B. Huang, J. Huang, G. C. Yam, J. P. Vistan, E. Pali, J. Vialard, M. Janicot, J. B. Lorens, D. G. Payan, and Y. Hitoshi. 2005. Critical role of the ubiquitin ligase activity of UHRF1, a nuclear RING finger protein, in tumor cell growth. *Mol Biol Cell* 16: 5621-5629.

107. Du, Z., J. Song, Y. Wang, Y. Zhao, K. Guda, S. Yang, H. Y. Kao, Y. Xu, J. Willis, S. D. Markowitz, D. Sedwick, R. M. Ewing, and Z. Wang. 2010. DNMT1 stability is regulated by proteins coordinating deubiquitination and acetylation-driven ubiquitination. *Sci Signal* 3: ra80.

108. Qin, W., H. Leonhardt, and F. Spada. 2011. Usp7 and Uhrf1 control ubiquitination and stability of the maintenance DNA methyltransferase Dnmt1. *J Cell Biochem* 112: 439-444.

109. Mudbhary, R., Y. Hoshida, Y. Chernyavskaya, V. Jacob, A. Villanueva, M. I. Fiel, X. Chen, K. Kojima, S. Thung, R. T. Bronson, A. Lachenmayer, K. Revill, C. Alsinet, R. Sachidanandam, A. Desai, S. SenBanerjee, C. Ukomadu, J. M. Llovet, and K. C. Sadler. 2014. UHRF1 overexpression drives DNA hypomethylation and hepatocellular carcinoma. *Cancer Cell* 25: 196-209.

110. Hervouet, E., L. Lalier, E. Debien, M. Cheray, A. Geairon, H. Rogniaux, D. Loussouarn, S. A. Martin, F. M. Vallette, and P. F. Cartron. 2010. Disruption of Dnmt1/PCNA/UHRF1 interactions promotes tumorigenesis from human and mice glial cells. *PLoS One* 5: e11333.

111. Pacaud, R., E. Brocard, L. Lalier, E. Hervouet, F. M. Vallette, and P. F. Cartron. 2014. The DNMT1/PCNA/UHRF1 disruption induces tumorigenesis characterized by similar genetic and epigenetic signatures. *Sci Rep* 4: 4230.

112. Blanc, R. S., and S. Richard. 2017. Arginine Methylation: The Coming of Age. *Mol Cell* 65: 8-24.

113. Yang, Y., and M. T. Bedford. 2013. Protein arginine methyltransferases and cancer. *Nat Rev Cancer* 13: 37-50.

114. Larsen, S. C., K. B. Sylvestersen, A. Mund, D. Lyon, M. Mullari, M. V. Madsen, J. A. Daniel, L. J. Jensen, and M. L. Nielsen. 2016. Proteome-wide analysis of arginine monomethylation reveals widespread occurrence in human cells. *Sci Signal* 9: rs9.

115. Gayatri, S., and M. T. Bedford. 2014. Readers of histone methylarginine marks. *Biochim Biophys Acta* 1839: 702-710.

116. Bedford, M. T., and S. Richard. 2005. Arginine methylation an emerging regulator of protein function. *Mol Cell* 18: 263-272.

117. Cerami, E., J. Gao, U. Dogrusoz, B. E. Gross, S. O. Sumer, B. A. Aksoy, A. Jacobsen, C. J. Byrne, M. L. Heuer, E. Larsson, Y. Antipin, B. Reva, A. P. Goldberg, C. Sander, and N. Schultz. 2012. The cBio cancer genomics portal: an open platform for exploring multidimensional cancer genomics data. *Cancer Discov* 2: 401-404.

118. Gao, J., B. A. Aksoy, U. Dogrusoz, G. Dresdner, B. Gross, S. O. Sumer, Y. Sun, A. Jacobsen, R. Sinha, E. Larsson, E. Cerami, C. Sander, and N. Schultz. 2013. Integrative analysis of complex cancer genomics and clinical profiles using the cBioPortal. *Sci Signal* 6: pl1.

119. Cheung, N., L. C. Chan, A. Thompson, M. L. Cleary, and C. W. So. 2007. Protein arginine-methyltransferase-dependent oncogenesis. *Nat Cell Biol* 9: 1208-1215.

120. Elakoum, R., G. Gauchotte, A. Oussalah, M. P. Wissler, C. Clement-Duchene, J. M. Vignaud, J. L. Gueant, and F. Namour. 2014. CARM1 and PRMT1 are dysregulated in lung cancer without hierarchical features. *Biochimie* 97: 210-218.

121. Yoshimatsu, M., G. Toyokawa, S. Hayami, M. Unoki, T. Tsunoda, H. I. Field, J. D. Kelly, D. E. Neal, Y. Maehara, B. A. Ponder, Y. Nakamura, and R. Hamamoto. 2011. Dysregulation of PRMT1 and PRMT6, Type I arginine methyltransferases, is involved in various types of human cancers. *Int J Cancer* 128: 562-573.

122. Singh, V., T. B. Miranda, W. Jiang, A. Frankel, M. E. Roemer, V. A. Robb, D. H. Gutmann, H. R. Herschman, S. Clarke, and I. F. Newsham. 2004. DAL-1/4.1B tumor suppressor interacts with protein arginine N-methyltransferase 3 (PRMT3) and inhibits its ability to methylate substrates in vitro and in vivo. *Oncogene* 23: 7761-7771.

123. Habashy, H. O., E. A. Rakha, I. O. Ellis, and D. G. Powe. 2013. The oestrogen receptor coactivator CARM1 has an oncogenic effect and is associated with poor prognosis in breast cancer. *Breast Cancer Res Treat* 140: 307-316.

124. Cheng, H., Y. Qin, H. Fan, P. Su, X. Zhang, H. Zhang, and G. Zhou. 2013. Overexpression of CARM1 in breast cancer is correlated with poorly characterized clinicopathologic parameters and molecular subtypes. *Diagn Pathol* 8: 129.

125. Kim, D., J. Lee, D. Cheng, J. Li, C. Carter, E. Richie, and M. T. Bedford. 2010. Enzymatic activity is required for the in vivo functions of CARM1. *J Biol Chem* 285: 1147-1152.

126. Shilo, K., X. Wu, S. Sharma, M. Welliver, W. Duan, M. Villalona-Calero, J. Fukuoka, S. Sif, R. Baiocchi, C. L. Hitchcock, W. Zhao, and G. A. Otterson. 2013. Cellular localization of protein arginine methyltransferase-5 correlates with grade of lung tumors. *Diagn Pathol* 8: 201.

127. Wang, L., S. Pal, and S. Sif. 2008. Protein arginine methyltransferase 5 suppresses the transcription of the RB family of tumor suppressors in leukemia and lymphoma cells. *Mol Cell Biol* 28: 6262-6277.

128. Yan, F., L. Alinari, M. E. Lustberg, L. K. Martin, H. M. Cordero-Nieves, Y. Banasavadi-Siddegowda, S. Virk, J. Barnholtz-Sloan, E. H. Bell, J. Wojton, N. K. Jacob, A. Chakravarti, M. O. Nowicki, X. Wu, R. Lapalombella, J. Datta, B. Yu, K. Gordon, A. Haseley, J. T. Patton, P. L. Smith, J. Ryu, X. Zhang, X. Mo, G. Marcucci, G. Nuovo, C. H. Kwon, J. C. Byrd, E. A. Chiocca, C. Li, S. Sif, S. Jacob, S. Lawler, B. Kaur, and R. A. Baiocchi. 2014. Genetic validation

of the protein arginine methyltransferase PRMT5 as a candidate therapeutic target in glioblastoma. *Cancer Res* 74: 1752-1765.

129. Vieira, F. Q., P. Costa-Pinheiro, J. Ramalho-Carvalho, A. Pereira, F. D. Menezes, L. Antunes, I. Carneiro, J. Oliveira, R. Henrique, and C. Jeronimo. 2014. Deregulated expression of selected histone methylases and demethylases in prostate carcinoma. *Endocr Relat Cancer* 21: 51-61.

130. Thomassen, M., Q. Tan, and T. A. Kruse. 2009. Gene expression meta-analysis identifies chromosomal regions and candidate genes involved in breast cancer metastasis. *Breast Cancer Res Treat* 113: 239-249.

131. Nicholson, T. B., N. Veland, and T. Chen. 2015. Chapter 3 - Writers, Readers, and Erasers of Epigenetic Marks A2 - Gray, Steven G. In *Epigenetic Cancer Therapy*. Academic Press, Boston. 31-66.

132. Zhao, Q., G. Rank, Y. T. Tan, H. Li, R. L. Moritz, R. J. Simpson, L. Cerruti, D. J. Curtis, D. J. Patel, C. D. Allis, J. M. Cunningham, and S. M. Jane. 2009. PRMT5-mediated methylation of histone H4R3 recruits DNMT3A, coupling histone and DNA methylation in gene silencing. *Nat Struct Mol Biol* 16: 304-311.

133. Girardot, M., R. Hirasawa, S. Kacem, L. Fritsch, J. Pontis, S. K. Kota, D. Filipponi, E. Fabbrizio, C. Sardet, F. Lohmann, S. Kadam, S. Ait-Si-Ali, and R. Feil. 2014. PRMT5-mediated histone H4 arginine-3 symmetrical dimethylation marks chromatin at G + C-rich regions of the mouse genome. *Nucleic Acids Res* 42: 235-248.

134. Hatanaka, Y., T. Tsusaka, N. Shimizu, K. Morita, T. Suzuki, S. Machida, M. Satoh, A. Honda, M. Hirose, S. Kamimura, N. Ogonuki, T. Nakamura, K. Inoue, Y. Hosoi, N. Dohmae, T. Nakano, H. Kurumizaka, K. Matsumoto, Y. Shinkai, and A. Ogura. 2017. Histone H3 Methylated at Arginine 17 Is Essential for Reprogramming the Paternal Genome in Zygotes. *Cell Rep* 20: 2756-2765.

135. Kirmizis, A., H. Santos-Rosa, C. J. Penkett, M. A. Singer, M. Vermeulen, M. Mann, J. Bahler, R. D. Green, and T. Kouzarides. 2007. Arginine methylation at histone H3R2 controls deposition of H3K4 trimethylation. *Nature* 449: 928-932.

136.   Dowhan, D. H., M. J. Harrison, N. A. Eriksson, P. Bailey, M. A. Pearen, P. J. Fuller, J. W. Funder, E. R. Simpson, P. J. Leedman, W. D. Tilley, M. A. Brown, C. L. Clarke, and G. E. Muscat. 2012. Protein arginine methyltransferase 6-dependent gene expression and splicing: association with breast cancer outcomes. *Endocr Relat Cancer* 19: 509-526.

137.   Sun, Y., H. H. Chung, A. R. Woo, and V. C. Lin. 2014. Protein arginine methyltransferase 6 enhances ligand-dependent and -independent activity of estrogen receptor alpha via distinct mechanisms. *Biochim Biophys Acta* 1843: 2067-2078.

138.   Harrison, M. J., Y. H. Tang, and D. H. Dowhan. 2010. Protein arginine methyltransferase 6 regulates multiple aspects of gene expression. *Nucleic Acids Res* 38: 2201-2216.

139.   Mann, M., Y. Zou, Y. Chen, D. Brann, and R. Vadlamudi. 2014. PELP1 oncogenic functions involve alternative splicing via PRMT6. *Mol Oncol* 8: 389-400.

140.   Phalke, S., S. Mzoughi, M. Bezzi, N. Jennifer, W. C. Mok, D. H. Low, A. A. Thike, V. A. Kuznetsov, P. H. Tan, P. M. Voorhoeve, and E. Guccione. 2012. p53-Independent regulation of p21Waf1/Cip1 expression and senescence by PRMT6. *Nucleic Acids Res* 40: 9534-9542.

141.   Stein, C., S. Riedl, D. Ruthnick, R. R. Notzold, and U. M. Bauer. 2012. The arginine methyltransferase PRMT6 regulates cell proliferation and senescence through transcriptional repression of tumor suppressor genes. *Nucleic Acids Res* 40: 9522-9533.

142.   Kleinschmidt, M. A., P. de Graaf, H. A. van Teeffelen, and H. T. Timmers. 2012. Cell cycle regulation by the PRMT6 arginine methyltransferase through repression of cyclin-dependent kinase inhibitors. *PLoS One* 7: e41446.

143.   Nakakido, M., Z. Deng, T. Suzuki, N. Dohmae, Y. Nakamura, and R. Hamamoto. 2015. PRMT6 increases cytoplasmic localization of p21CDKN1A in cancer cells through arginine methylation and makes more resistant to cytotoxic agents. *Oncotarget* 6: 30957-30967.

144.   Ma, W. L., L. Wang, L. X. Liu, and X. L. Wang. 2015. Effect of phosphorylation and methylation on the function of the p16INK4a protein in non-small cell lung cancer A549 cells. *Oncol Lett* 10: 2277-2282.

145. Neault, M., F. A. Mallette, G. Vogel, J. Michaud-Levesque, and S. Richard. 2012. Ablation of PRMT6 reveals a role as a negative transcriptional regulator of the p53 tumor suppressor. *Nucleic Acids Res* 40: 9513-9521.

146. Czechanski, A., C. Byers, I. Greenstein, N. Schrode, L. R. Donahue, A. K. Hadjantonakis, and L. G. Reinholdt. 2014. Derivation and characterization of mouse embryonic stem cells from permissive and nonpermissive strains. *Nat Protoc* 9: 559-574.

147. Eram, M. S., Y. Shen, M. M. Szewczyk, H. Wu, G. Senisterra, F. Li, K. V. Butler, H. U. Kaniskan, B. A. Speed, C. dela Sena, A. Dong, H. Zeng, M. Schapira, P. J. Brown, C. H. Arrowsmith, D. Barsyte-Lovejoy, J. Liu, M. Vedadi, and J. Jin. 2016. A Potent, Selective, and Cell-Active Inhibitor of Human Type I Protein Arginine Methyltransferases. *ACS Chem Biol* 11: 772-781.

148. Dan, J., P. Rousseau, S. Hardikar, N. Veland, J. Wong, C. Autexier, and T. Chen. 2017. Zscan4 Inhibits Maintenance DNA Methylation to Facilitate Telomere Elongation in Mouse Embryonic Stem Cells. *Cell Rep* 20: 1936-1949.

149. Kumaki, Y., M. Oda, and M. Okano. 2008. QUMA: quantification tool for methylation analysis. *Nucleic Acids Res* 36: W170-175.

150. Mohn, F., M. Weber, D. Schubeler, and T. C. Roloff. 2009. Methylated DNA immunoprecipitation (MeDIP). *Methods Mol Biol* 507: 55-64.

151. Ren, J., V. Briones, S. Barbour, W. Yu, Y. Han, M. Terashima, and K. Muegge. 2015. The ATP binding site of the chromatin remodeling homolog Lsh is required for nucleosome density and de novo DNA methylation at repeat sequences. *Nucleic Acids Res* 43: 1444-1455.

152. Jorgensen, H. F., V. Azuara, S. Amoils, M. Spivakov, A. Terry, T. Nesterova, B. S. Cobb, B. Ramsahoye, M. Merkenschlager, and A. G. Fisher. 2007. The impact of chromatin modifiers on the timing of locus replication in mouse embryonic stem cells. *Genome Biol* 8: R169.

153. Veland, N., S. Hardikar, Y. Zhong, S. Gayatri, J. Dan, B. D. Strahl, S. B. Rothbart, M. T. Bedford, and T. Chen. 2017. The Arginine Methyltransferase PRMT6 Regulates DNA

Methylation and Contributes to Global DNA Hypomethylation in Cancer. *Cell Rep* 21: 3390-3397.

154. Mahe, M. M., E. Aihara, M. A. Schumacher, Y. Zavros, M. H. Montrose, M. A. Helmrath, T. Sato, and N. F. Shroyer. 2013. Establishment of Gastrointestinal Epithelial Organoids. *Curr Protoc Mouse Biol* 3: 217-240.

155. Schneider, C. A., W. S. Rasband, and K. W. Eliceiri. 2012. NIH Image to ImageJ: 25 years of image analysis. *Nat Methods* 9: 671-675.

156. Gu, H., Z. D. Smith, C. Bock, P. Boyle, A. Gnirke, and A. Meissner. 2011. Preparation of reduced representation bisulfite sequencing libraries for genome-scale DNA methylation profiling. *Nat Protoc* 6: 468-481.

157. Varley, K. E., J. Gertz, K. M. Bowling, S. L. Parker, T. E. Reddy, F. Pauli-Behn, M. K. Cross, B. A. Williams, J. A. Stamatoyannopoulos, G. E. Crawford, D. M. Absher, B. J. Wold, and R. M. Myers. 2013. Dynamic DNA methylation across diverse human cell lines and tissues. *Genome Res* 23: 555-567.

158. Martin, M. 2011. Cutadapt removes adapter sequences from high-throughput sequencing reads. *2011* 17.

159. Krueger, F., and S. R. Andrews. 2011. Bismark: a flexible aligner and methylation caller for Bisulfite-Seq applications. *Bioinformatics* 27: 1571-1572.

160. Langmead, B., C. Trapnell, M. Pop, and S. L. Salzberg. 2009. Ultrafast and memory-efficient alignment of short DNA sequences to the human genome. *Genome Biol* 10: R25.

161. Akalin, A., M. Kormaksson, S. Li, F. E. Garrett-Bakelman, M. E. Figueroa, A. Melnick, and C. E. Mason. 2012. methylKit: a comprehensive R package for the analysis of genome-wide DNA methylation profiles. *Genome Biol* 13: R87.

162. Pruitt, K. D., G. R. Brown, S. M. Hiatt, F. Thibaud-Nissen, A. Astashyn, O. Ermolaeva, C. M. Farrell, J. Hart, M. J. Landrum, K. M. McGarvey, M. R. Murphy, N. A. O'Leary, S. Pujar, B. Rajput, S. H. Rangwala, L. D. Riddick, A. Shkeda, H. Sun, P. Tamez, R. E. Tully, C. Wallin, D.

Webb, J. Weber, W. Wu, M. DiCuccio, P. Kitts, D. R. Maglott, T. D. Murphy, and J. M. Ostell. 2014. RefSeq: an update on mammalian reference sequences. *Nucleic Acids Res* 42: D756-763.

163.   Mendez, J., and B. Stillman. 2000. Chromatin association of human origin recognition complex, cdc6, and minichromosome maintenance proteins during the cell cycle: assembly of prereplication complexes in late mitosis. *Mol Cell Biol* 20: 8602-8612.

164.   Hackett, J. A., and M. A. Surani. 2013. DNA methylation dynamics during the mammalian life cycle. *Philos Trans R Soc Lond B Biol Sci* 368: 20110328.

165.   Robertson, K. D. 2005. DNA methylation and human disease. *Nat Rev Genet* 6: 597-610.

166.   Gowher, H., K. Liebert, A. Hermann, G. Xu, and A. Jeltsch. 2005. Mechanism of stimulation of catalytic activity of Dnmt3A and Dnmt3B DNA-(cytosine-C5)-methyltransferases by Dnmt3L. *J Biol Chem* 280: 13341-13348.

167.   Suetake, I., F. Shinozaki, J. Miyagawa, H. Takeshima, and S. Tajima. 2004. DNMT3L stimulates the DNA methylation activity of Dnmt3a and Dnmt3b through a direct interaction. *J Biol Chem* 279: 27816-27823.

168.   Van Emburgh, B. O., and K. D. Robertson. 2011. Modulation of Dnmt3b function in vitro by interactions with Dnmt3L, Dnmt3a and Dnmt3b splice variants. *Nucleic Acids Res* 39: 4984-5002.

169.   Zhang, Z. M., R. Lu, P. Wang, Y. Yu, D. Chen, L. Gao, S. Liu, D. Ji, S. B. Rothbart, Y. Wang, G. G. Wang, and J. Song. 2018. Structural basis for DNMT3A-mediated de novo DNA methylation. *Nature* 554: 387-391.

170.   Jurkowska, R. Z., N. Anspach, C. Urbanke, D. Jia, R. Reinhardt, W. Nellen, X. Cheng, and A. Jeltsch. 2008. Formation of nucleoprotein filaments by mammalian DNA methyltransferase Dnmt3a in complex with regulator Dnmt3L. *Nucleic Acids Res* 36: 6656-6663.

171.   Smallwood, S. A., S. Tomizawa, F. Krueger, N. Ruf, N. Carli, A. Segonds-Pichon, S. Sato, K. Hata, S. R. Andrews, and G. Kelsey. 2011. Dynamic CpG island methylation landscape in oocytes and preimplantation embryos. *Nat Genet* 43: 811-814.

172.	Shirane, K., H. Toh, H. Kobayashi, F. Miura, H. Chiba, T. Ito, T. Kono, and H. Sasaki. 2013. Mouse oocyte methylomes at base resolution reveal genome-wide accumulation of non-CpG methylation and role of DNA methyltransferases. *PLoS Genet* 9: e1003439.

173.	Choi, J., K. Clement, A. J. Huebner, J. Webster, C. M. Rose, J. Brumbaugh, R. M. Walsh, S. Lee, A. Savol, J. P. Etchegaray, H. Gu, P. Boyle, U. Elling, R. Mostoslavsky, R. Sadreyev, P. J. Park, S. P. Gygi, A. Meissner, and K. Hochedlinger. 2017. DUSP9 Modulates DNA Hypomethylation in Female Mouse Pluripotent Stem Cells. *Cell Stem Cell* 20: 706-719 e707.

174.	Guenatri, M., D. Bailly, C. Maison, and G. Almouzni. 2004. Mouse centric and pericentric satellite repeats form distinct functional heterochromatin. *J Cell Biol* 166: 493-505.

175.	Komissarov, A. S., E. V. Gavrilova, S. J. Demin, A. M. Ishov, and O. I. Podgornaya. 2011. Tandemly repeated DNA families in the mouse genome. *BMC Genomics* 12: 531.

176.	Chedin, F., M. R. Lieber, and C. L. Hsieh. 2002. The DNA methyltransferase-like protein DNMT3L stimulates de novo methylation by Dnmt3a. *Proc Natl Acad Sci U S A* 99: 16916-16921.

177.	Meissner, A., A. Gnirke, G. W. Bell, B. Ramsahoye, E. S. Lander, and R. Jaenisch. 2005. Reduced representation bisulfite sequencing for comparative high-resolution DNA methylation analysis. *Nucleic Acids Res* 33: 5868-5877.

178.	Meissner, A., T. S. Mikkelsen, H. Gu, M. Wernig, J. Hanna, A. Sivachenko, X. Zhang, B. E. Bernstein, C. Nusbaum, D. B. Jaffe, A. Gnirke, R. Jaenisch, and E. S. Lander. 2008. Genome-scale DNA methylation maps of pluripotent and differentiated cells. *Nature* 454: 766-770.

179.	Smith, Z. D., H. Gu, C. Bock, A. Gnirke, and A. Meissner. 2009. High-throughput bisulfite sequencing in mammalian genomes. *Methods* 48: 226-232.

180.	Guenatri, M., R. Duffie, J. Iranzo, P. Fauque, and D. Bourc'his. 2013. Plasticity in Dnmt3L-dependent and -independent modes of de novo methylation in the developing mouse embryo. *Development* 140: 562-572.

181. Chen, Z. X., J. R. Mann, C. L. Hsieh, A. D. Riggs, and F. Chedin. 2005. Physical and functional interactions between the human DNMT3L protein and members of the de novo methyltransferase family. *J Cell Biochem* 95: 902-917.

182. Borgel, J., S. Guibert, Y. Li, H. Chiba, D. Schubeler, H. Sasaki, T. Forne, and M. Weber. 2010. Targets and dynamics of promoter DNA methylation during early mouse development. *Nat Genet* 42: 1093-1100.

183. Sakai, Y., I. Suetake, F. Shinozaki, S. Yamashina, and S. Tajima. 2004. Co-expression of de novo DNA methyltransferases Dnmt3a2 and Dnmt3L in gonocytes of mouse embryos. *Gene Expr Patterns* 5: 231-237.

184. Ma, P., E. de Waal, J. R. Weaver, M. S. Bartolomei, and R. M. Schultz. 2015. A DNMT3A2-HDAC2 Complex Is Essential for Genomic Imprinting and Genome Integrity in Mouse Oocytes. *Cell Rep* 13: 1552-1560.

185. Duymich, C. E., J. Charlet, X. Yang, P. A. Jones, and G. Liang. 2016. DNMT3B isoforms without catalytic activity stimulate gene body methylation as accessory proteins in somatic cells. *Nat Commun* 7: 11453.

186. Liu, X., Q. Gao, P. Li, Q. Zhao, J. Zhang, J. Li, H. Koseki, and J. Wong. 2013. UHRF1 targets DNMT1 for DNA methylation through cooperative binding of hemi-methylated DNA and methylated H3K9. *Nat Commun* 4: 1563.

187. Qin, W., P. Wolf, N. Liu, S. Link, M. Smets, F. La Mastra, I. Forne, G. Pichler, D. Horl, K. Fellinger, F. Spada, I. M. Bonapace, A. Imhof, H. Harz, and H. Leonhardt. 2015. DNA methylation requires a DNMT1 ubiquitin interacting motif (UIM) and histone ubiquitination. *Cell Res* 25: 911-929.

188. Harrison, J. S., E. M. Cornett, D. Goldfarb, P. A. DaRosa, Z. M. Li, F. Yan, B. M. Dickson, A. H. Guo, D. V. Cantu, L. Kaustov, P. J. Brown, C. H. Arrowsmith, D. A. Erie, M. B. Major, R. E. Klevit, K. Krajewski, B. Kuhlman, B. D. Strahl, and S. B. Rothbart. 2016. Hemi-methylated DNA regulates DNA methylation inheritance through allosteric activation of H3 ubiquitylation by UHRF1. *Elife* 5.

189.   Rothbart, S. B., K. Krajewski, N. Nady, W. Tempel, S. Xue, A. I. Badeaux, D. Barsyte-Lovejoy, J. Y. Martinez, M. T. Bedford, S. M. Fuchs, C. H. Arrowsmith, and B. D. Strahl. 2012. Association of UHRF1 with methylated H3K9 directs the maintenance of DNA methylation. *Nat Struct Mol Biol* 19: 1155-1160.

190.   Hu, L., Z. Li, P. Wang, Y. Lin, and Y. Xu. 2011. Crystal structure of PHD domain of UHRF1 and insights into recognition of unmodified histone H3 arginine residue 2. *Cell Res* 21: 1374-1378.

191.   Wang, C., J. Shen, Z. Yang, P. Chen, B. Zhao, W. Hu, W. Lan, X. Tong, H. Wu, G. Li, and C. Cao. 2011. Structural basis for site-specific reading of unmodified R2 of histone H3 tail by UHRF1 PHD finger. *Cell Res* 21: 1379-1382.

192.   Lallous, N., P. Legrand, A. G. McEwen, S. Ramon-Maiques, J. P. Samama, and C. Birck. 2011. The PHD finger of human UHRF1 reveals a new subgroup of unmethylated histone H3 tail readers. *PLoS One* 6: e27599.

193.   Fang, J., J. Cheng, J. Wang, Q. Zhang, M. Liu, R. Gong, P. Wang, X. Zhang, Y. Feng, W. Lan, Z. Gong, C. Tang, J. Wong, H. Yang, C. Cao, and Y. Xu. 2016. Hemi-methylated DNA opens a closed conformation of UHRF1 to facilitate its histone recognition. *Nat Commun* 7: 11197.

194.   Tsumura, A., T. Hayakawa, Y. Kumaki, S. Takebayashi, M. Sakaue, C. Matsuoka, K. Shimotohno, F. Ishikawa, E. Li, H. R. Ueda, J. Nakayama, and M. Okano. 2006. Maintenance of self-renewal ability of mouse embryonic stem cells in the absence of DNA methyltransferases Dnmt1, Dnmt3a and Dnmt3b. *Genes Cells* 11: 805-814.

195.   Karahan, G., N. Sayar, G. Gozum, B. Bozkurt, O. Konu, and I. G. Yulug. 2015. Relative expression of rRNA transcripts and 45S rDNA promoter methylation status are dysregulated in tumors in comparison with matched-normal tissues in breast cancer. *Oncol Rep* 33: 3131-3145.

196.   Du, J., L. M. Johnson, S. E. Jacobsen, and D. J. Patel. 2015. DNA methylation pathways and their crosstalk with histone methylation. *Nat Rev Mol Cell Biol* 16: 519-532.

197.   Goodell, M. A., H. Nguyen, and N. Shroyer. 2015. Somatic stem cell heterogeneity: diversity in the blood, skin and intestinal stem cell compartments. *Nat Rev Mol Cell Biol* 16: 299-309.

198.   Scott-Browne, J. P., L. Cw, and A. Rao. 2017. TET proteins in natural and induced differentiation. *Curr Opin Genet Dev* 46: 202-208.

199.   Cheng, Y., N. Xie, P. Jin, and T. Wang. 2015. DNA methylation and hydroxymethylation in stem cells. *Cell Biochem Funct* 33: 161-173.

200.   Cullen, S. M., and M. A. Goodell. 2013. Rising from the crypt: decreasing DNA methylation during differentiation of the small intestine. *Genome Biol* 14: 116.

201.   Elliott, E. N., and K. H. Kaestner. 2015. Epigenetic regulation of the intestinal epithelium. *Cell Mol Life Sci* 72: 4139-4156.

202.   Elliott, E. N., K. L. Sheaffer, J. Schug, T. S. Stappenbeck, and K. H. Kaestner. 2015. Dnmt1 is essential to maintain progenitors in the perinatal intestinal epithelium. *Development* 142: 2163-2172.

203.   Yu, D. H., M. Gadkari, Q. Zhou, S. Yu, N. Gao, Y. Guan, D. Schady, T. N. Roshan, M. H. Chen, E. Laritsky, Z. Ge, H. Wang, R. Chen, C. Westwater, L. Bry, R. A. Waterland, C. Moriarty, C. Hwang, A. G. Swennes, S. R. Moore, and L. Shen. 2015. Postnatal epigenetic regulation of intestinal stem cells requires DNA methylation and is guided by the microbiome. *Genome Biol* 16: 211.

204.   Sheaffer, K. L., R. Kim, R. Aoki, E. N. Elliott, J. Schug, L. Burger, D. Schubeler, and K. H. Kaestner. 2014. DNA methylation is required for the control of stem cell differentiation in the small intestine. *Genes Dev* 28: 652-664.

205.   Kaaij, L. T., M. van de Wetering, F. Fang, B. Decato, A. Molaro, H. J. van de Werken, J. H. van Es, J. Schuijers, E. de Wit, W. de Laat, G. J. Hannon, H. C. Clevers, A. D. Smith, and R. F. Ketting. 2013. DNA methylation dynamics during intestinal stem cell differentiation reveals enhancers driving gene expression in the villus. *Genome Biol* 14: R50.

206.   Huang, C. Z., T. Yu, and Q. K. Chen. 2015. DNA Methylation Dynamics During Differentiation, Proliferation, and Tumorigenesis in the Intestinal Tract. *Stem Cells Dev* 24: 2733-2739.

207.   Elliott, E. N., K. L. Sheaffer, and K. H. Kaestner. 2016. The 'de novo' DNA methyltransferase Dnmt3b compensates the Dnmt1-deficient intestinal epithelium. *Elife* 5.

208.   Forn, M., A. Diez-Villanueva, A. Merlos-Suarez, M. Munoz, S. Lois, E. Carrio, M. Jorda, A. Bigas, E. Batlle, and M. A. Peinado. 2015. Overlapping DNA methylation dynamics in mouse intestinal cell differentiation and early stages of malignant progression. *PLoS One* 10: e0123263.

209.   Hammoud, S. S., B. R. Cairns, and D. A. Jones. 2013. Epigenetic regulation of colon cancer and intestinal stem cells. *Curr Opin Cell Biol* 25: 177-183.

210.   Ko, M., J. An, H. S. Bandukwala, L. Chavez, T. Aijo, W. A. Pastor, M. F. Segal, H. Li, K. P. Koh, H. Lahdesmaki, P. G. Hogan, L. Aravind, and A. Rao. 2013. Modulation of TET2 expression and 5-methylcytosine oxidation by the CXXC domain protein IDAX. *Nature*.

211.   Esteve, P. O., Y. Chang, M. Samaranayake, A. K. Upadhyay, J. R. Horton, G. R. Feehery, X. Cheng, and S. Pradhan. 2011. A methylation and phosphorylation switch between an adjacent lysine and serine determines human DNMT1 stability. *Nat Struct Mol Biol* 18: 42-48.

212.   Fellinger, K., U. Rothbauer, M. Felle, G. Langst, and H. Leonhardt. 2009. Dimerization of DNA methyltransferase 1 is mediated by its regulatory domain. *J Cell Biochem* 106: 521-528.

213.   Chen, T., Y. Ueda, S. Xie, and E. Li. 2002. A novel Dnmt3a isoform produced from an alternative promoter localizes to euchromatin and its expression correlates with active de novo methylation. *J Biol Chem* 277: 38746-38754.

214.   Fortini, M. E. 2002. Gamma-secretase-mediated proteolysis in cell-surface-receptor signalling. *Nat Rev Mol Cell Biol* 3: 673-684.

215.   Taylor, R. C., S. P. Cullen, and S. J. Martin. 2008. Apoptosis: controlled demolition at the cellular level. *Nat Rev Mol Cell Biol* 9: 231-241.

216.   Ying, Q. L., J. Wray, J. Nichols, L. Batlle-Morera, B. Doble, J. Woodgett, P. Cohen, and A. Smith. 2008. The ground state of embryonic stem cell self-renewal. *Nature* 453: 519-523.

217.   von Meyenn, F., M. Iurlaro, E. Habibi, N. Q. Liu, A. Salehzadeh-Yazdi, F. Santos, E. Petrini, I. Milagre, M. Yu, Z. Xie, L. I. Kroeze, T. B. Nesterova, J. H. Jansen, H. Xie, C. He, W. Reik, and H. G. Stunnenberg. 2016. Impairment of DNA Methylation Maintenance Is the Main Cause of Global Demethylation in Naive Embryonic Stem Cells. *Mol Cell* 62: 983.

218. Musselman, C. A., and T. G. Kutateladze. 2011. Handpicking epigenetic marks with PHD fingers. *Nucleic Acids Res* 39: 9061-9071.

219. Wrangle, J., W. Wang, A. Koch, H. Easwaran, H. P. Mohammad, F. Vendetti, W. Vancriekinge, T. Demeyer, Z. Du, P. Parsana, K. Rodgers, R. W. Yen, C. A. Zahnow, J. M. Taube, J. R. Brahmer, S. S. Tykodi, K. Easton, R. D. Carvajal, P. A. Jones, P. W. Laird, D. J. Weisenberger, S. Tsai, R. A. Juergens, S. L. Topalian, C. M. Rudin, M. V. Brock, D. Pardoll, and S. B. Baylin. 2013. Alterations of immune response of Non-Small Cell Lung Cancer with Azacytidine. *Oncotarget* 4: 2067-2079.

220. Li, H., K. B. Chiappinelli, A. A. Guzzetta, H. Easwaran, R. W. Yen, R. Vatapalli, M. J. Topper, J. Luo, R. M. Connolly, N. S. Azad, V. Stearns, D. M. Pardoll, N. Davidson, P. A. Jones, D. J. Slamon, S. B. Baylin, C. A. Zahnow, and N. Ahuja. 2014. Immune regulation by low doses of the DNA methyltransferase inhibitor 5-azacitidine in common human epithelial cancers. *Oncotarget* 5: 587-598.

221. Kim, K., A. D. Skora, Z. Li, Q. Liu, A. J. Tam, R. L. Blosser, L. A. Diaz, Jr., N. Papadopoulos, K. W. Kinzler, B. Vogelstein, and S. Zhou. 2014. Eradication of metastatic mouse cancers resistant to immune checkpoint blockade by suppression of myeloid-derived cells. *Proc Natl Acad Sci U S A* 111: 11774-11779.

222. Wang, L., Z. Amoozgar, J. Huang, M. H. Saleh, D. Xing, S. Orsulic, and M. S. Goldberg. 2015. Decitabine Enhances Lymphocyte Migration and Function and Synergizes with CTLA-4 Blockade in a Murine Ovarian Cancer Model. *Cancer Immunol Res* 3: 1030-1041.

223. Chiappinelli, K. B., P. L. Strissel, A. Desrichard, H. Li, C. Henke, B. Akman, A. Hein, N. S. Rote, L. M. Cope, A. Snyder, V. Makarov, S. Budhu, D. J. Slamon, J. D. Wolchok, D. M. Pardoll, M. W. Beckmann, C. A. Zahnow, T. Merghoub, T. A. Chan, S. B. Baylin, and R. Strick. 2015. Inhibiting DNA Methylation Causes an Interferon Response in Cancer via dsRNA Including Endogenous Retroviruses. *Cell* 162: 974-986.

224. Roulois, D., H. Loo Yau, R. Singhania, Y. Wang, A. Danesh, S. Y. Shen, H. Han, G. Liang, P. A. Jones, T. J. Pugh, C. O'Brien, and D. D. De Carvalho. 2015. DNA-Demethylating Agents

Target Colorectal Cancer Cells by Inducing Viral Mimicry by Endogenous Transcripts. *Cell* 162: 961-973.

225.   Weintraub, K. 2016. Take two: Combining immunotherapy with epigenetic drugs to tackle cancer. *Nat Med* 22: 8-10.

226.   Dear, A. E. 2016. Epigenetic Modulators and the New Immunotherapies. *N Engl J Med* 374: 684-686.

VITA

Jaime Nicolas Veland was born in Lima, Peru on April 6th, 1984. After completing his work at Santa Maria Marianistas High School, Lima, Peru in 2001, he entered Universidad Peruana Cayetano Heredia (UPCH) in Lima, Peru. He received the degree of Bachelor in Science with a major in Biology from UPCH in May, 2007. For the next five years, he worked as a research assistant in the Institute of Tropical Medicine "Alexander von Humboldt" at UPCH. In August of 2012 he entered The University of Texas MD Anderson Cancer Center UTHealth Graduate School of Biomedical Sciences.

Permanent address:

3950 Highway 71 East Apt 924

Bastrop, Texas 78602